VAASAN YLIOPISTO

CHAO GAO

Performance and Energy Efficiency in Wireless Self-Organized Networks

ACTA WASAENSIA NO 215

COMPUTER SCIENCE 8
TELECOMMUNICATIONS ENGINEERING

UNIVERSITAS WASAENSIS 2009

Reviewers

Professor Carlos Pomalaza-Raez
University of Oulu
Telecommunication Laboratory
P.O. Box 4500
90014 University of Oulu

Professor Kim Seong-Lyun
School of Electrical & Electronic Engineering
Yonsei University
134 Sinchon-Dong, Seodaemun-Gu
Seoul 120–749
Korea

Julkaisija	**Julkaisuajankohta**	
Vaasan yliopisto	Marraskuu 2009	
Tekijä(t) Chao Gao	**Julkaisun tyyppi** Monografia	
	Julkaisusarjan nimi, osan numero Acta Wasaensia, 215	
Yhteystiedot Vaasan Yliopisto Teknillinen tiedekunta Tietotekniikan laitos PL 700 65101 Vaasa	**ISBN** 978–952–476–279–3	
	ISSN 0355–2667, 1455–7339	
	Sivumäärä 206	**Kieli** Englanti

Julkaisun nimike

Suorituskyky ja energiatehokkuus itseorganisoituvissa langattomissa verkoissa

Tiivistelmä

Itseorganisoituvat pakettiradioverkot (ad hoc -verkot) ovat keränneet paljon huomiota viimeaikoina. Yksi kyseisten verkkojen keskeisistä ongelmista on energia tehokkuus, sillä verkon solmut ovat tyypillisesti akkukäyttöisiä. Käytettyjen protokollien energiatehokas suunnittelu voi oleellisesti parantaa verkkojen stabiilisuutta ja pidentää niiden elinikää.

Tässä työssä tarkastellaan ad hoc-verkkojen ja langattomien anturiverkkojen energiatehokkuutta eri protokollakerroksilla. Fyysisen kerroksen ja MAC-kerroksen osalta tutkitaan verkkosolmujen energian kulutusta. Korkeampien kerrosten osalta tutkitaan protokollien signalointikuormaa. Verkkokerroksen osalta työssä tutkitaan erityisesti reaktiivisia reititysprotokollia. Tarvittavien hyppyjen määrän analyysin perusteella työssä esitetään muutoksia AODV-protokollaan. Reaktiivisten reititysprotokollien ominaisuuksista johtuen, lyhyimmällä polulla on suhteellisen pieni todennäköisyys tulla valituksi – erityisesti suurissa verkoissa. Lyhyimmän polun reititys olisi kuitenkin toivottavaa tiedon päästä päähän kuluvan energian minimoimiseksi. Työssä esitetään kaksi menetelmää lyhimmän polun valitsemistodennäköisyyden kasvattamiseksi. Simulaatiotulokset indikoivat, että esitetyt menetelmät kykenevät vähentämään sekä energian kulutusta sekä siirtoviivettä.

Työssä tarkastellaan tehotason säätöä osana verkon klusterointia. Klusteroinilla pyritään verkon skaalautuvuuden sekä energiatehokkuuden parantamiseen. Työssä esitetään klusterointimenetelmä, joka hyödyntää mitattuja linkin tilatietoja sekä mahdollisuutta eri tehotasojen asettamiseen klusterin sisäiselle ja klustereiden väliselle tiedonsiirrolle. Klusteroinnin yhteydessä esitetään myös globaali synkronisointiprotokolla.

Työssä tutkitaan lisäksi monihyppyisten solukkoverkkojen itseorganisoituvuutta ja esitetään yläsuunnan peittoalueen ja energiatehokkuuden parantamiseksi kahden hypyn kahden aikavälin tiedonsiirtomenetelmä.

Asiasanat

Langaton ad-hoc -verkko, langaton anturiverkko, itse-organisaatio

Publisher	**Date of publication**	
Vaasan yliopisto	November 2009	
Author(s) Chao Gao	**Type of publication** Monograph	
	Name and number of series Acta Wasaensia, 215	
Contact information University of Vaasa Faculty of Technology Department of Computer Sciences P.O. Box 700 FI–65101 Vaasa, Finland	**ISBN** 978–952–476–279–3	
	ISSN 0355–2667, 1455–7339	
	Number of pages 206	**Language** English

Title of publication
Performance and Energy Efficiency in Wireless Self-Organized Networks

Abstract

Self-organized packet radio networks (ad-hoc networks) and wireless sensor networks have got massive attention recently. One of critical problems in such networks is the energy efficiency, because wireless nodes are usually powered by battery. Energy efficiency design can dramatically increase the survivability and stability of wireless ad-hoc/sensor networks.

In this thesis the energy efficiency has been considered at different protocol layers for wireless ad-hoc/sensor networks. The energy consumption of wireless nodes is inspected at the physical layer and MAC layer.

At the network layer, some current routing protocols are compared and special attention has been paid to reactive routing protocols. A minimum hop analysis is given and according to the analysis result, a modification of AODV routing is proposed.

A variation of transmit power can be also applied to clustering algorithm, which is believed to be able to control the scalability of network. Clustering a network can also improve the energy efficiency. We offer a clustering scheme based on the link state measurement and variation of transmit power of intra-cluster and inter-cluster transmission. Simulation shows that it can achieve both targets. In association with the clustering algorithm, a global synchronization scheme is proposed to increase the efficiency of clustering algorithm.

The research attention has been also paid to self-organization for multi-hop cellular networks. A 2-hop 2-slot uplink proposal to infrastructure-based cellular networks. The proposed solution can significantly increase the throughput of uplink communication and reduce the energy consumption of wireless terminals.

Keywords
Wireless ad-hoc networks, wireless sensor networks, self-organization

ACKNOWLEDGEMENTS

First of all, I would like to give my heartfelt thanks to my advisor Professor Riku Jäntti for his innumerable support and advise during these years of research. It is my whole-life good memory and pleasure to discuss with him, not only about academic topics, but also about all the world around us. His scientifical spirit and academical attitude will always inspirit me to face the researches in my future life.

I would like also to thank Professor Matti Linna who was my first advisor. He helped me to start this study life and gave me instructions to make the first step of research, thus I can complete my licentiate degree. As the head of the faculty of technology, he also helped me a lot in the office to get clear information of study.

I am also grateful to Professor Seong-Lyun Kim, who had supported me to visit his laboratory twice in year 2004 and 2006. His instructions and advice are very precious to extend my research ability.

My cordial thanks should also go to Mr. Kalevi Ylinen, the head of the department of Information Technology of Vaasa University of Applied Sciences. He arranged the my teaching courses so that I was able to have time to make this achievement. The same thanks must be given to Mr. Pentti Ruotsala, the formal Rector of Vaasa University of Applied Sciences, for those priceless support and encouragement.

I would like to show my gratitude to Professor Kimmo Salmonjoki and Professor Merja Wanne, and Päivi, the secretary of department, who also gave me support during the study and research.

The office staff of Computer Science department of Vaasa University have helped me during the years of thesis working.

This thesis is specially dedicated to my family — my wife Sanna, my children Otto and Johanna. I am sorry that I did not take care of you very much during these years because of this hard job.

CONTENTS

LIST OF FIGURES

LIST OF TABLES

LIST OF ABBREVIATIONS

ACK	ACKnowledgement
ADC	Analog-to-Digital Converter/Conversion
ALOHA	Areal Location of Hazardous Atmospheres
AODV	Ad-hoc On-demand Distance Vector
AP	Access Point
BEAC	BEAcon for Clustering
BEB	Binary Exponential Backoff
BER	Bit Error Rate
BREP	Beacon REPly
BSS	Basic Service Set
CBR	Constant Bit Rate
CCA	Clear Channel Assessment
CDF	Cumulative Density Function
CDMA	Code Division Multiple Access
CFP	Collision-Free Period
CGZ	Communication Gray Zone
CMOS	Complementary Metal Oxide Semiconductor
CSMA	Carrier Sense Medium Access
CSMA/CA	CSMA with Collision Avoidance
CTS	Clear To Send
CW	Contention Window
DAC	Digital-to-Analog Converter/Conversion
DCF	Distributed Coordinate Function
DIFS	DCF IFS
DSDV	Destination-Sequenced Distance Vector
DSR	Dynamic Source Routing
ESS	Extended Service Set
FDMA	Frequency Division Multiple Access
HVAC	Heating, Ventilating and Air-Conditioning
IC	Integrated Circuits
iCAR	integrated Cellular and Ad-hoc Relay
IEEE	Institute of Electrical and Electronics Engineers
IETF	Internet Engineering Task Force
IFS	Inter-Frame Space
LAN	Local Area Networks

LMNR	Localized Multiple Nexthop Routing
LNA	Low-Noise Amplifier
LPA	Linear Power Amplifier
LSCA	Link State Clustering Algorithm
MAC	Medium Access Control
MACA	Multiple Access with Collision Avoidance
MANET	Mobile Ad-hoc NETworks
MCFA	Minimum Cost Forwarding Algorithm
MCU	Microcontroller Unit
MEMS	MicroElectroMechanical Systems
MST	Minimum Spanning Tree
NAV	Network Allocation Vector
NIC	Network Interface Card
NS-2	Network Simulator version 2
OSI	Open System Interconnection
PAR	Power Aware Routing
PCF	Point Coordinate Function
PDA	Personal Data Assistant
PDF	Probability Density Function
PER	Packet Error Rate (a.k.a. FER – Frame Error Rate)
PRNET	Packet Radio NETworks
RERR	Route Error
RF	Radio Frequency
RREP	Route REPly
RREQ	Route REQuest
RSSI	Receive Signal Strength Indication
RTS	Request To Send
SB	Synchronization Beacon
SCAN	Slave CANcel
SIFS	Short IFS
S-MAC	Sensor-MAC
SNR	Signal-to-Noise Ratio
SPIN	Sensor Protocols for Information via Negotiation
SURAN	SUrvivable Adaptive Radio Networks
SWIN	Synchronization WINdow
TCP	Transport Control Protocol
TDMA	Tiem Division Multiple Access
TPSN	Time-sync Protocol for Sensor Networks
TTL(1)	Transistor-Transistor Logic
TTL(2)	Time-To-Live
UDP	User Datagram Protocol
VSF-DS-CDMA	Variable Spreading Factor Direct Sequence CDMA
WLAN	Wireless LAN
WPAN	Wireless Personal Area Networks
WSN	Wireless Sensor Networks

WW	Waiting Window
WWT	WW Timer

1 INTRODUCTION

1.1 Definition and Properties

Wireless self-organized network research and applications have gained excessive attentions in recent years. This is not only caused by that the self-organized networking design presents a lot of technical challenges to researchers, but also by that networked microsensor technology is predicted as a key technology for the future (Business Week 1999). The trend of wireless communications will be based on micro- and nanotechnologies that will enable the smart spaces of the future. A network constructed by the nodes using these technologies will incorporate a high level of integration as well as low-power operation in a small physical package,(Darrin, Carkhuff & Mehoke 2004) and a key feature of such a network is self-organization.

1.1.1 Self-organization

Self-organization is a process in which pattern at the global level of a system emerges solely from numerous interactions among the lower-level components of the system. Self-organization is often referred to as the multitude of algorithms and methods that organize the global behavior of a system based on inter-system communication (Dressler 2006).

Key features of self-organization include:

Self-healing : the network is able to automatically fix the network failures. Network failures include node failure due to the battery off or node hardware abnormity, path/route failures due to the mobility or node failure, channel access failure due to the strong external noise, etc.

Self-configuration : the network is able to be automatically configured when

it is deployed. This includes automatic functions such as channel selection, node role configuration in a heterogenerous network, neighbor finding, topology awareness, etc.

Self-management : the network is able to automatically manage its operations and communications, such as scheduling the transmission, wake-up/sleep synchronization, clustering, etc.

Self-optimization : the network is able to optimize its parameters during the operation. This includes energy optimization such as transmit power control, network optimization for connectivity and routing, scheduling optimization, etc.

Basically, wireless ad-hoc networks and sensor networks are self-organization networks due to the high dynamics of these networks.

1.2 History Overview

The first generation of ad hoc networking goes back to 1972. At the time, the name was called PRNET (Packet Radio Networks) (Minoli 1979). In conjunction with ALOHA (Areal Locations of Hazardous Atmospheres) and CSMA (Carrier Sense Medium Access), approaches for medium access control and a kind of distance-vector routing, PRNET were used on a trial basis to provide different networking capabilities in a combat environment.

The second generation of ad hoc networks emerged in 1980s, when the ad-hoc network systems were further enhanced and implemented as a part of the SURAN (Survivable Adaptive Radio Networks) program (Beyer 1990), which provided a packet-switched network to the mobile battlefield devices in an environment without infrastructure. This program proved to be beneficial in improving the radios' performance by making them smaller, cheaper, and resilient to electronic attacks.

In the 1990s, the concept of commercial wireless ad-hoc networks arrived with notebook computers and other viable communications equipment portable and small-size . At the same time, the idea of a collection of mobile nodes was proposed at several research conferences.(Ramanathan & Redi 2002)

After year 2000, the concept and application of wireless communications extended to large-scale sensing and actuating networks. This was driven by the factors that, 1) Microeletromechanical Systems (MEMS) technology had made the sensors smaller(Wameke & Pister 2002), and 2) circuit integration had made the processing circuits and radio circuits smaller. Wireless sensor netwroking is considered to be applied to military, enviromental, habitat, industry/business, health, and many more potential areas.

1.2.1 Wireless Ad-hoc Networks

An ad-hoc network is a (possibly mobile) collection of communications devices (nodes) that wish to communicate, but have no fixed infrastructure available, and have no pre-determined organization of available links. Individual nodes are responsible for dynamically discovering which other nodes they can directly communicate with. A key assumption is that not all nodes can directly communicate with each other, so nodes are required to relay packets on behalf of other nodes in order to deliver data across the network. A significant feature of ad hoc networks is that repid changes in connectivity and link characteristics are introduced due to node mobility and power control practices. Ad hoc networks can be built around any wireless technology, including infrared and RF (Radio Frequency). (Ramanathan & Redi 2002)

Wireless ad-hoc networks are sometimes also called *Mobile Ad-hoc Networks* (MANET). In this thesis, these two terms hereafter refer to the same issue.

Wireless ad-hoc networks are desirable in case that infrastructure is either not available, not trusted, or not able to be established in time. Examples of wireless ad-hoc network application include exchanging data in conference meeting, catastrophy rescue, vehicles/fleet communication on road/sea, military communication on hostile ground, etc. Figure 1.1 shows a conceptual ad hoc network consisting of laptops, mobile terminals, and PDAs (Personal Data Asistant).

Wireless ad-hoc networks exhibit great difference from their wired counterparts. Most critical issues are:(Sikora 2004)

- **Topology control and routing** are very difficult in a spontaneous network. This is caused by 1) node mobility, and 2) random, autonomous power on and off of the mobile nodes.

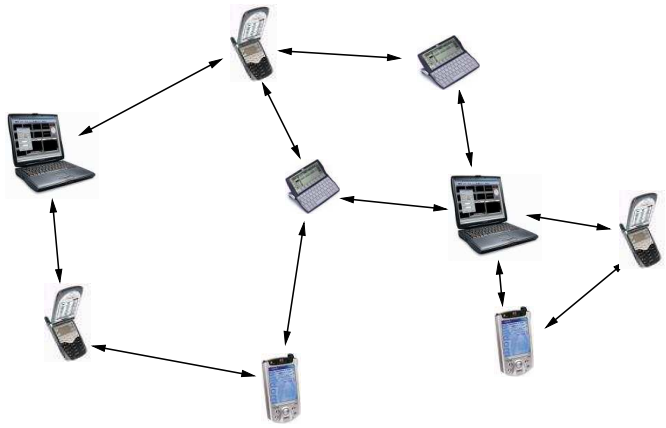

Figure 1.1: An example of ad hoc network

- **Mobility** must be considered in most applications. Mobility can change the network topology, routing performance, radio transmission range, avaibility of services and data, etc.
- The number of devices in the field may vary from only two to some thousands. This is regarded as **scalability problem**.
- **Quality of service**, in terms of packet delivery delay, jittering, transmission error, etc., is difficult to be achieved.
- Mobile nodes and sensor nodes are battery operated. Changing battery is not convenient or totally impossible. Thus **energy efficiency** design is very important.

1.2.2 Wireless Sensor Networks

A Wireless Sensor Network (WSN) consists hundreds or even thousands of wireless sensor nodes that are low cost and small in size. The sensor nodes monitor or sense the environment parameters, and the sensed data can be collected by one or a set of central points called *sinks*, or be processed in a distributed manner. Due to the larger scale of network and more nodes than that of Ad-hoc networks, some high-capacity nodes dedicated to network communication and/or management may be deployed together with sensor nodes. These nodes can take care of data frame relaying, clustering, transmission scheduling, and network diagnosis, etc. A typical WSN usually has a structure shown in Fig. 1.2.

WSNs are similar to wireless ad-hoc networks in many aspects. A wireless sensor

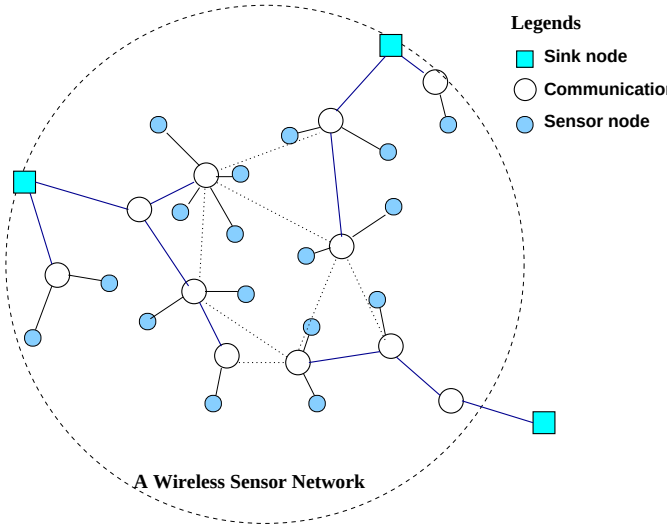

Figure 1.2: A typical wireless sensor network structure

network with a large number of nodes that are usually distributed randomly in a target field. Major issues of wireless ad-hoc networks such as multihop communication, energy efficiency, routing, and topology control also present in wireless sensor networks. However, WSNs have some special features that are different from traditional MANET. These features include data aggregation, localization, tracing, coverage, etc.(Tubaishat & Madria 2003)

WSNs can be applied to following fields:(Sikora 2004)

- Control of machines and devices in the process and automation industry, but also in home appliance.
- Temperature, pressure or gas sensors, valves and actuators, e.g., for *heating, ventilating and air-conditioning* (HVAC)
- Medical monitoring (intra- and extra-corporal)
- Environmental monitoring, e.g., distributed in towns, forests, farming fields, etc.

1.3 Objectives of the Study

In this thesis, the main goal is to improve the energy efficiency and communication performance of wireless ad-hoc/sensor networks when mobility and scalability is

considered. In order to achieve this goal, other self-organization problems such as routing, clustering, synchronization, and throughput improvement are also studied because usually a solution is a combination or trade-off of several aspects of network property.

To achieve this goal, mathematical models of MANETs and WSNs in different aspects such as energy consumption model, routing model, traffic delivery model, and mobility model have been established and analysed.

In order to understand energy consumption behaviour of a mobile node, the structure and functionality of wireless transceiver has been inspected and the results have been referred by later modelings and analysis.

We evaluate our proposals by software simulations. All the simulation processes are written either within Network Simulator version 2 (NS-2)(Fall & Varadhan 2003) or individually in C++/Matlab(The Mathworks, Inc. n.d.).

1.4 Scope and Contributions

This thesis covers the lower layers of communication protocol stack of MANET and WSN. We focus on the energy characteristics of physical layer, data link layer, and network layer. At the physical layer, the details of energy cost in transmitting, receiving, and sleeping mode are inspected. At the data link layer, especially the Medium Access Control (MAC) sublayer, we study the connectivity of the network caused by transmit power control. At the network layer, the energy cost by network overheads and different routing protocols is studied.

Need to say that there are also tremendous research in upper layers of wireless network protocol stack that contribute to performance and energy efficiency. However, due to the limit of possibility and capability, they are not included in this research.

The thesis is a monograph, but most parts of context are the research results have been published earlier in conference proceedings. Chapter 4 is based on the work of (Gao & Jäntti 2004*a*). Chapter 5 is based on the work of (Gao & Jäntti 2005*a*). Chapter 6 is based on the work of (Gao & Jäntti 2004*b*). Chapter 7 is based on the work of (Gao & Jäntti 2005*c*). Chapter 8 is based on the work of (Gao & Jäntti 2005*b*). Chapter 9 is based on the work of (Gao & Jäntti 2006*a*).

Chapter 10 is based on the work of (Gao, Nethi & Jäntti 2007). Chapter 11 is based on the work of (Nethi, Gao & Jäntti 2007), in which I contributed to the system modeling and protocol design, whileas Mr. Shekar Nethi contributed to the coding and simulating in NS-2. Chapter 12 is based on the work of (Gao & Jäntti 2006*c*).

1.5 Organization of the Thesis

The rest of the thesis is organized as follows. In Chapter 2 a brief introduction to the current status of research of ad-hoc/sensor networks is presented. We give special attention to energy efficiency at issues of connectivity, capacity, and routing of ad-hoc networks. Chapter 3 discusses the energy consumption of a typical wireless transceiver. This discussion gives essential concepts of how much energy a wireless node consumes in different phases of participating the network activities. In Chapter 4, in order to increase the energy efficiency, we analyse the probability of finding a minimum-hop route by typical reactive routing protocols. A minimum-hop route is believed to cost less energy and shorten the packet delivery delay. Chapter 5 illustrates the network capacity in term of how many bits of user data can be delivered in multi-hop ad-hoc networks. We found that different transmit power levels result to different network connectivities and topologies. Thus a routing protocol will find different routes in term of hop counts. Consider the energy cost by transmitting and receiving, an optimal transmitting power level is expected to give best energy performance. In Chapter 6 a reactive routing protocol based on transmit power control is proposed. A modification of this protocol to cope with communication gray zone is given in Chapter 7. Chapter 8 focuses on the scalability problem of ad-hoc networks. A link-state clustering algorithm is proposed to reduce the network overhead and increase the scalability. A global synchronization scheme that can be integrated with the link-state clustering algorithm is discussed in Chapter 9. Chapters 10 and 11 focus on multipath routing protocols which are believed to give energy fairness and throughput improvement to MANET and WSN in the situations that a single route is fragile due to the bursty traffic or interference from other systems or nodes. Chapter 12 deals with self-organization solutions for cellular-based multihop networks. A 2-hop 2-slot uplink scheme is proposed to improve uplink throughput for elastic traffic and its performance is analysed and evaluated. Chapter 13 concludes the research.

2 FUNDAMENTAL OF WIRELESS AD-HOC/SENSOR NETWORKS

2.1 Radio Frequency Signal Properties

Many critical problems of MANET and WSN are caused by a simple fact: wireless communication is more difficult than that of the wired counterpart. Radio communication is much more subjected to the change of environment and the interference present, due to its open-to-air feature. Basically, one can find following properties of radio communication(Schwartz 2005):

1. the *average* power measured over a distance from a transmitter decreases inversely with the distance in term of $d^{-\alpha}$, here α is call *path lose factor*, and the power decrease is hence called *path loss*.

2. the instantaneous power measured is found to vary randomly about this *average* power. The power probability distribution is commonly a *log-normal* distribution with variance typically 6-10dBm. This phenomenon is commonly referred to as *shadow fading*. The overall effect of *path loss* and *shadow fading* is called *large-scale fading*.

3. As a receiver moves the order of a half wavelength, the measured result may vary many dB. This *small-scale* variation of the received signal is caused by the destructive/constructive phase interference of many received signal paths. The phenomenon is thus referred to as *multipath fading*. Different statistical models have been applied to different environments. For a relatively long path case, the signal received follows *Rayleigh* distribution; in shorter distances a *Ricean* distribution fits better.

Putting these factors together, the statistical received signal power of a receiver at d meters away from a transmitter can be expressed:

$$P_R = y^2 10^{x/10} d^{-\alpha} P_T G_T G_R \tag{2.1}$$

where P_T is the transmitter power, G_T, G_R are antenna gain of the transmitter and receiver, respectively, and these three terms are usually constant. x is a random variable representing *shadow fading*, and follows a zero-mean gaussian distribution with variance σ:

$$f(x) = \frac{e^{-\frac{x^2}{2\sigma^2}}}{\sqrt{2\pi\sigma^2}} \tag{2.2}$$

where y is a random variable representing *small-scale fading*, and usually follows Rayleigh statistics with Probability Density Function (PDF):

$$p(y) = \frac{y}{\sigma^2} e^{-y^2/2\sigma^2},\ y \geq 0 \tag{2.3}$$

where σ^2 is the time-average power of the received signal before envelope detection.

Rayleigh fading is suitable for a communication environment in which there is no line of sight between the transmitter and receiver and many objects attenuate, reflect, refract and diffract the signal. In case that there exists a dominant signal, usually the one in line of sight, Ricean model is a better estimation. Ricean fading is denoted as

$$p(y) = \frac{2y}{\sigma^2} e^{-\frac{y^2+A^2}{2\sigma^2}} I_0(\frac{Ay}{\sigma^2}) \tag{2.4}$$

where A denotes the peak amplitude of the dominant signal and $I_0(\cdot)$ is the modified Bessel function of the first kind and zero-order.

2.2 Network Architecture and Protocol Stack

A wireless ad-hoc/sensor network consists of a number of wireless devices (also called nodes) sharing the same radio interface, thus working in packet-delivery mode. The devices are usually mobile in an area and operated by battery power. The communication between the nodes can be either point-to-point, multicast, or broadcast. The type of communication data can be any format, such as real-time sensed information (in small amount), non-realtime files/databases (in large size), realtime audio or video (in streamed format), etc. Because of the limit of radio signal propagation distance and the purpose of efficiently reusing the radio resource, a wireless ad hoc/sensor network usually works in multihop mode. In

an ad-hoc network, communications between the nodes are distributed and balanced, i.e., communication may happen between any two nodes; whileas a wireless sensor network is usually data-collective and thus unbalanced, i.e., sensed data is collected by one or several data sinking nodes. The sinks can be located at the edge or in the middle of the network, or totally random. The number of nodes in wireless sensor networks is usually much greater than their ad-hoc counterparts.

The protocol stack of such a network usually follows the OSI (Open System Interconnection) 7-layer model, as shown in Figure 2.1. However, the lower layers are specialized in order to cope with wireless communication features. Especially, the MAC sublayer copes with radio interface collision problem and the network layer copes with multihop routing problem.

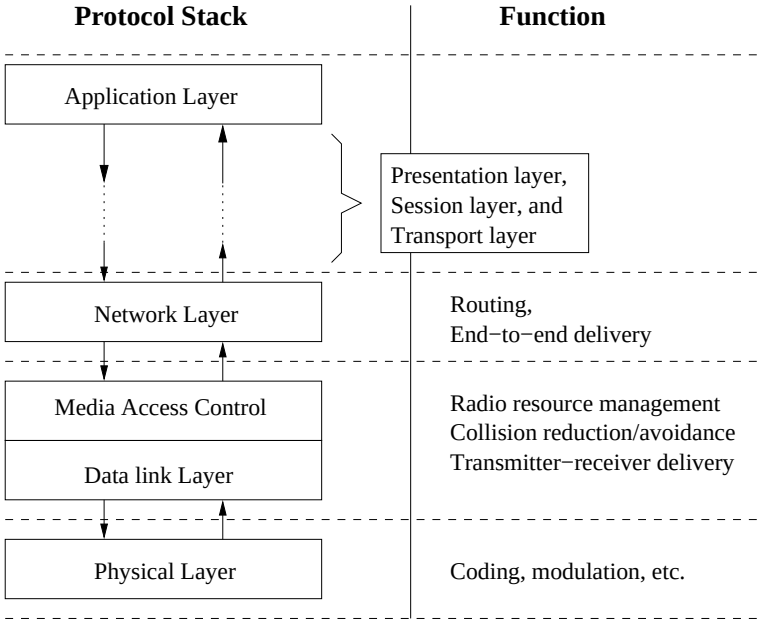

Figure 2.1: Wireless ad hoc network protocol stack and functions of layers.

2.3 Media Access Control

Media Access Control (MAC) is a sublayer at layer 2 of OSI 7-layer model. MAC protocol must be deployed when a group of communication devices is sharing the same physical medium. In wireless ad-hoc/sensor networks, MAC protocol design is not a trivial issue. On one hand, we must consider the functionality of MAC protocol, i.e., to avoid collisions when two or more nodes have data to transmit at the same time; on the other hand, MAC layer design should also consider 1) the

energy efficiency of the network, because MAC signaling is considered as overhead of the communications, and 2) the fairness, because every node should have the same opportunity to access the channel.

Cellular mobile systems usually use a scheduleling-based MAC protocol, because in cellular systems the infrastructure can allocate/schedule the radio resource to the mobile devices in its service area. Typical scheduling-based techniques include FDMA (Frequency-Division Multiple Access), TDMA (Time-Division Multiple Access), and CDMA (Code-Division Multiple Access). In a scheduling-based system, the collision of communication is totally avoided. However, in wireless self-organized networks, since there is no infrastructure that can schedule the communication, distributed processes have to be deployed to make the nodes schedule the communication by themselves. This makes scheduling techniques not very favorable in wireless self-organized networks.

Another class of MAC protocols is based on random access. The simplest and most fundamental random access MAC protocols for wireless networks are ALOHA and slotted-ALOHA. A mobile node using ALOHA starts the transmission immediately when it has data to send. In a slotted-ALOHA network, the whole network is synchronized by time slots. A node that has data to send waits for the beginning of next time slot. Both ALOHA and slotted-ALOHA protocols have no mechanism to prevent collisions. If the transmitted data packet collided, the dedicated receiver cannot send back an acknowledgement (ACK) and the sending node will retransmit after its ACK waiting timer expires.

A more sophisticated MAC protocol used in wireless self-organized networks is CSMA/CA (Carrier Sense Multiple Access with Collision Avoidance). In CSMA/CA, a node first senses the radio channel (the carrier) for a period; if the channel is free the node sends the packet, otherwise it backs-off the transmission with a random period to avoid collision. CSMA/CA is adopted as IEEE Wireless LAN protocol in IEEE 802.11b standard (IEEE 1999). A modified CSMA/CA protocol with synchronization features is applied in IEEE Wireless Personal Area Network (WPAN) standard IEEE 802.15.4 (IEEE 2003).

Many more MAC protocols are proposed for energy efficiency and/or throughput improvement, such as PAMAS (Singh & Raghavendra 1998), S-MAC (Ye, Heidemann & Estrin 2002), T-MAC (van Dam & Langendoen 2003), and X-MAC(Buettner, Yee, Anderson & Han 2006). A modified CSMA protocol known as CSMA/CF (Collision Freeze) aimed to solve hidden node problem for IEEE

802.15.4 beacon-based WSN is proposed in (Sheu, Shih & Lee 2009). A hybrid Z-MAC (Zebra-MAC) proposed in (Rhee, Warrier, Aia, Min & Sichitiu 2008) for WSN tries to borrow the advantages from both random access methods and TDMA methods. There are also some MAC proposals that involve either multi-channel radio or smart antenna. Some of these aforementioned protocols are shortly illustrated in 2.3.3.

2.3.1 CSMA/CA

CSMA was first proposed in (Kleinrock & Tobagi 1975). In this protocol, a node senses the wireless channel for ongoing transmissions before sending a packet. If the channel is already in use, the node sets a random backoff timer and then waits this period of time before re-attempting the transmission. On the other hand, if the channel is not currently in use, the node begins transmission. A flaw of this version CSMA is the hidden node problem(Tobagi & Kleinrock 1975), as illustrated in Figure 2.2(a). In the figure, nodes A, B, and C are seperated in distance so that nodes A and C cannot hear each other. When A is transmitting to B, C cannot sense the transmission and thus starts its own transmission at the same time. The result is that collision occurs on B.

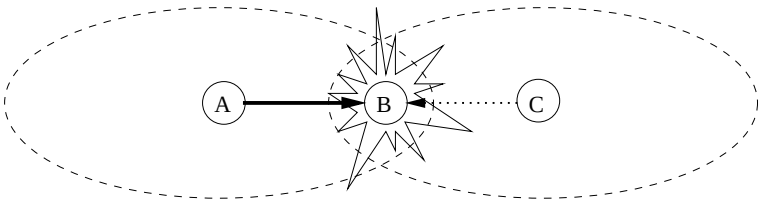

a) Hidden node C causes collision at B

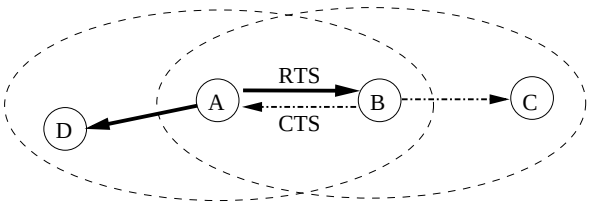

b) RTS−CTS handshake deffers C's transmit

Figure 2.2: Hidden node problem with CSMA and the RTS/CTS solution

An elaborated version of CSMA is called MACA (Multiple Access with Collision Avoidance) (Karn 1990). MACA defines Request-To-Send (RTS) and Clear-To-

Send (CTS) control packets to announce an upcoming data transmission. A node wishing to send a data packet broadcasts a RTS message containing the length of the data frame that will follow. Upon receiving the RTS, the receiver responds by broadcasting a CTS packet which also contains the length of the upcoming data frame. Any node hearing either of these two control packets must be silent long enough for the data packet to be transmitted. In this way, neighboring nodes will not transmit during the data transmission, and the probability of collision is reduced. An example of RTS/CTS solving hidden node problem can be seen in Figure 2.2(b).

CSMA/CA is adopted by IEEE 802.11 as Wireless Local Area Network (WLAN) MAC protocol with slight modifications, and known as CSMA/CA with Distributed Coordinate Function (DCF). In IEEE 802.11 CSMA, first the transmission of data packet must wait DIFS (DCF Interframe Space), and the transmission of ACK must wait SIFS (Short Interframe Space). Second, in IEEE 802.11 MAC, an ACK (Acknowledgement) frame is sent from destination back to source when the receiver has correctly received the packet.

It is worth noting that CSMA/CA without RTS/CTS and CSMA/CA with RTS/CTS (i.e., MACA) can work together in one network. In IEEE 802.11 specification, both of these schemes are adopted.

The mechanism of IEEE 802.11 MAC is shown in Figure 2.3. In the figure, the node wishing to transmit (Src node) first waits for DIFS time, and keeps sensing the channel during DIFS. If no channel activity has been dectected, the node sends a RTS frame. If the receiver (Dst) node can hear this RTS, it differs SIFS time before sending the CTS frame back. After the reception of the CTS, the sending node differs also SIFS time before sending the data frame. The Dst node differs another SIFS time between the end of receiving Data frame and the start of sending ACK frame. DIFS is necessary for the RF transceiver to switch between transmitting and receiving modes.

IEEE 802.11 introduced a timing information called Network Allocation Vector (NAV), which is embedded into both RTS and CTS frames. Because frame size of RTS and CTS is fixed, and SIFS is also a fixed value, a sending node is able to calculate the time that how long the channel will be occupied by the upcoming

transmission, including all the interframe spaces, denoted as:

$$NAV_{RTS} = SIFS + T_{CTS} + SIFS + T_{data} \tag{2.5}$$

where $T_{data} = L_{data}/R$, is the time of sending the data frame. L_{data} and R are the data frame length in bits and the transmitting rate in bit per second, respectively. T_{CTS} is the transmitting time of CTS frame.

The receiver calculates another NAV after the receiving of RTS, and puts it into the CTS frame. It is denoted as

$$NAV_{CTS} = NAV_{RTS} - SIFS - T_{CTS} \tag{2.6}$$

The nodes that have heard the RTS and/or the CTS thus are informed that the channel will be occupied during NAV time, as shown in Figure 2.3. So they can devote themselve into other activities rather than keeping sensing the channel during the this time. A common use of NAV is to put these nodes into sleep mode to save energy (Ye et al. 2002, van Dam & Langendoen 2003).

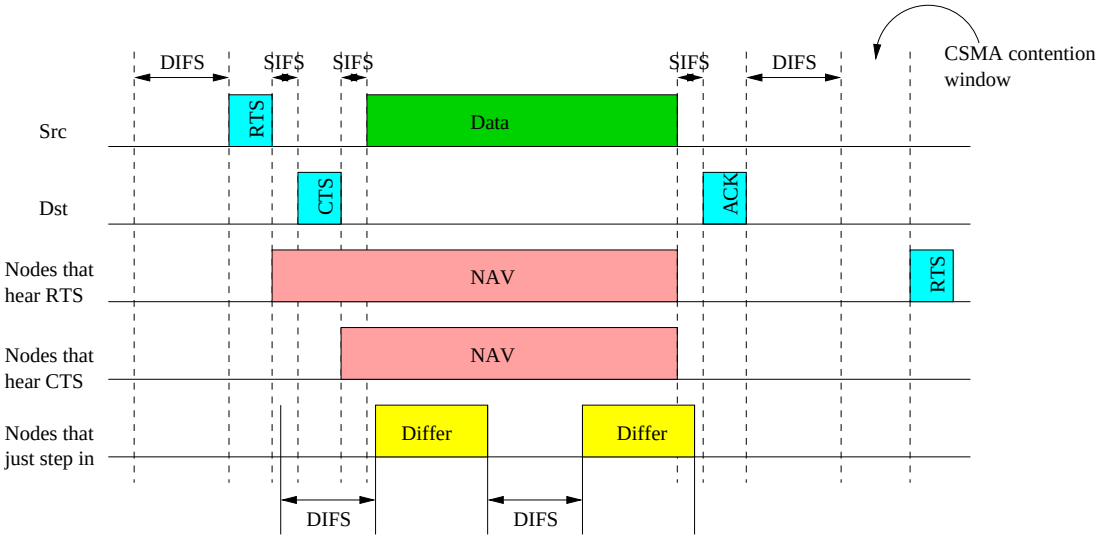

Figure 2.3: IEEE 802.11 MAC with DCF

In order to cope with multiple transmitter problem, i.e., a number of nodes intending to send at the same time, and one must note that this number is dependently variable, CSMA/CA uses a Binary Exponential Backoff (BEB) algorithm to set the contention window before DIFS sensing. The contention window (as shown in Figure 2.3) is divided into a number fixed length time sections denoted as *time slot*. Each node, after sensing the channel for DIFS time will set a random

number μ uniformly distributed in $[0, CW - 1]$, where $CW = CW_{min}$ at the first transmission attempt.

The sending node counts down the generated random number and monitors the channel at the end of each time slot. When CW reaches zero and the channel is still idle, the node sends the DATA frame (in the case without RTS/CTS) or the RTS frame (in the case with RTS/CTS handshake). If at the end of one time slot the channel is sensed occupied, the node will halt the counter, and continues the decrement when the channel is free again.

CW doubles by the following equation when the current attempt is failed, i.e., the channel is busy when μ counts to zero:

$$CW = \min[2 \cdot CW, CW_{max}] \tag{2.7}$$

After a sucessful transmission, CW will be reset to CW_{min}.

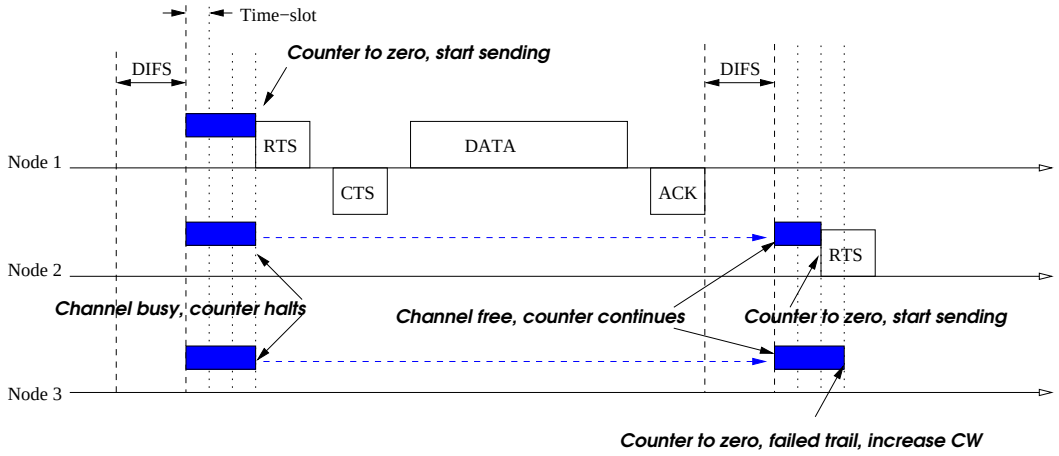

Figure 2.4: IEEE 802.11 Binary Exponential Backoff

Figure 2.4 shows an example of three nodes competing for the channel using BEB. In the figure, node 1 caputres the channel first; nodes 2&3 halt their backoff counter and continue after node 1's transmission has finished. Then, node 2 captures the channel due to a smaller random number generated; and node 3 finds the channel is still busy when its counter counts to zero and uses BEB to increase its CW. BEB is a heuristic algorithm to increase the efficiency of channel utilization and gives fairness to the nodes (G.Bianchi 2000). However, Song, Kwak, Song & Miller (2003) argue that an exponential increase with exponential decrease backoff algorithm will give better throughput to the network.

IEEE 802.11 also supports an infrastructure mode of WLAN, in which user nodes

are associated with one or more infrastructure nodes called Access Point (AP). In a small network, one AP is enough to cover all the user nodes and this mode is called Basic Service Set (BSS). In case the user nodes are scattered and a number of APs are deployed to support them, then it is called Extended Service Set (ESS). In ESS mode, different frequency channels have to be allocated to adjacent APs in order to avoid collision, and handover mechanism must be invoked to cope with node mobility. Figure 2.5 shows the examples of BSS and ESS respectively.

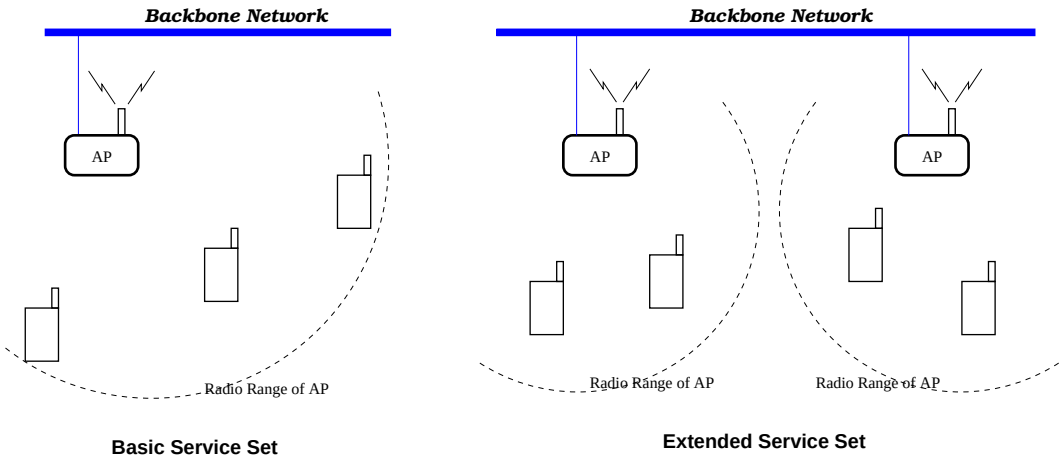

Figure 2.5: IEEE 802.11 infrastructure modes

In the infrastructure mode, there is an enhanced Point Coordinate Function (PCF) designed for access points. An AP running in PCF mode is able to control the channel access by deploying a Collision-Free Period (CFP), in which the AP uses a polling protocol to allocate access time for different user nodes. PCF mode enables throughput control for each individual user node.

2.3.2 S-MAC for WSN

As mentioned in previous sections, WSN shares many common features with MANET. However, they are specialized by their own characteristics, such as larger network size in node number, more energy-constrained, unbalanced communication pattern, usually unattended after the deployment, etc.

There are a number of MAC protocols proposed for WSN. Among them the Sensor-MAC (S-MAC) protocol (Ye et al. 2002) and its extensions have received excessive attentions.

S-MAC is highlit by the following features:

1. Energy saving by periodic sleeping and listening

2. Synchronization and Scheduling with neighbors

3. Passive clustering by scheduling

In a network that S-MAC is applied, neighbor nodes are synchronized by exchanging *timestamps*, or SYNC packets. A SYNC contains a *schedule* that will be executed by the sending node. A node that has received a SYNC is able to follow this schedule, i.e., synchronized with the sender. All timestamps exchanged are relative rather than absolute, i.e., only between the transmitter and the receiver. All the nodes periodically wake up and listen to the channel, and the listen period is significantly longer than clock error or drift.

When a node is powered on, it first listens to the channel for a certain moment of time. If it has not heard a schedule from another node at end of this phase, it then chooses a random sleep time and immediately broadcasts its schedule in a SYNC message. A node that has received a schedule from a neighbor will follow that schedule by setting its schedule to be the same. If a node receives a different schedule after it has selected and broadcast its own schedule, it adopts both schedules. Virtually, the whole network is passively clustered by the nodes that broadcast the SYNC messages. A network forming/scheduling scenario example can be seen in Figure 2.6. In this example, nodes B and D took the channel and broadcast their SYNCs ahead of other nodes, thus are passively raised as cluster heads. Node C has heard SYNC message from both B and D, as shown in the example, will follow both schedules.

As shown in Figure 2.6, the S-MAC protocol applies a sleep mode to save energy. In each period of SYNC broadcasting, The scheduled nodes wake up for two time phases: a phase that a new SYNC schedule may come from the cluster head, and a phase for communications, with the second phase right follows the first one. In the second phase, the nodes who wish to send data message will broadcast RTS in CSMA/CA fashion, shown as blue-colored time regions in the figure. Note there may be multiple potential senders, thus a contention-based CSMA with RTS/CTS is applied in this phase. After the second phase, only the nodes involved in the current communication (i.e., the senders and intended receivers) remain awaken. The other nodes in this cluster will turn off their radio and go into the sleep mode.

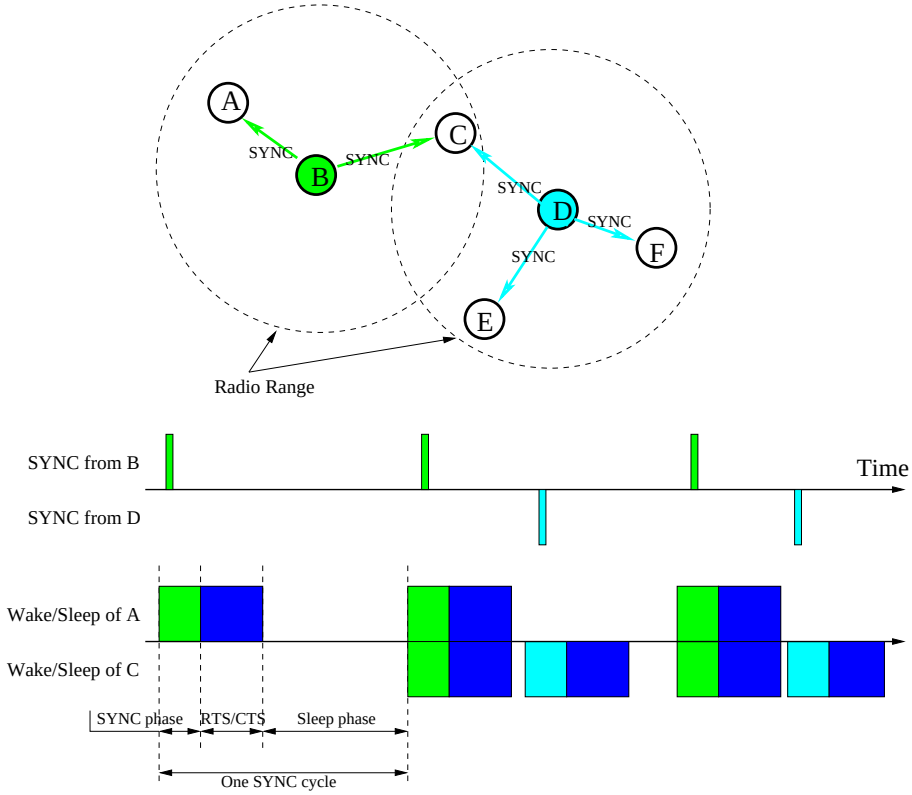

Figure 2.6: A network forming/scheduling example using S-MAC protocol

2.3.3 Other MAC protocols for WSN

T-MAC (van Dam & Langendoen 2003) is an improved version of S-MAC. In T-MAC, the length of awake period is reduced by listening to the channel for only a short time after the synchronization phase. If no data is received during this awake window, the node returns to sleep mode; if data is received, the node remains awake until no further data is received or the awake period ends. The trade-off of shorten the awake period is the reduction of throughput and increament of latency.

Both S-MAC and T-MAC are synchronous duty-cycled MAC protocols, in which the nodes are (locally) synchronized by exchanging SYNC schedules periodically. Such an awake-sleep duty-cycle increases the latency of communication which is proportional to the sleep duty-cycle, by which the energy efficiency relies on. Based on this consideration, some asynchronous approaches are proposed. A highlit one of these asynchronous protocols is known as X-MAC(Buettner et al. 2006).

X-MAC is an asynchronous protocol so that the energy overhead for synchroniza-

tion is eliminated. All the nodes in a network chooses their own sleep schedule. When a node has data to send, it sends out *short preambles* periodically. Each short preamble contains receiver's address. The dedicated receiving node wakes up by its own sleep schedule, and keeps the awaken time longer than one period of short preamble to guarantee that a preamble will be heard. The receiving node sends back an *early ACK* immediately after a preamble is received. By receiving this early ACK, the sending node will send the data frame. The mechanism of X-MAC is illustrated in Figure 2.7 with comparison to *long preamble* Low Power Listening (LPL) solution.

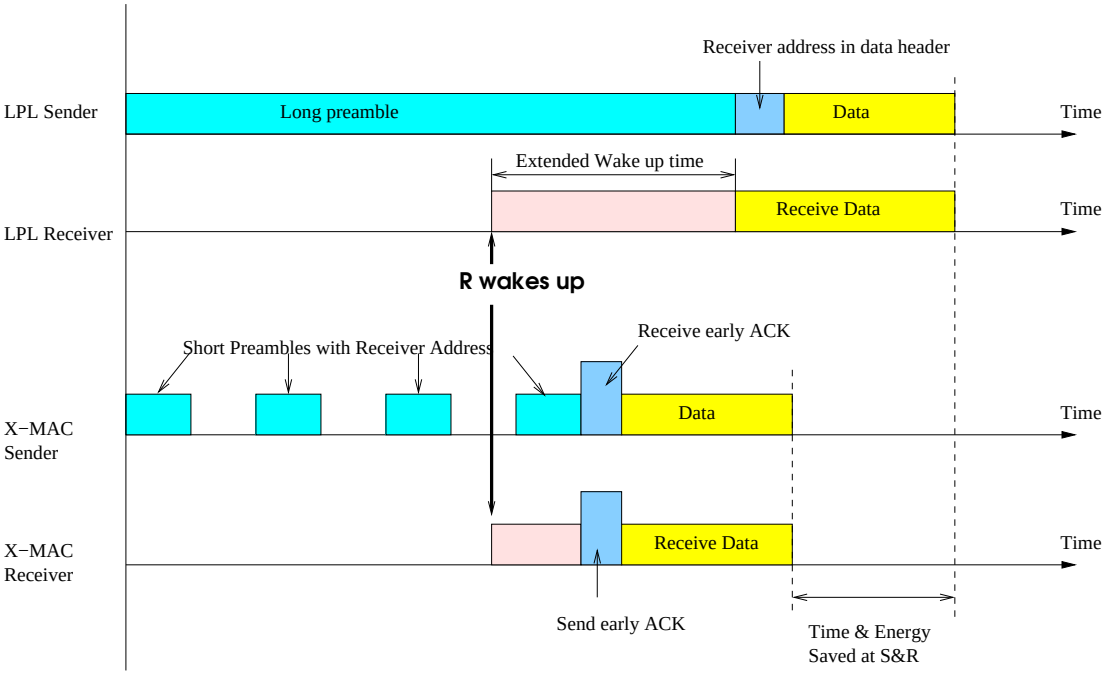

Figure 2.7: Comparison of the timelines between LPL and X-MAC

(Rhee et al. 2008) propose a hybrid MAC protocol named Z-MAC for WSN. This protocol combines both CSMA/CA and TDMA for high channel utilization under heavy traffic situations and latency reduction. In Z-MAC, first an efficient scalable channel-scheduling algorithm DRAND(Rhee, Warrier, Min & Xu 2006) is deployed and by which each node will be allocated one time slot by marking the ownership of that slot. The owner of a time slot has higher priority to access the channel, which can be achieved by minimizing the contention window of CSMA. However, if the owner of the current time slot has no data to send, other nodes can *steal* this time slot by CSMA contention with the contention window size set larger than that of the owner.

(Sheu et al. 2009) proposed a MAC protocol known as CSMA/CF for IEEE

802.15.4 beacon-based multihop networks. The protocol aims to cope with hidden node problem in such networks. In order to achieve the goal, the RF transceivers are demanded to perform *capture effect*[1]. When a collision has been detected but the early-arrived frame header has been successfully decoded, the receiving device (the coordinator) will schedule the retransmission of the first frame into Collision-Free Period (CFP) of the next beacon interval and inform the sending node by the next beacon frame. CSMA/CF can significantly improve the throughput and reduce the average access delay in dense networks. By reducing the retransmission attempts, the protocol is also more energy efficient.

2.4 Network Layer and Routing

Routing in multi-hop MANET/WSN is a function to find one or more routes from the source node to the destination node. All the intermediate nodes on a selected route must be aware to forward packets to the next one, until the packets reach the destination node. Routing protocol in the network layer plays an important role in energy conservation. A well-designed ad hoc routing protocol will improve the energy efficiency of the network in following ways:

1. The route-finding packets are overheads of communication. This requires the reduction of packet length and the amount of occurances, thus will reduce the power consumption.

2. In a given network topology, there exists an optimal route, along which minimum energy consumption can be achieved.

3. A better route will suffer less congestions so that the chance of retransmission is reduced.

4. A node with poor battery residual shall not participate in routing, if there are substituting nodes available.

[1]A function that enables the receiver to decode the un-collided part of the early-arrived frame. In IEEE 802.15.4 it is frame header part, which contains frame control and address data.

2.4.1 Routing in MANET

Basically there are three categories of routing protocols proposed for ad-hoc networks: proactive, reactive, and the combination of these two.

2.4.1.1 Proactive and Reactive Routing

Proactive routing attempts to maintain routes to all destinations at all times, regardless of whether they are needed. To support this, every node propagates information updates about a network's topology or connectivity throughout the network. This propagation must be done periodically because the node mobility will make the connectivity information out of date. Destination-Sequenced Distance Vector (DSDV) routing (Perkins & Bhagwat 1994) is an example of proactive routing protocol. In contrast, reactive or on-demand routing protocols determine routes only when there is data to send. If a route is unknown, the source node initiates a search to find one, which tends to cause a traffic surge as the query is propagated through the network. Nodes that receive the query and have a route to the requested destination respond to the query. Typical reactive routing protocols include Ad-hoc On-demand Distance Vector (AODV) (Perkins & Royer 2001) and Dynamic Source Routing (DSR) (Johson, Maltz, Hu & Jetcheva 2001).

The advantages of proactive routing include:

1. Every node in the network has the full topology information of the network. This decreases the time of finding a route.

2. Full topology information also helps the nodes to select optimal route in terms of latency, energy efficiency, or stability.

However, because proactive routing protocols need to periodically broadcast connectivity information throughout the whole network, even though no data transmission is going on, this increases the cost of routing overheads. This disadvantage is exaggerated in wireless sensor networks, because in these networks the communication usually occurs far less frequently than that of ad-hoc networks, thus resulting more severe energy loss by routing protocol.

The advantages of reactive routing is the reduction of network overhead. The

routing overheads are sent only when there is data need to be transmitted. The disadvantage of reactive routing include:

1. The time to find a route is longer than that of proactive schemes.
2. Because the route finding packet is broadcast throughout the whole network in a flooding fashion, reactive routing schemes usually generate a so-called "flooding storm" which impacts the data transmission during the routing time.
3. It is more difficult to find an optimal route by reactive routing.

2.4.1.2 Ad-hoc On-demand Distance Vector Routing

AODV is the most popular routing protocol accepted by ad hoc network researchers. AODV is the first routing protocol proposed by IETF (The Internet Engineering Task Force) as the standard routing scheme for mobile ad-hoc networks (Perkins & Royer 2001) and IEEE 802.15.4 standard (IEEE 2006). Since AODV is used in our research as the default routing protocol, here we give an elaborated description of its mechanism.

AODV is a reactive routing protocol, which means that a route is established on fly whenever a node has data destined to another node. In AODV, each node has a *route table* in which a route to a destination node is held as a piece of record. A piece of record contains following information:

1. Destination node identity
2. Next hop node identity
3. The number of hops to the destination
4. A sequence number used for route updating

When a node S has data packet(s) to send to another node D, it first checks its route table. If the D's identity cannot be found in the table, node S starts a route finding procedure by broadcasts a Route REQuest (RREQ) message. Every neighbor of S that has received the RREQ will look up its route table for D. If D is not in table, the node broadcasts the RREQ again and record this RREQ

and the precursor node in its local buffer. The RREQ is rebroadcast in such a way until it reaches D or a node that has a route to D. In this case either D or the node that has a route to D will send a Route REPly (RREP) message back to its precursor node. Upon the reception of RREP, the intermediate nodes and source node will put a route entry to the destination into the route table. This procedure is illustrated in Figure 2.8.

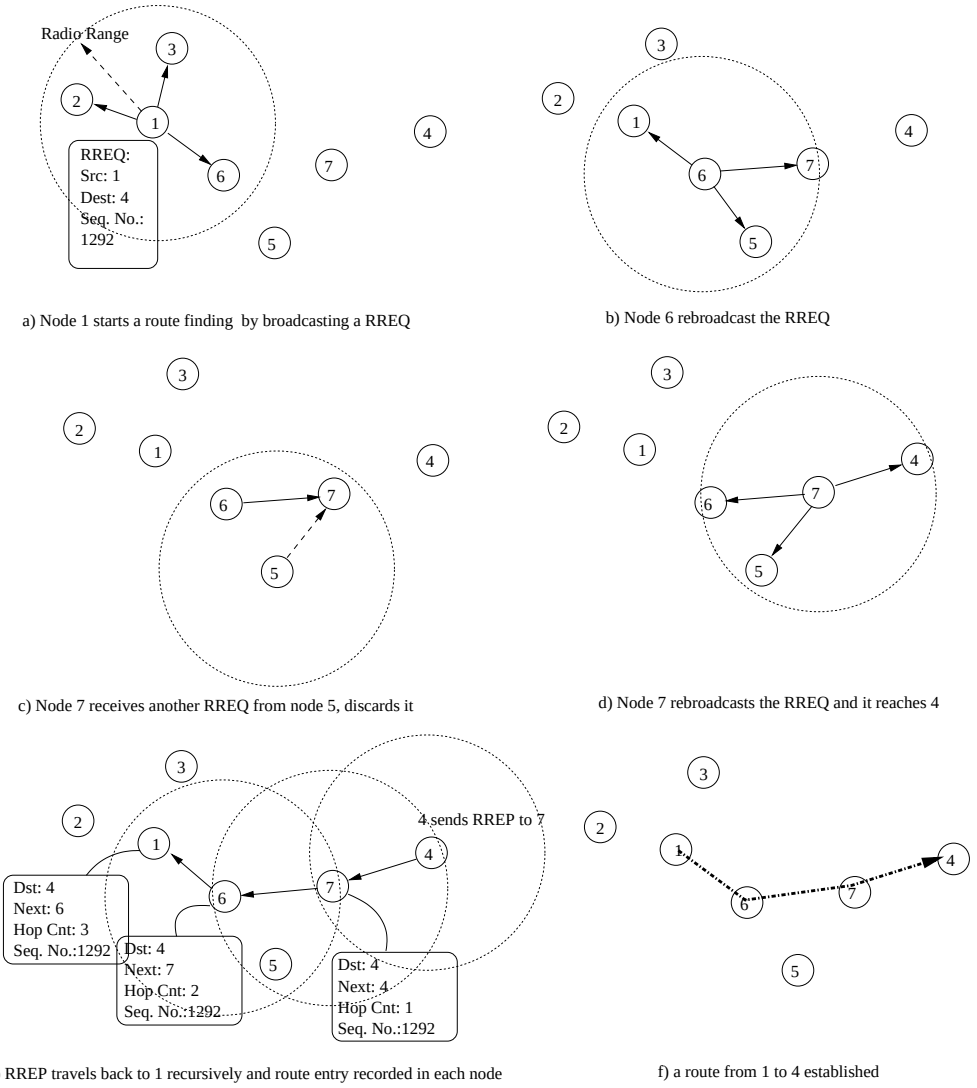

Figure 2.8: AODV routing procedure

A number of works have been concentrated on improving AODV for different aspects, inlucding Multirate Ad-hoc On-demand Distance Vector Routing Protocol (MR-AODV) (Guimaraes & Cerda 2007), Reliable Ad-hoc On-demand Distance Vector Routing Protocol R-AODV (Khurana, Gupta & Aneja 2006), Ant Colony Optimization and Ad-hoc On-demand Multipath Distance Vector (ACO-

AOMDV) (bing Wang, zhao Zhan, min Wang & ping Jiang 2008), etc.

2.4.1.3 Energy-Efficient Routing

Energy efficient routing have been extensively studied. Singh, Woo & Raghavendra (1998) present a detailed discussion of energy efficient route optimization. There are basically two ways to improve energy efficiency in routing protocols:

- **Minimizing energy consumption over a route.** The idea of such a routing protocol is to find a path from the source to the destination that delivering of packet(s) through this route cost minimum energy. Usually those distance vector routing protocols are aimed to this purpose.

- **Maximizing lifetime of the network.** A routing protocol aimed for this purpose does not focus on the energy consumption over a route, instead, it focuses on the balancing of battery resource of all the nodes involved in the routing procedure. More sophisticated algorithms also consider other balancing metrics such as the amount of traffic a node has dealt with, the location of nodes, etc.

- **Minimizing the routing overhead**. Overhead of routing protocol include topology exploration packets, route request broadcasting packets, route maintainence packets, neighbor greeting packets, etc. They are necessary to cope with mobility of the nodes or topology change caused by node power-down or additions.

2.4.2 Routing in WSN

Energy-efficient routing for WSN differs from tranditional routing protocols for ad-hoc networks. Tranditional ad-hoc routing algorithms focus more on avoiding congestion or maintaining connectivity when faced with mobility (Broch, Maltz, Johnson, Hu & Jetcheva 1998), and usually the communications is end-to-end fashion, address-centric. On the contrary in WSN, the communications is more data-centric, many-to-one fashion, and energy constrained. (Krishnamachari, Estrin & Wicher 2002). Also, since sensor nodes are resource poor, and number of nodes in the network could be very large, sensor nodes cannot afford the storage

space for "huge" routing table. Therefore reactive and hybrid routing protocols are attractive in sensor networks.(Singh, Vyas & Tiwari 2008)

The concept of *data-centric* is based on the following features of WSN:

1. Global address is not feasible (too many nodes and frequent removals/affiliations)
2. Data query is often region-based.
3. Data is usually transmitted from every sensor node within the deployment region with significant redundancy. Thus local data with high redundancy must be processed and combined before being sent to sink.

Based on this concept, a number of routing protocols for WSN have been proposed, such as SPIN (Sensor Protocols for Information via Negotiation) (Heinzelman, Kulik & Balakrishnan 1999), Directed diffusion (Intanagonwiwat, Govindan, Estrin, Heidemann & Silva 2003), Rumor Routing (Braginshhy & Estrin 2002), Gradient-based Routing (Schurgers & Sribastava 2001), Minimum Cost Forwarding Algorithm (MCFA) (Ye, Chen, Liu & Zhang 2001).

Some research focus on energy efficiency of WSN. These include Reliable Energy Aware Routing Protocol (REAR) (Shin, Song, Kim, Yu & Mah 2007), Pairs Energy Efficient Routing protocol (PEER) (Elshakankiri, Moustafa & Dakroury 2008), Reliable and Energy Effcient Protocol (REEP) (Zabin, Misra, Woungang, Rashvand, Ma & Ahsan Ali 2008) and many other solutions.

2.4.2.1 Case Study: SPIN

SPIN is a family of data-centric protocols proposed by (Kulik, Henzelman & Balakrishnan 2002). In SPIN, it is assumed that all nodes in the network are potential sinks, and sensed data is described by a high-level name called *meta-data*. Nodes running SPIN assign a high-level name to completely describe their collected meta-data and perform meta-data negotiations before the transmissions. This guaranttees that no redundant data is send throughout the network.

The SPIN family of protocols use three messages for communication:

- ADV : When a SPIN node has some new data, it sends an ADV message to its neighbors containing meta-data(data descriptor)

- REQ : When a SPIN node wished to receive some data, it sends an REQ message.
- DATA : These are actual data messages with a meta-data header.

An example of SPIN can be seen in Figure 2.9. In this example, node A has sensed some data and announces (broadcasts) by an ADV message. Upon the reception of this ADV, node B may send back a request so the sensed data can be delivered to B. Node B can announce that it has received such a meta-data so that its neighbors may be interested. The interested nodes may send REQ to fetch the data. However, if B is not interested of A's data but B's neighbors are, steps (4) and (5) may happen earlier than steps (2) and (3). From this example it can be seen that 1) information is delivered on request, 2) minimum routing overhead is achieved, and 3) routing is data-centric instead of address-centric.

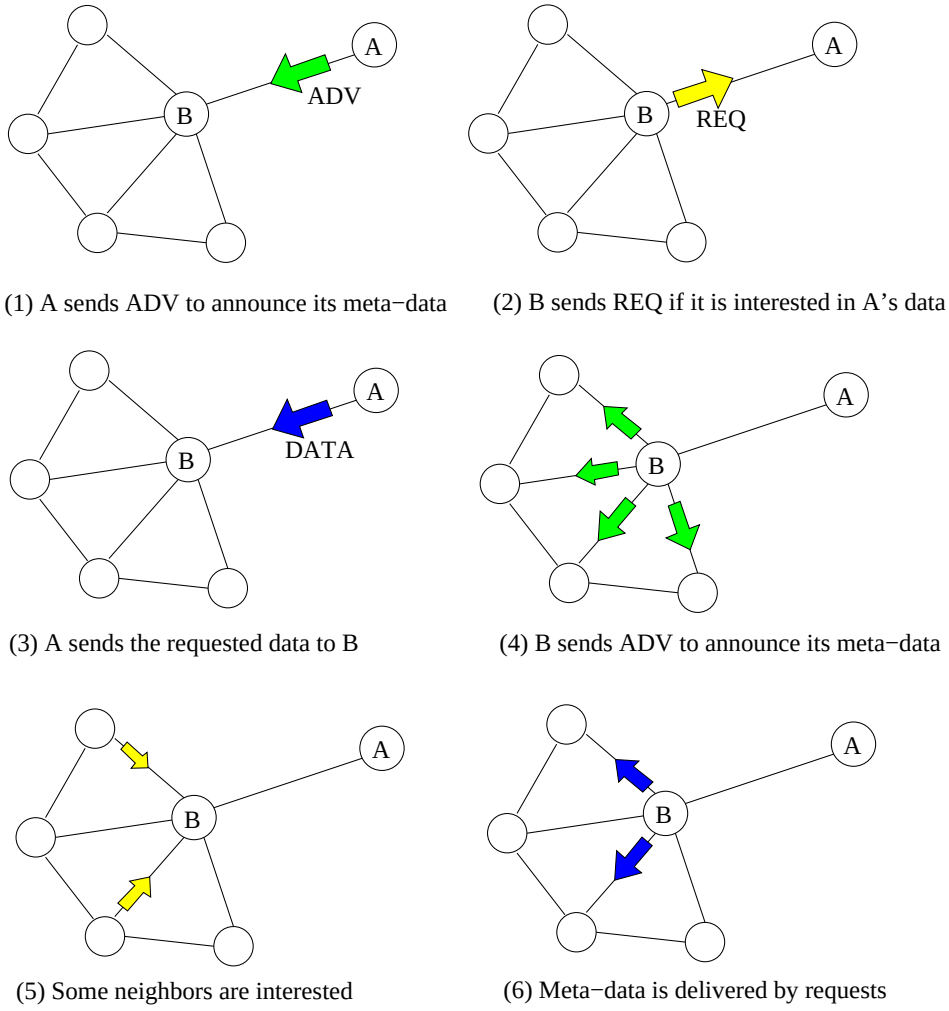

Figure 2.9: SPIN protocol

2.4.2.2 Case Study: LEACH

Low-Energy Adaptive Clustering Hierarchy (LEACH) (Handy, Haase & Timmermann 2002) is one of the most popular hierarchical routing algorithms for WSN. The idea is to form clusters of the sensor nodes based on received signal strength and use local cluster heads as routers to the sink.

The operation of LEACH is separated into two phases: the setup phase and the steady phase. In the setup phase, the clusters are organized and cluster heads are selected. In the steady state phase, the actual data transfer to the base station takes place. Cluster-heads can stochastically be chosen by:

$$T(n) = \frac{P}{1 - P \times \left(r \mod \frac{1}{P}\right)}, \quad \forall n \in G \tag{2.8}$$

$$T(n) = 0, \quad \forall n \notin G \tag{2.9}$$

with P as the cluster-head probability, r as the number of the current round and G as the set of nodes that have not been cluster-head in the last 1/P rounds. Each node n determines a random number between 0 and 1. If the number is less than $T(n)$, the node becomes a cluster-head for the current round.

An approach to increase the lifetime of LEACH-network is to include the remaining energy level available in each node. The threshold $T(n)$ is modify by:

$$T(n)_{er} = \frac{P}{1 - P \times \left(r \mod \frac{1}{P}\right)} \times \frac{E_{n\_current}}{E_{n\_max}} \tag{2.10}$$

However, $T(n)_{er}$ in 2.10 will eventually decrease to a certain value so that the cluster-head election fails, because of the presence of the second part in the equation. A solution to this is to add a factor that increases the threshold for any node that has not been clusterhead for the last $1/P$ rounds:

$$T(n)'_{er} = \frac{P}{1 - P \times \left(r \mod \frac{1}{P}\right)} \times \left[\frac{E_{n\_current}}{E_{n\_max}} + \left\lfloor \frac{r_s}{P} \right\rfloor \left(1 - \frac{E_{n\_current}}{E_{n\_max}}\right)\right] \tag{2.11}$$

with r_s as the number of consecutive rounds the node has not been cluster-head, and $\lfloor\rfloor$ floor operation.

The modification can increase the network lifetime by 20-30%.(Handy et al. 2002)

LEACH is completely distributed and requires no global knowledge of network.

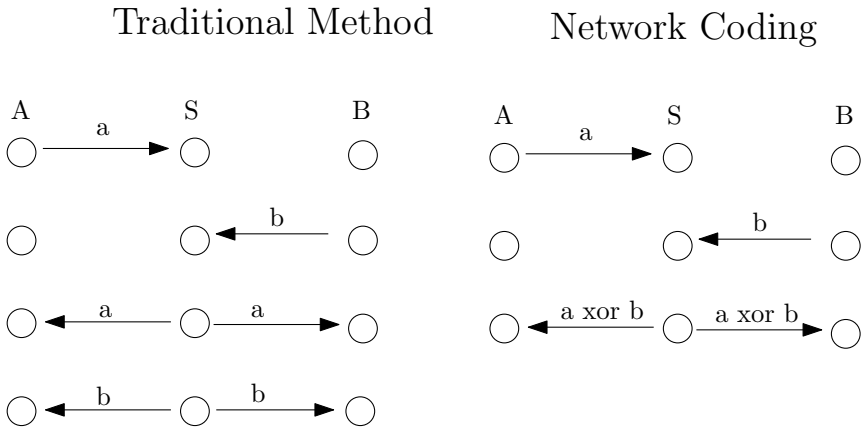

Figure 2.10: An example comparing Network Coding with Traditional Method

However, LEACH uses single-hop routing where each node can transmit directly to the cluster head and the sink. Therefore, it is not applicable to networks deployed in large regions.

2.4.3 Network Coding

Network Coding (NC) is a new research area that may have interesting applications in practical networking systems. With network coding, intermediate nodes may send out packets that are linear combinations of previously received information. There are two main benefits of this approach: potential throughput improvements and a high degree of robustness(Fragouli, Le Boudec & Widmer 2006).

A simple example shown in Fig. 2.10 illustrates the advantage of NC over tranditional communication method. In the example two nodes (A and B) needs to send a packet to each other via a relay (S). In traditional method, each packet is transmitted and relayed individually so that the whole procedure requires four steps to accomplish. Using network coding method, the two packets (a and b) are linearly combined (XOR is used in the example) and sent out by S, and nodes A and B are able to extract the data packet from the other source by subtracting the received packet from its own packet. The whole procedure takes only three steps.

Basically NC consists of two functions: encoding and decoding.

2.4.3.1 Encoding

Assume that a number of original packets $M^1, \ldots, M^n$ are generated by one or several sources in the network. In linear NC, each packet is associated with a sequence of coefficients $g_1, \ldots, g_n$ so that the combination is $X = \sum_{i=1}^{n} g_i M^i$. We call $g = g_1, \ldots, g_n$ *encoding vector* and the encoded data X *information vector*. Due to the linearity of combination, this encoding can be performed recursively, which means each node can generate a new encoded packet by a new *encoding vector* from an *infromation vector*.

2.4.3.2 Decoding

Assume that a node has received the set $(g^1, X^1), \ldots, (g^m, X^m)$. In order to retrieve the original packets, it needs to solve the system $\{X^j = \sum_{i=1}^{n} g_i^j M^j\}$. This is a linear system with m equations and n unknowns M^i. The system is solvable only in the case $m \geq n$, i.e., the number of received packets has to be larger than the number of original packets. And due to the fact that some combinations might be linearly dependent, $m \geq n$ is not sufficient. In practice, an efficient algorithm is to use random network coding. (Lim & Lee 1994) show that the probability of generating linearly-dependent combinations is negligible even with a sequence lenght of 8.

2.4.3.3 Applications

Network Coding has been applied to WSN in many aspects. Due to its nature, NC is very suitable in multicasting, data distribution, multipath routing, network lifetime improvement, etc. For multicasting applications one can refer to (Tan & Zou 2007, Goel & Khanna 2008),and (Shah-Mansouri & Wong 2008). (Oliveira & Barros 2008) applied NC to distribute secret key throughout a sensor network. (Wang & Lin 2008, Jardosh, Zunnun, Ranjan & Srivastava 2008) focus on buffer management and distribution of data in sensor nodes. (Geng, Lu, Liang & Chin 2008, Toledo & Wang 2006) applied network coding in multipath data delivery and routing.

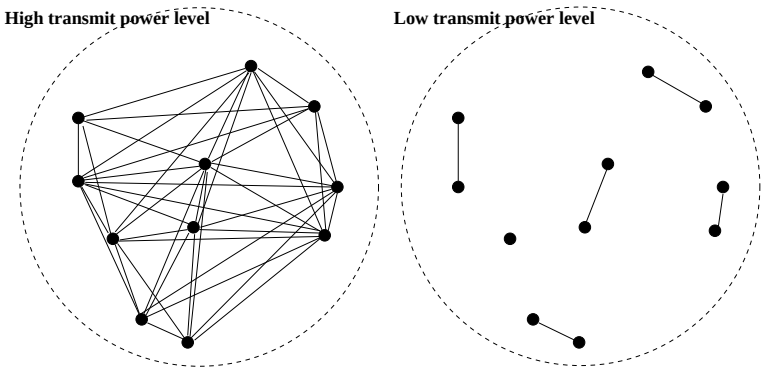

Figure 2.11: Connectivity results if the transmit power level is either too high or too low

2.5 Connectivity

Wireless transceivers can be designed to control the transmission power level. The power level of a node determines its neighbor node set, i.e., the nodes it can directly communicate with. Thus, different power levels of nodes generate different connectivity structures and topologies of the network. It is desirable to choose a low level transmit power in order to save energy and increase instantaneous throughput of the whole network. However, a low transmit power may cause the network partially or entirely disconnected. On the other hand, choosing a very high power level at all the nodes may cause the network totally congested at the radio interface and the energy cost is high. Figure 2.11 shows the connectivity results using different power levels.

In most literature, it is assumed that wireless nodes use omni-directional radio antenna and the coverage of radio signal is idealized as a circle centering at the node. Disc shaped connectivity model can be justified by referring to (Booth, Bruck, Cook & Franceschetti 2003), (Kwon & Gerla 2002), (Koskinen 2004), and (Yu & Li 2003) and a number of related works. However, some other authors argue that radio propagation characteristics must be considered, yielding the shape of radio coverage irregular.

3 POWER CONSUMPTION ANALYSIS OF WIRELESS NODE

3.1 Introduction

There are many MAC and network layer proposals for energy conservation for different MANET/WSN applications. However, energy consumption is a matter more related to the physical layer, especially to the circuit design of radio transceivers, therefore a thorough understanding of transceiver energy dissipation characteristics is necessary for practical energy-efficient upper layer protocol design.

In this chapter, we inspect the properties of radio transceiver circuits of wireless ad-hoc sensor node hardware from an energy consumption point of view. The energy consumption of transmitting, receiving, and sleeping states are calculated and compared. By the results of this inspection, we will analyse the energy-efficient protocols currently proposed for the wireless ad-hoc/sensor networks.

3.2 Structure and Power Properties of Radio Transceiver

A radio transceiver consists of two parallel parts: a transmitter and a receiver. The main difference of power consumption between transmitting and receiving locates at the physical layer, because upper layer functions, e.g., encoding/decoding, fragmenting/defragmenting, encrypting/decrypting, frame error generating/detecting, etc., are performed by logic processing devices such as a microprocessor, which nowadays are low power CMOS (Complementary Metal Oxide Semiconductor) ICs (Integrated Circuits). CMOS circuits consume much less power than that of TTL (Transistor-Transistor Logic) devices, which are used in air-interfacing circuits. In (Monks, Ebert, Wolisz & Hwu 2001), the authors

studied WLAN transceiver hardware and claimed that the power consumed at the MAC layer is less than 200mW whereas the physical layer circuits, especially the air-interfacing circuits, consume more than 1000mW of power. Secondly, the power consumed by these functions depends on the processing complexity, for a symmetrical duplex communication, digital processing complexity is almost equivalent for both transmit and receive.

Figure 3.1 shows a typical block diagram of an 802.11b Network Interface Card (NIC) transceiver circuits (MAXIM Semiconductor 2001). From the figure one can see that there are two function blocks that deffer from each other between the transmitter and receiver sections. The first different place is at the antenna interfacing: the transmitter applies a Linear Power Amplifier (LPA) whereas the receiver applies a Low-Noise Amplifier (LNA). Another distinguishing place is at the baseband processing block: the transmitter needs to convert the (modulated) digital signal into analog form, thus a Digital-to-Analog Converter (DAC) circuit is applied; the receiver needs to do the reverse function thus an Analog-to-Digital Converter (ADC) is required.

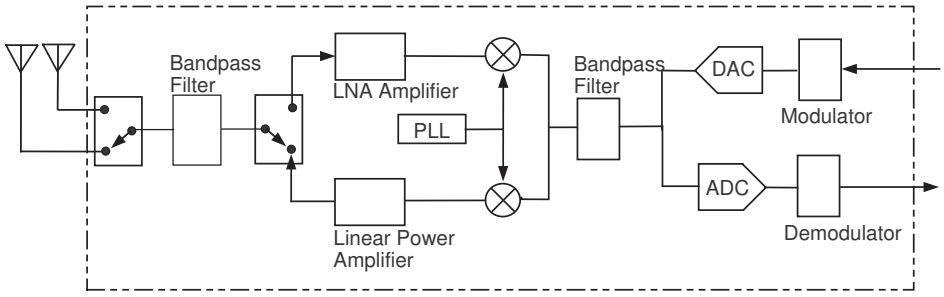

Figure 3.1: A typical WLAN transceiver block diagram

3.2.1 Amplifications

We can find that the power consumed by an LNA at receiver is lower than that of an LPA at transmitter. For example MAX2644 is a typical WLAN LNA IC. Its standard power consumption is 245mW. On the contrary, an LPA IC MAX2242 consumes approximately 900mW when the output power is 22dBm (MAXIM Semiconductor 2003). The reason is that the output of an LPA is used to drive an antenna circuit, which requires a necessary current value to radiate electromagnetic waves.

3.2.2 ADC and DAC

Take a look inside the ADC and the DAC circuits, we can find that the power consumed by a DAC is usually much lower than that of an ADC. For example, MAX1186 is a 10-bit ADC working at 40Msps (samples-per-second) with a typical power consumption of 105mW (MAXIM Semiconductor 2003). Analog Devices (Analog Device 2004) also offers a similar IC (part number: AD9203, 10-bit, 40Msps) with power dissipation of 108mW. Another Analog Devices product AD9050 working at +5V consumes power as high as 400mW.

For DAC, the power consumption is much lower. MAX5185 is a 10-bit DAC working at the same sampling rate as MAX1186. It consumes only 20mW of power (MAXIM Semiconductor 2003). The reason of this is that the structure of high-speed ADC circuit is much more complex than that of DAC circuit at the same sampling rate and quantization level. One should be aware that ADC/-DAC circuits are located in front of modulation/demodulation circuits, as shown in Figure 3.1, therefore if the modulation is an M-ary phase modulation such as DQPSK at 2Mbps or CCK at higher bit rates as specified by IEEE 802.11b, two sets ADC/DAC circuits are necessary for in-phase and quadrature-phase respectively. This will make the power consumption gap between ADC and DAC even bigger.

Table 3.1: 802.11b WLAN PC card power consumption

Manufacturer	**Product**	**Tx Power**	**Rx Power**
InstantWare	NWH1610	500mA	300mA
Proxim Co.	ORiNOCO	600mA	330mA
Socketcom	N/A	170-280mA	N/A
BreezeCom	SA-PCR	360mA	285mA
Cisco	Cisco352	450mA	270mA
Fujitsu/Siemens	E-1100	285mA	185mA
Average	—	403mA	274mA

Overall, for a typical WLAN transceiver, the amplification of transmitter consumes more energy than that of the receiver. The difference is about 500-600mW when the transmitter gives maximum output. The reception process consumes more energy at the ADC circuits, comparing to the DAC of the transmitting. The difference is between 100mW to 700mW depending on the detail circuit design. This result explains that most present WLAN products have the same level

of power consumption for transmitting and receiving. Table 3.1 lists the power consumption feature of some WLAN products. On average the receive power consumption is 68% of the transmit power consumption. (Veijalainen, Ojanen, Haq, Vahteala & Matsumoto 2002) show that similar results hold in GSM terminals.

3.2.3 Hardware Architecture of Sensor Node

As shown in Figure 3.2, a wireless sensor node usually consists of four sub-systems, namely computing subsystem, communication subsystem, sensing subsystem, and power-supply subsystem (Raghunathan, Schurgers, Park & Srivastava 2002).

- A computing subsystem consisting of a microprocessor (or microcontroller unit - MCU) and certain amount of memory (RAM, ROM, or flash memory).
- A communication subsystem consisting of a short range radio.
- A sensing subsystem consisting of one or a group of sensors or/and actuators that link the node to the outside world.
- A power supply subsystem consisting of a battery and usually some supporting circuits.

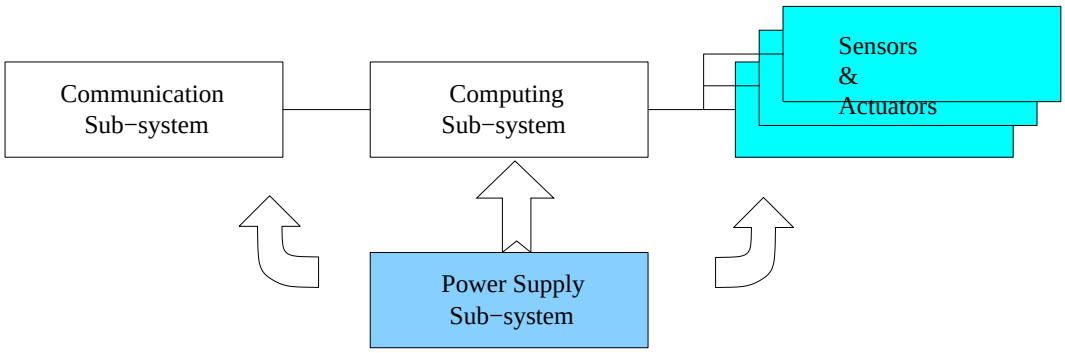

Figure 3.2: Sensor node architecture

The computing subsystem, i.e., the MCU, usually operates under various operating modes for power management purposes. For example, ATMEL's AT90S2313, a typical 8-bit MCU for sensor node development, has three operating modes (Atmel 2006), with active mode power consumption 2.8mA, idle mode power consumption 0.8mA, and power-down mode power consumption $< 0.1\mu A$.

The communication subsystem for sensor node also contains two parallel parts for transmitting and receiving respectively. Due to the short range communication feature, the power consumption is significantly less than that of a WLAN transceiver. For example, Chipcon's 2.4GHz cc2420 transceiver consumes 18.8mA power at transmitting mode, 17.4mA power at receiving mode, and only $20\mu A$ at the power-down mode (Texas inst. 2007*a*).

The power consumption of sensors and actuators is entirely dependent on the type of sensor. It can be varied from $45\mu A$ for a temperature sensor (Texas Inst. 2007*b*) to some amperes for a motor-driven actuator. However, the real energy consumption also depends on how the sensors and actuators are scheduled to be active in operation.

There are quite a few sensor node projects or testbed designs available nowadays, and many more are emerging when this document is being written. A more detailed survey can be found in (Healy, Newe & Lewis 2008). Table 3.2 shows some well-known WSN projects in details such as frequency band, power consumption, etc.

3.2.4 Energy Estimation of Sensor Node

In the previous section the energy consumption of different parts/modules of a sensor node is investigated. Many MAC and network layer protocols discussed/refered in this thesis rely on energy/power measurement. However, many WSN hardware platforms do not provide energy measurement function as a hardware solution. (Dunkels, Osterlind, Tsiftes & He 2007) provide a software-based on-line energy estimation approach for sensor nodes. This method calculates durations every time a hardware component is switched on or off. When a component is on, the estimation mechanism stores a time stamp. The energy model is denoted as

$$\frac{E}{V} = I_m t_m + I_l t_l + I_t t_t + I_r t_r + \sum_i I_{C_i} t_{C_i} \tag{3.1}$$

where V is the supply voltage, I_m the current draw of the microprocessor when running, t_m the time in which the microprocessor has been running, I_l and t_l the current draw and the time of microprocessor in low power mode, I_t and t_t the current draw and the time of communication device in transmit mode, I_r and t_r the current draw and the time of communication device in receive mode, and I_{C_i}

Table 3.2: Sensor node projects

Name	**Platform**	**Frequency**	**Node Power Cons.**	**Research Team**
i-BEAN	N/A	868MHz or 2.4GHz	12mA at stand-by	Millennial Net Co.
BTnode	ATmega 128L	Chipcon CC1000 (433-915 MHz) and Bluetooth (2.4 GHz)	9.9mW min., 102.3mW max.	ETH Zurich
iMote 2.0	ARM PXA271	TI CC2420 2.4GHz	0.13W at stand-by, 0.26W at transmit	Inter Co.
Mica2	ATmega128L	Chipcon CC1000	30 mW sleep, 33 mW active, 21 mW radio	UC Berkeley
SenseNode	MSP430F1611	Chipcon CC2420	N/A	GenetLab
EYES	MSP430F149	RFM TR1001	15μW at dormant, 20mW at transmit	Twente Univ.
Cinet	ATmega128L	Chipcon CC2420	40mA active, 20μA powersave	Chydenius Inst.

and t_{C_i} the current draw and time of other components such as sensors and LEDs.

Fig. 3.3 shows the detail current drain when a IEEE802.15.4-based sensor node sends out a data frame using CSMA/CA. The node consists of ATmega128L 8-bit microcontroller and Chipcon CC2420 IEEE802.15.4-compatible RF module. The measurement is achieved by adding a 5.25Ω resistor next to the power supply. We measured the voltage over the resistor and calculated the current using Ohm's rule. Similar method has been used in (Erdogan, Ozev & Collins 2008, Hohlt, Doherty & Brewer 2004).

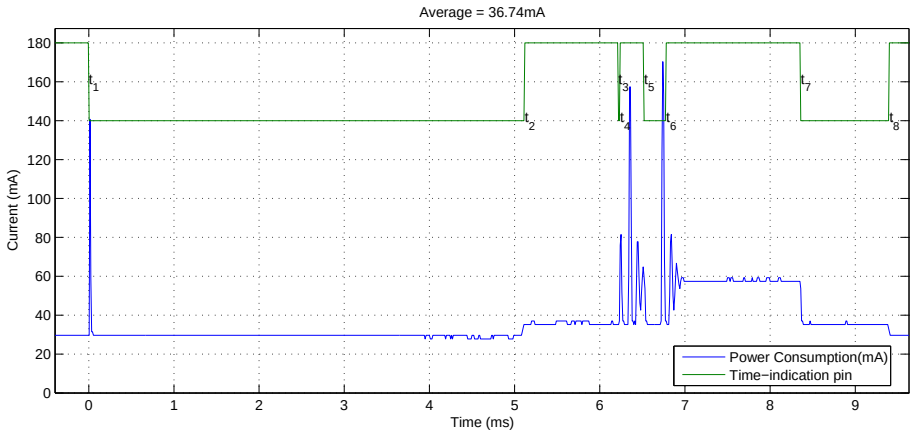

Figure 3.3: Power consumption measurement of Cinet sensor node

3.2.4.1 Case Study: Power Consumption of Cinet Node

We are interested in the real-time power consumption when the sensor node is active and its radio is turned on[1]. Totally five phases are needed to send a frame (Texas inst. 2007*a*):

1. Initialize radio module: the radio transceiver is turned on and transceiver's oscillator starts to oscillate. This phase takes several milliseconds.

2. Frame formatting: a frame is copied to the radio buffer using the serial bus. This phase duration varies, depending on the frame length.

3. Waiting RSSI: the radio module waits for a clearance of channel. This phase duration varies, depending on the channel situation.

4. Random backoff: IEEE 802.15.4 uses CSMA/CA MAC, so a random backoff will reduce the chance of collision.

5. Sending the frame: the frame is sent out. The duration is proportional to the frame length.

The above phases can be seen in Fig. 3.3.

As the time transitions given by the green line in Fig. 3.3, the duration $t_2 - t_1$ is the radio initialization phase, which takes approximately 5ms. There is an impulse power consumption at the beginning of this time when the radio circuits oscillator starts to run.

[1]we have observed less than 1mA current drain during the sleeping mode using Cinet node.

The second duration $t_3 - t_2$ indicates the local communication between ATmega128 and CC2420. In our test, a total of 37 bytes (including MAC header 9 bytes, IP header 20 bytes and payload 8 bytes) were copied to CC2420. SPI was set at a bus clock rate 7.7MHz/16 so that 37 bytes will take 0.615ms to transmit. Together with SPI bus commands, we have observed approximately 1ms for this phase. The power consumption raises 5mA from a floor of 30mA during this time.

The third duration is short. This is the time that CC2420 acknowledges to the μC that frame buffer is ready.

The next duration $t_5 - t_4$ is the channel access time. CC2420 must find a valid RSSI (Received Signal Strength Indicator) before the attempting of transmission. During this time the radio module keeps listening to the channel so several power consumption peaks are observed.

The duration $t_6 - t_5$ is the random backoff time of CSMA/CA, and $t_7 - t_6$ the frame transmitting time. During the transmission, the power consumption stays on a floor of 60mA.

At last, during $t_8 - t_7$ the radio module is turned off.

In average, sending a frame consumes 36.74mA in approximately 10ms.

3.3 Energy-Efficient Solutions

So far, energy-efficient design has been considered in the lower three layers (i.e., physical, data link/MAC, network/routing) by implementing sleep mode of the transceiver or the whole node, transmitter power control, data aggregation, minimum hop routing, etc.

3.3.1 Sleep Mode

Most WLAN products and WSN radio transceivers provide a sleep mode or power-down mode, dormant mode, etc.) when the communication is scheduled not active, or no data is sensed. The power consumption of sleep mode is much less than that of transmit/receive mode. A typical value from Fujitsu/Siemens E-1100 802.11b WLAN PC card is 9mA, two magnitudes lower than that of the active

states.

So far, the solutions using sleep mode in wireless ad-hoc/sensor networks can be classified into following categories:

- The implementation can be a pure MAC layer protocol, such as PAMAS and S-MAC. In PAMAS a node turns off its radio when it overhears a packet not addressed to it. In S-MAC, a mechanism called *message passing* is deployed to modify the Network Allocation Vector for a burst of message. During the burst all the irrelavent nodes will turn the radio off.
- There are also some proposals that apply this function to dynamically change the network topology to result to a better energy-efficient performance (BECA, AFECA in (Ya, Heidemann & Estrin 2000), and GAF in (Xu, Heidemann & Estrin 2001)).
- Other proposals set the ad-hoc network to be hierarchical or clustered; a cluster head coordinates the nodes in its cluster to be either active or sleeping, e.g. (Chavalit & Chien-Chung 2002), (Liu & Lin 2003), (Chen, Jamieson, Balakrishnan & Morris 2002). IEEE 802.15.4 specification proposes a cluster-tree topology and cluster-heads can synchronize their cluster members to be in sleep mode periodically (IEEE 2006).

The tradeoff of using sleep mode is the increament of transmission delay. A sleeping node can immediately turns back to transmit mode when it has data to send. But when the sleeping node is the destination, other nodes have to wait for its sleep time-out if they have data destinated to this node. Sleep mode does not show advantages in some communication types. For example, if the transport layer has a consecutive packet series to transmit, putting a routing node into sleep will degrade the performance.

3.3.2 Transmit Power Control

Power control can be implemented by varying the output strength of LPA. One straightforward idea is to vary the amplification factor. In practice the amplification factor of an analog amplifier is hard to be dynamically modified. A more convenient solution to implement power control is to put a scaling processor between the modulator and the DAC, as proposed in Figure 3.4. Because the output

power of an LPA is linear proportional to its input (Figure 3.5 shows the input-output power property of MAX2242), thus we can control the output power by scaling the value of input signal strength. Since the power control is usually applied by the MAC layer or network layer protocols, a digital scaling processor is more suitable to interface the upper layer control signals.

By dynamically controlling the transmit power, a radio link consumes less energy and reduces the interference to other nodes, hence the network throughput increases. As depicted in our previous discussion, power control is technically feasible at radio transceiver. However, we should paid attention to the so-called *power imbalance* problem. Authors of (Poon & Li 2003) claimed that *flows that use lower power levels generally have a higher probability of transmission failure.*

A remarkable energy property should be noticed: the transmit power control does not affect to the receive power consumption. Whatever the received signal quality is, **the receive power consumption is constant**, as shown in Figure 3.4.

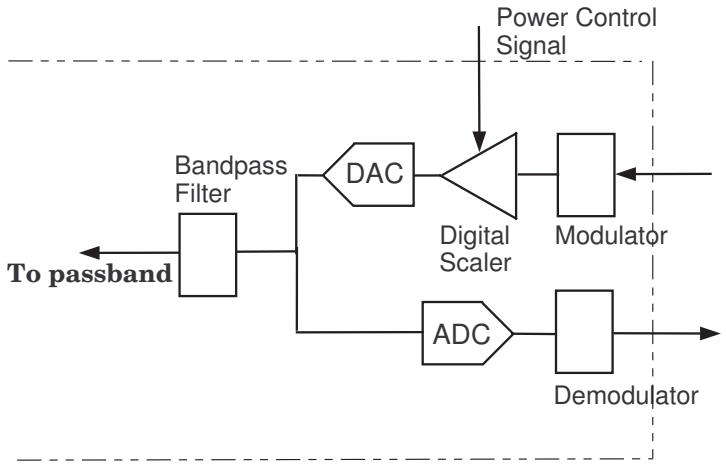

Figure 3.4: Power control implementation by a digital scaler

Another important principle in power control protocol design is that receive power consumption CANNOT be ignored. In this respect we need to consider the researches in (Doshi & Brown 2002), (Li, Aslam & Rus 2001), (Floreen, Kaski, Kohonen & Orponen 2003), (Bergamo, Maniezzo, Giovanardi, Mazzini & Zorzi 2002) to give more detailed power consumption discussion. To make one step further, we assert that *dividing a long hop into some shorter links does NOT ALWAYS save energy* by current transceiver circuit design, even power control is available. For example in Figure 3.6, a single hop from A to C consumes power P_{AC} can be

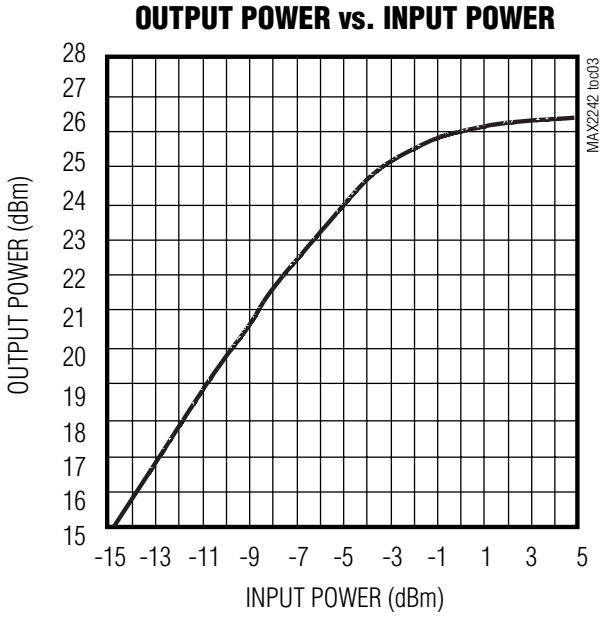

Figure 3.5: Power input-output property of MAX2242 LPA

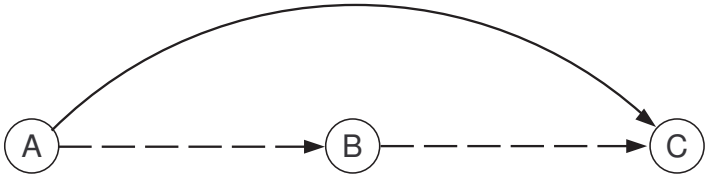

Figure 3.6: Single hop link vs. multihop link

denoted as

$$P_{AC} = P_{tx:A-C} + P_{rx} \tag{3.2}$$

where P_{rx} is the constant power taken by the receiver. As we have discussed, P_{rx} is constant. When $P_{tx:A-C} = P_{max}$, this link will consume maximum power.

If the packet is relayed by an intermediate node B, the power consumed by the link A-B-C is

$$P_{ABC} = P_{tx:A-B} + P_{rx} + P_{tx:B-C} + P_{rx} \tag{3.3}$$

The optimal position of B is at the middle point between A and C. If we assume that the path loss factor of radio propagation $\alpha = 4$, i.e., $P_{tx:A-B} = P_{tx:B-C} =$

$(\frac{1}{2})^4 P_{tx:A-C}$, and $P_{rx} = 0.68 P_{max}$ as we discussed previously, we have

$$P_{AC} = 1.68 P_{max} \tag{3.4}$$

$$P_{ABC} = 1.49 P_{max} \tag{3.5}$$

One can see that the energy conservation of the two-hop link is very limited. We should also be aware that node B locating at such a perfect place is very idealistic, since so far there is no routing protocol that can select relaying node close to this position. To make it clear, Figure 3.7 shows the power comparison between these two scenarios when B's location is changing between A and C, with different path loss factors. The zero line in the figure indicates the energy consumption by one hop, and the curves indicate the overall energy consumed by deploying a relaying node B. We can see for the typical wireless environment (α varies from 2 to 5), energy saved by multihop link is very limited or completely worse than that of a single hop link (when $\alpha = 5$). Furthermore, if a link is separated into several sections, it will suffer more transmission failures than a single link thus retransmission will consume more power than a single hop link.

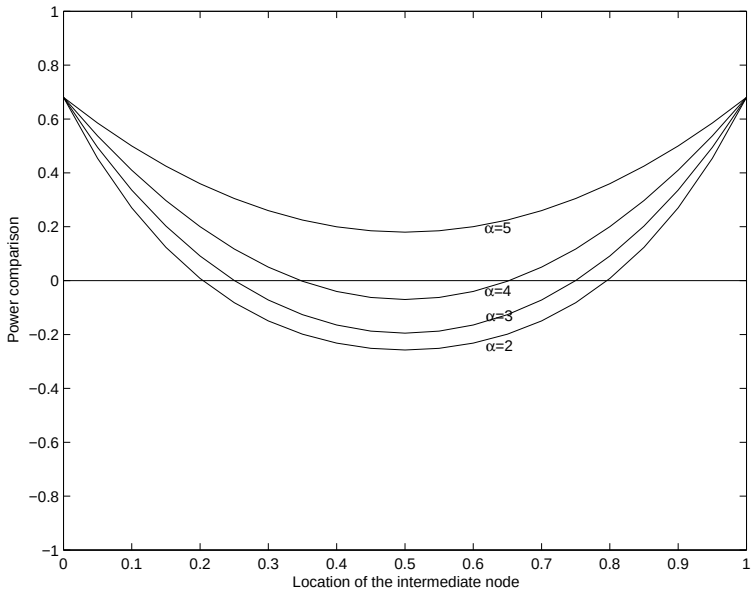

Figure 3.7: Energy saved when an intermediate node deployed

3.3.3 Impacts to Energy-Efficient Routing Protocols

A proper routing protocol can also contribute to saving energy. There are several ways to achieve energy conservation by a routing protocol:

1. To find a route that consumes minimum energy when a packet is delivered through it.

2. To find a route that excludes those nodes with less battery residual.(Tan & Bose 2005)

3.3.4 Using Energy Efficient Coding

Using proper encoding scheme for the data to be transferred can also save energy. Error detection/correction codings such as Reed-Solomon and convolutional codes applied in cellular networks have been applied to wireless data link layer since long time ago. In WSN, the advantage of applying coding scheme can reduce the retransmission thus save energy. However, due to the limited capability of sensor node, complex encoding/decoding algorithms may require unaffordable resources such as storage, memory, and energy. (Howard, Schlegel & Iniewski 2006) gave an analysis of energy consumption when Error Control Coding (ECC) is applied in WSN. The authors claim that In an urban outdoor setting, at higher frequencies, ECC can be practical for sensor networks placed between buildings, especially when implemented with analog decoders. For indoor environments, ECC is energy-efficient at high frequencies, for sensors placed at opposite ends of hallways or in adjacent rooms, or on multiple floors or in a dense urban environment at all frequencies.

Another direction is Distributed source coding (DSC). DSC has recently been considered as an efficient approach to data compression in wireless sensor networks (WSN). Using this coding method multiple sensor nodes compress their correlated observations without inter-node communications. Therefore energy and bandwidth can be efficiently saved(Tang, Glover, Evans & He 2007).

3.4 Concluding Remarks

In this chapter we inspected the power dissipation property of typical wireless transceivers for ad-hoc networks and wireless sensor networks. The conclusions are:

- Due to the circuit complexity of ADC, the energy cost at receiving phase is not negligible.
- Putting a node into sleeping mode can save energy significantly.
- In short range communications, it is not energy-efficient to divide a direct radio link into smaller multiple hops.

4 LEAST-HOP ROUTING ANALYSIS OF ON-DEMAND ROUTING PROTOCOLS

4.1 Introduction

Since the radio coverage of mobile nodes is limited, wireless ad hoc networks usually work in multihop mode, which means that some intermediate nodes may participate as routers into a communication session between the source node and the destination node. Multihop ad hoc networks have better performance of energy efficiency and throughput than that of single hop peer-to-peer networks (Doshi & Brown 2002, Gupta & Kumar 2000). However, to find a path from source to destination raises the routing problems in multihop ad hoc networks. Basically there are two categories of routing protocols for ad hoc networks: proactive and on-demand. For energy conservation point of view, on-demand protocols give better performance than those proactive ones (Cano & Manzoni 2000). The authors of (Broch et al. 1998) also showed that on-demand routing protocols are better in packet delivery goodput and generate less overhead. In (Perkins & Royer 2001, Perkins & Bhagwat 1994, Johson et al. 2001, Park & Corson 2001), some routing protocols are presented and among them we use AODV routing protocol (Perkins & Royer 2001), which is an on-demand protocol, later in our discussion.

One of the major international standards for wireless ad hoc networks is IEEE 802.11 (IEEE 1999). Since power control is not available for ad hoc mode in this standard, it means that transmit power is fixed as a constant. Thus we can assert that **the minimum energy consumption route equals to the least-hop route**. If the traffic load is uniformly distributed in the network, then a least-hop path suffers less congestions when delivering a packet, thus results in a faster transmission. This is very important in real-time communications.

In (Raju, Hernandez & Zou 2000), the authors used a fuzzy logic algorithm to find a least cost route using hop count in ad hoc networks. In (Sheu & Chen 2001), a

shortest path routing protocol based on proactive scheme was introduced for the consideration of propagation delay. In (Li, Wan, Wang & Frieder 2001), energy-sensitive routing algorithms are discussed by both centralized and distributed implementations and the authors declared that a route with less hops can achieve better energy conservation performance.

In this chapter we will analyse on-demand routing protocols for the possibility that an optimal route (least-hop) will be selected in different scenarios. Later two new methods are proposed to improve the possibility of optimal route discovery. Since the analysis is based on on-demand routing protocol, which is only applicable to Ad-hoc networks, and the it is difficult to imagine a similar WSN scenario, the rest of this chapter focus only Ad-hoc cases.

4.2 Least-hop Routing Analysis

In an on-demand routing ad hoc network such as AODV, suppose from the source node S to the destination node D there are N paths noted as $\{N_i\}$. For each N_i there are H_i hops. So we can denote the path set as $\{(N_i, H_i)\}$ $i = 1, 2, ..., N$. Figure. 4.1 shows an example of path set, which is denoted as $\{(N_1, 3), (N_2, 4)\}$.

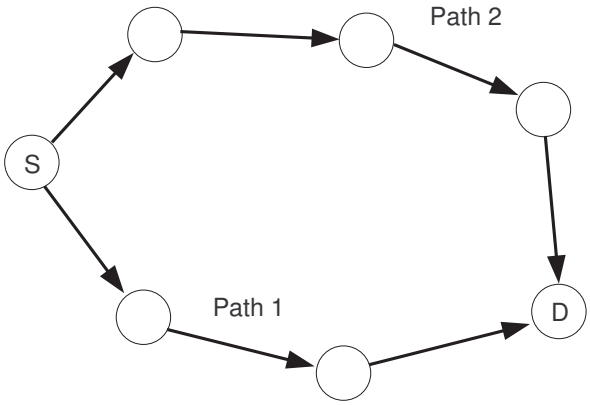

Figure 4.1: A communication link with two paths

We consider a multihop ad hoc network, which is symmetric and normalized, i.e., every node has approximately equal number of neighbors and generates equal amount of traffic. In that case, the probability that the air interface is occupied (i.e. congestion) when a RREQ packet is to be broadcast is p for all nodes. In a large random network this assumption holds well.

Because the processing delay eventually happens at every hop that propagates the RREQ packet, with a path of H hops, the time to propagate the RREQ with k congestions is denoted as

$$T_{H,k} = k\tau_c + H\tau_p \tag{4.1}$$

Here τ_c is congestion delay (the back-off interval a node has to do when it detects the channel busy); τ_p is the processing delay.

In equation (4.1), the second term $H\tau_p$ is a constant and dependent only on the hop count H. The first term $k\tau_c$ depends on the probability of occurrence of k congestions in H hops. The probability can be given by

$$\Pr(H,k) = \binom{H-1+k}{k} p^k (1-p)^H, k = 0, 1, 2... \tag{4.2}$$

The derivation of this can be found in Appendix 13.

4.2.1 Expected Delay

It is possible to explore the expected delay of propagation of a packet through an H-hop path.

$$E(T_H) = \sum_{i=0}^{\infty} T_{H,i} \Pr(H,i) \tag{4.3}$$

Substitute equations (4.1) and (4.2) into (4.3) we can evaluate the expected propagation delay (see Appendix 13):

$$E(T_H) = H\left[\tau_p + \tau_c \frac{p}{(1-p)}\right] \tag{4.4}$$

Equation (4.4) shows that the expected propagation delay consists of two parts: the first part is the processing delay $H\tau_p$ and the second part is the congestion delay $H\tau_c p/(1-p)$ dependent on congestion probability p.

Because equation (4.4) is proportional to the hop count H, it is clear that in a given path set $\{(N_i, H_i)\}$ $i = 1, 2, ..., N$, the least-hop path has the shortest expected time to reach the destination if τ_c, τ_p, p are fixed.

When a congestion happens, the node will defer the transmission in NAV (network allocation vector) interval (IEEE 1999). Time of processing a RREQ usually is

much shorter than it, therefore $\tau_p \ll \tau_c$. Then equation (4.4) becomes:

$$E(T_H) = H\tau_c \frac{p}{(1-p)} \tag{4.5}$$

Though the result shows that the least-hop path has the maximum probability to be selected, in a complex network topology, there exist many paths from the source to the destination. In this case the probability of selecting least-hop path becomes rather small as the results of numerical analysis show in next section. Equation (4.5) also indicates that when the congestion probability p increases, the expected delay will also increase, as shown in Figure 4.2. If p goes to 1 (always congested), $E(T_H)$ goes to infinity, i.e. the packet will never reach the destination.

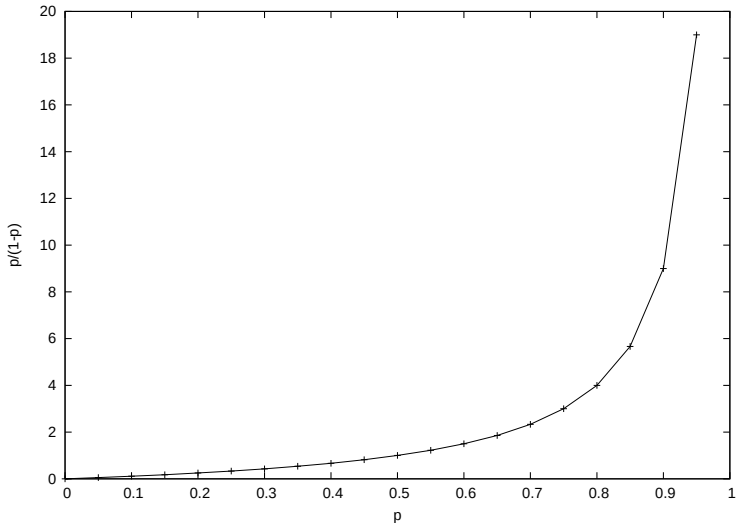

Figure 4.2: Propagation time $E(T)$ vs. congestion probability p

4.2.2 Numerical Analysis for Grid and Random Topologies

First let's think of the probability that the least-hop path is selected. The condition that the least-hop path (without losing generality, always denoted as N_1) with H_1 hops and along the path there are k congestions, will have less propagation time than all other paths N_i that have longer propagation delay is represented as

$$\Pr_{H_1,k|less} = \Pr\{T_{H1} < T_{H2}, ..., T_{H1} < T_{Hn} | H_1, k\} \tag{4.6}$$

This is the probability that when the least-hop path N_1 suffers k congestions, all other paths will suffer more than k congestions. When two or more paths suffer the same number of congestions, they have a contention to reach the destination and the chance is equal ($1/m$ if there are m competitors). The overall probability for the least-hop path is

$$\Pr_{H_1,k} = \Pr_{H_1,k|less} + \sum_{m=1}^{N-1} C_{N-1}^{m} \Pr\{\underbrace{T_{H_i} = T_{H_1}}_{m} \text{ and } T_{H_j} > T_{H_1}\}/(m+1) \tag{4.7}$$

Probability $\Pr_{H_1,k|less}$ can be derived as

$$\Pr_{H_1,k|less} = \Pr_{H_1,k} \prod_{i=2}^{N} \Pr(H_i, k_i > k) \tag{4.8}$$

Here $\Pr(H_i, k_i > k)$ is the probability that path N_i will suffer more than k congestions

$$\Pr(H_i, k_i > k) = \sum_{j=k+1}^{\infty} \Pr(H_i, j),\ i = 2, ..., N \tag{4.9}$$

and

$$\Pr\{\underbrace{T_{H_i} = T_{H_1}}_{m} \text{ and } T_{H_j} > T_{H_1}\} = \prod_{i=1}^{m} \Pr(H_i, k) \prod_{i=m+1}^{N-1} \Pr(H_i, k_i > k) \tag{4.10}$$

If we substitute equations above to equation (4.7), we can find the probability of least-hop route N_1 suffering k congestions. Therefore, the overall probability that the least-hop path will be selected is the summation for all the cases of k, that is, from 0 to ∞:

$$\Pr_{H_1} = \sum_{k=0}^{\infty} \Pr_{H_1,k}, \tag{4.11}$$

Equation (4.11) is too complex to be derived analytically, therefore we demonstrate some numerical and simulation results.

4.2.3 Numerical Results

It is clear that when the total number of paths increases, the probability that the least-hop path to be selected decreases. As shown in Figure 4.3, we keep the least-hop path to be 2 and 3 hops, other paths 3 and 4 hops, respectively in (a) and (b).

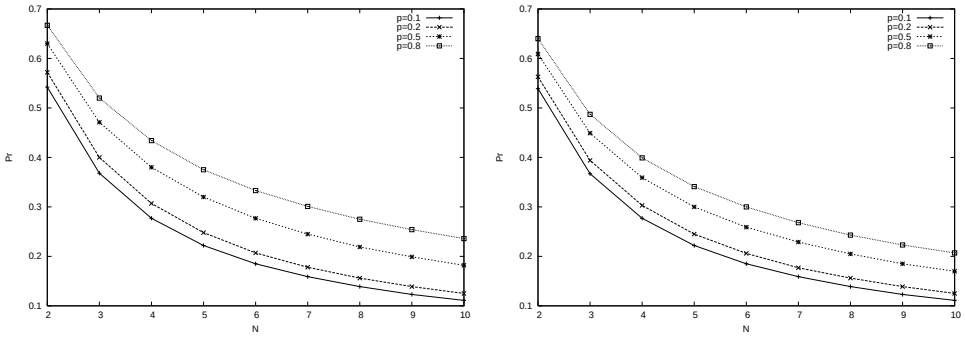

(a) $H_1 = 2, H_i = 3$ (b) $H_1 = 3, H_i = 4$

Figure 4.3: Probabilities in different scenarios, N is the number of paths except N_1.

It is also possible to see from Figure 4.3 that when the congestion probability increases, the least-hop probability $\Pr_{H_1}$ increases, too. This is caused by that a longer path has higher probability to suffer more congestions. To make it clear, Figure 4.4 shows the changes with different congestion rates p. Here $H_1 = 3, H_i = 4$.

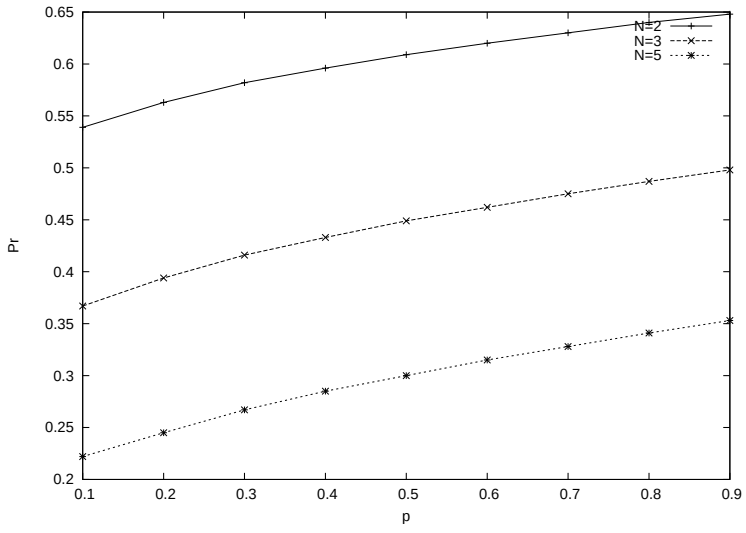

Figure 4.4: Pr with different p and N

Another factor is the network scale. As the network size increases, from the source to the destination there are more paths and the number of hops of each path also increases. In Figure 4.5 one example situation is considered: we fix the congestion probability and increase both N and H. In the figure, we present 5 situations. The values along X-axis are H_i, H_1, and N, respectively from up to down. We can see when the network scale increases, the least-hop route probability decreases.

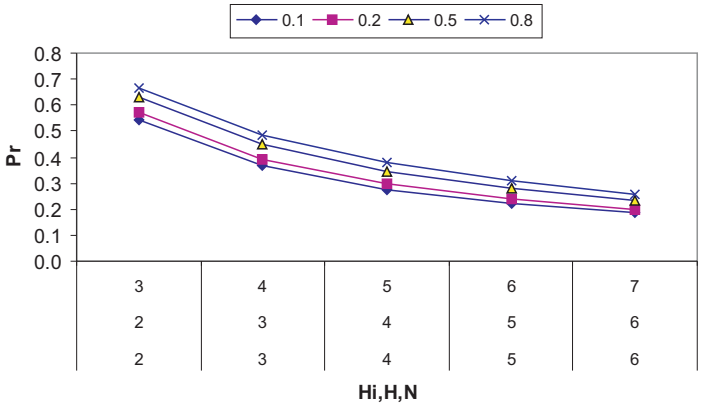

Figure 4.5: Pr vs. network scale

Need to mention that in a real wireless ad hoc network it is possible that there are more than one least-hop path. Thus the probability to select the one of them is $m \times \Pr$, here m is the number of least-hop paths and Pr is the probability that one of these paths will be selected.

4.3 Solution and Simulation Results

Here we suggest two methods that will increase the least-hop path probability.

4.3.1 Approach 1 - Waiting Window

In the current on-demand protocols such as AODV and DSR, the destination node will immediately send a RREP packet upon having received the first RREQ packet. This was based on response time consideration, i.e., to establish a path as soon as possible. From the previous analysis we know the first RREQ may not be the optimal one. A simple and slight change at the destination node can

improve the least-hop path probability if we set a *Waiting Window* (WW) at the destination node. Upon receiving the first RREQ packet, the node activates a *Waiting Window Timer* (WWT) instead of sending RREP packet immediately. Within the timer there might be some other RREQ packets coming by different paths. When the WWT expires, the node compares all the RREQ packets by hop counts data inside and selects the minimum one to send RREP. The RREQ packets that arrive after the WW will be discarded. This can be illustrated in Figure 4.6.

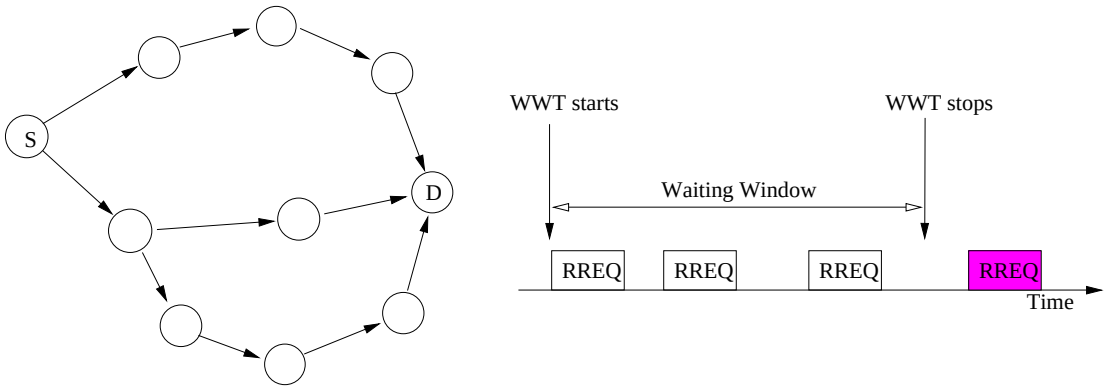

Figure 4.6: Waiting Window

One rule should be notified: if the source node and the destination node are neighbors, i.e. $H = 1$, it is not necessary to activate the waiting window at all.

The disadvantage of Waiting Window method is when the network size becomes large, hop count of routes increases. This implies potentially longer intervals between the arriving RREQs. Thus we have to increase the duration of WW. Finally it will be a rather significant impact to the system performance. In our simulations we have observed that it can be as long as 100ms between the first and second RREQ arrivals.

4.3.2 Approach 2 - Multiple Reply

Since the Waiting Window scheme increases the delay of route establishment phase. In order to overcome the problem, we propose an alternative method, in which the destination immediately sends a RREP upon having received the first RREQ. The RREP will be propagated back to the source and a route is established within the first time. The source can start sending data packets alone the first established route, which may not be the least-hop route. If we set that

the destination node will reply every arrived RREQ with a RREP. The source will receive several RREP packets. When a new RREP packet comes, the source compares the hop count field in RREP and either chooses the new one if the hop count is less than that of the current route or discards it otherwise. Figure 4.7 gives an example of this scheme.

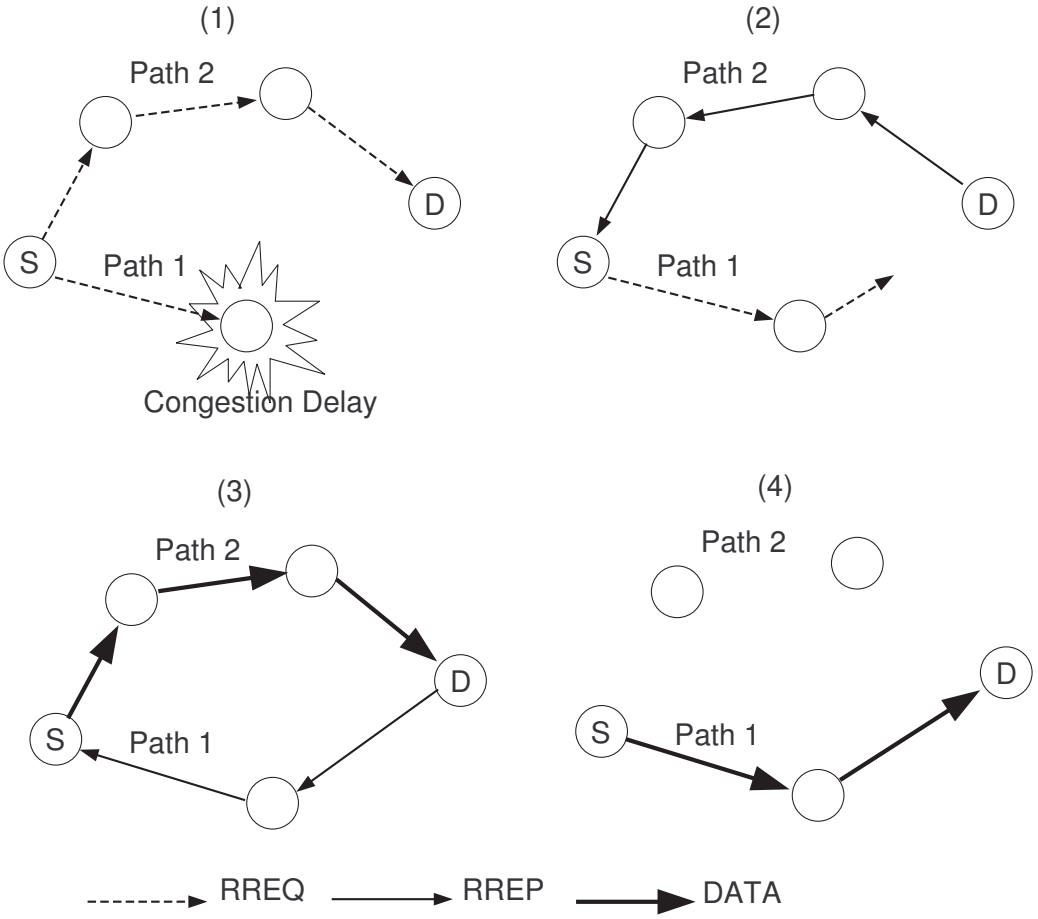

Figure 4.7: Multiple Reply

This approach can guarantee the shortest route establish time. The disadvantage is that sending multiple RREPs will increase network overhead. However, because the delivery of RREP is a point-to-point transmission, this overhead increment is not significant. Let's denote that a RREP packet has L_{RREP} bits and a data packet has L_{DATA} bits. Transmitting one bit takes unit energy. Total traffic (load + overhead) of Multiple Reply scheme will consume energy

$$E_{mr} = \sum_{i=1}^{N} H_i L_{RREP} + H_1 L_{DATA}, \tag{4.12}$$

In a typical on-demand routing protocol, a route is selected by the probability of $\Pr_{H_i}$, as discussed in equation (4.11). The energy cost by the traffic (load + overhead) is

$$E_o = (L_{DATA} + L_{RREP}) \sum_{i=1}^{N} \Pr_{H_i} H_i \tag{4.13}$$

According to the AODV specification (Perkins & Royer 2001), L_{RREP} is 44 bytes, L_{DATA} is usually 532 bytes. A communication session such as TCP or CBR usually have multiple data packets. Compare with the traffic load, multiple RREP overhead is negligible. When the number of data packets increases, the overall energy consumption E_{mr} is less than E_o because of the selection of least-hop route. Figure 4.8 shows some comparison results.

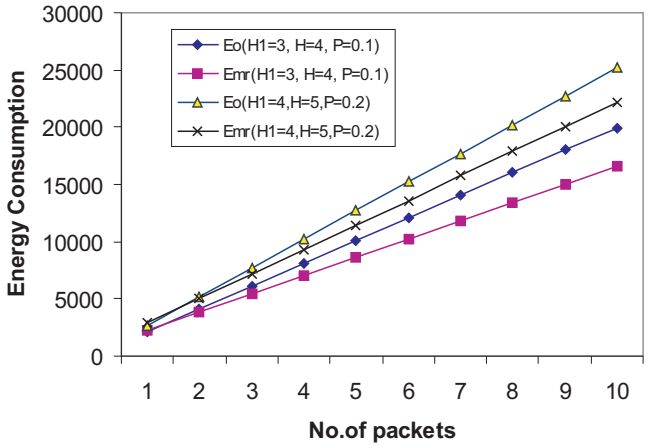

Figure 4.8: Energy Comparison: Multiple Reply vs. Original AODV

4.3.3 Intermediate Node Policy

The logic in intermediate nodes should be changed for these two new schemes. In the current on-demand protocols, an intermediate node will forward the RREQ only once upon having received it first time. Later arrivals are discarded. To guarantee the least-hop path, the node now should inspect the hop count data in every incoming RREQ and update its temporal route table if the hop count in the new RREQ is less than the current data. An example is illustrated in Figure 4.9.

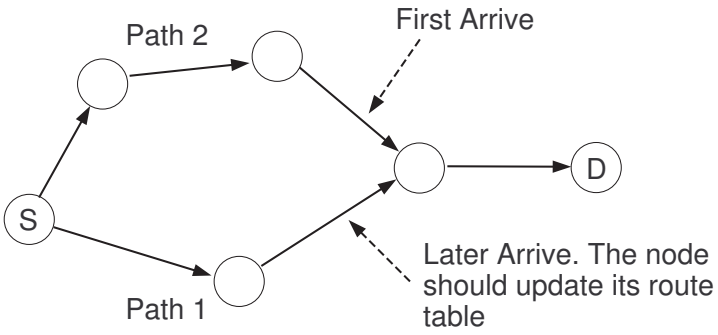

Figure 4.9: Intermediate node policy

4.3.4 Simulation Results

The simulations have been done in Network Simulator (NS-2 ver2.26) (Fall & Varadhan 2003). In the simulations, we set up a network with 25 mobile nodes in an area of 800x800 m^2. The nodes are fixed as a 5x5 grid as shown in Figure 4.10 and mobility is prohibited. The distance between nodes is $200m$ thus a node can hear from those neighbors at direct angles (e.g., node 7 can hear from nodes 2, 6, 8 and 12).

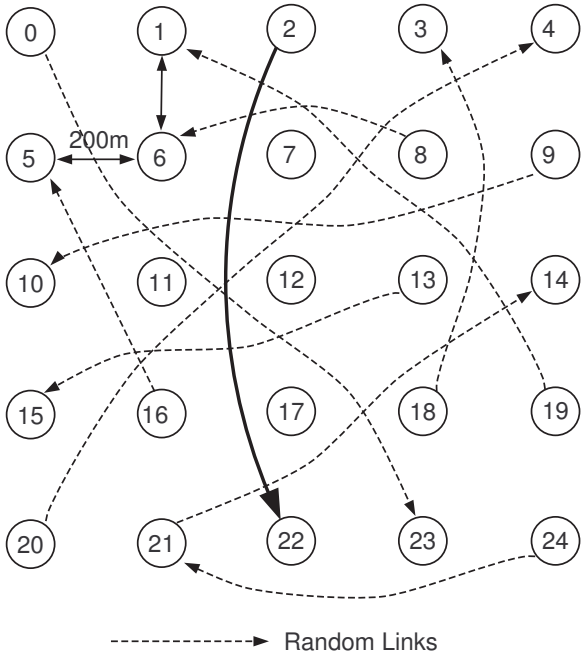

Figure 4.10: Simulation topology

The physical layer is Two Ray Ground and omnidirectional antennas with unity

gain. The MAC layer is IEEE 802.11 MAC. Routing protocol is AODV. The simulation time is 200 seconds. During the simulation, there are 10 *Constant Bit Rate* (CBR) connections randomly generated. The rate of each CBR connection is 1/2/4 packets per second respectively for different congestion rates. We observe a route between nodes 2 and 22, as shown in Figure 4.10, after 10 random CBR connections have been established.

Since waiting window is unscalable, we prefer to choose multiple reply scheme. We pay attention to two metrics between the original AODV and AODV with multiple reply: the average packet delivery delay, and the average power consumption over a link. The average packet delay comparision is given in Figure 4.11(a). The average power consumption over a link is equal to the average hop count over a link. Figure 4.11(b) shows the comparisons between two schemes with different packet rates. It can be seen that the least-hop route gives up to 30% energy saving and average delivery delay is only 50% compared to original AODV.

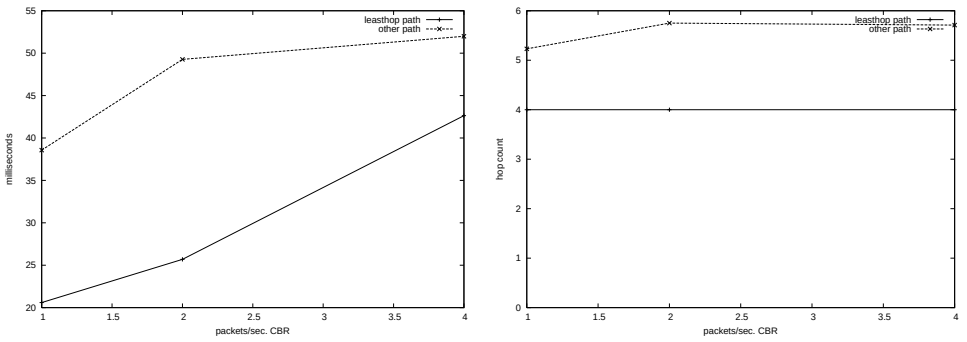

(a) Average packet delivery delay

(b) Average power consumption over a link

Figure 4.11: Average delivery delay and power consumption.

4.4 Concluding Remarks

In this chapter, we have inspected the route discovery properties of on-demand routing protocols. Based on the packet congestion probability p, we found that the expected packet delay along a path is proportional to its hop count H and $p/(1-p)$, here p is the congestion probability. We derived the probability that the least-hop path will be selected when using an on-demand routing protocol. It shows that when the network topology becomes complex, the probability of least-hop path to be selected decreases dramatically. For this problem we suggest

two solutions: 1) waiting window, and 2) multiple reply. The waiting window scheme allows the destination to select the least-hop path after several arrived RREQ packets; whiles the multiple reply scheme allows the source to do the route selection. The multiple reply scheme establishes a route as fast as possible and seemed to be a better choice.

5 ENERGY-LIMITED AD HOC NETWORK CAPACITY

5.1 Introduction

The capacity of mobile ad hoc networks can be considered in different aspects. Some researchers have paid attention to the instantaneous throughput of the network, i.e., how many bits can be transmitted in the network in a certain duration, or how many traffic links can be established simultaneously (Gupta & Kumar 2000), (Gupta & Das 2001) and (Toumpis & Goldsmith 2000). However, from another point of view, nodes in an ad hoc network are constrained by the battery energy. Thus we can define the network capacity as the ratio of the number of transmitted bits to the energy consumed by this transportation. Here the transportation means end-to-end communication through a multihop path. In a multi-hop ad hoc network, we need to consider the energy consumed by all the intermediate routing nodes. In (Rodoplu & Meng 2002) the authors have given the network capacity definition as **bit per joule**. In some specific type ad hoc networks such as sensor networks, the traffic is not very heavy, thus the network survivability—transmit as much as data before the batteries run out—is more important than the network instantaneous throughput.

One of the major energy-saving methods is power control. Power control at the MAC layer have been heavily discussed and it is found that power control can save energy significantly. On the other hand, by using different power levels, the network connectivity changes. Research shows that a lower transmit power will result to more simultaneous transmissions, because the co-channel interference is reduced (Gupta & Kumar 2000). However, the reduction of transmit power increases hop count from the source to the destination. This will 1) increase the energy consumption of the packet reception, because it is proportional to the route hop count, 2) increase the delay of packet propagation, 3) increase the overall probability of transmission failure, and 4) increase the network overhead.

In this chapter we inspect the network energy performance. Attention is focused on the energy consumption of the end-to-end transmission with different node densities and transmit power levels.

Power control is one of the major methods applied in ad hoc networks to save battery energy (See e.g. (Swetha, Kawadia, Screenivas & Kumar 2002) and the references therein). Increasing the transmit power will reduce the average hop count of routes. Since the number of hops is reduced, the end-to-end packet drop rate is potentially reduced. However, increasing the transmit power will increase the energy consumption of a single radio link. Meanwhile the co-channel interference will also increase thus increase the packet error rate (PER) at a single link. In (Imran, Sorav, Gupta, Misra, Razdan & Shorey 2002), the authors inspected the TCP performance of ad hoc networks by setting different transmit power levels. They established a model to analyse the change of packet error rate (PER) when transmit power varies. They asserted that a **medium power level** gives optimal energy performance in respect of packet retransmission. However, they inspected the energy performance only over a fixed source-destination couple by varying the distance between them. Another argument is the network instantaneous throughput. It is stated that lower transmit power can let more simultaneous transmissions thus the network throughput is increased. However, from a network point of view, for an end-to-end connection, lower transmit power will involve more nodes as routers. Consequently these nodes have less resource for their own traffic thereby reducing the network throughput. We leave these arguments for further research.

5.2 Energy-Aware Capacity

Besides the instantaneous throughput, the capacity of ad hoc networks also depends on the energy consumption. One of the basic gaols in battery-operated ad hoc networks is to make the whole network functioning as long as possible. We define the **energy-aware ad hoc network capacity** as the inverse value of **the expected energy** consumed by a single packet delivery, denoted as

$$C = \frac{1}{\overline{D}(P_t + P_r)} \tag{5.1}$$

here $\overline{D}$ is the expected route length, i.e., the number of hops alone a route. P_t, P_r are normalized transmit and receive power, respectively. Idle power consumption is assumed negligible. This formula is based on the assumption that every traffic link has equal amount of data to transmit[1].

Equation (5.1) is based on the assumption that the communication channel is error-free. If we take the packet delivery failures in to account, we can draw the conclusion in term of the packet error rate. We suppose that for each single hop the packet has probability p to be failed and retransmission will be triggered. Thus alone a route with D hops, the probability that there are k retransmissions is denoted as:

$$\Pr(D,k) = \binom{D-1+k}{D-1} p^k (1-p)^D, k = 0, 1, 2... \tag{5.2}$$

therefore the expected value of retransmission can be derived as

$$E(k,D) = \sum_{0}^{\infty} k \Pr(D,k) = Dp/(1-p) \tag{5.3}$$

The energy capacity regarding to transmission failure becomes

$$C(p) = \frac{1}{[\overline{D} + E(k,\overline{D})](P_t + P_r)} = \frac{1-p}{\overline{D}(P_t + P_r)} \tag{5.4}$$

It is clear from this equation that when p grows, the energy capacity of the network decreases.

5.3 Arbitrary Topology

We start the analysis from an arbitrary grid topology, i.e., the network is an $m \times n$ matrix. By this node distribution we can set different transmit power so that every node can reach a different set of nodes.

The power consumption taken by the data delivery depends on the established route. However, different transmit power levels will result to different network topologies, therefore establish different routes between the source and the desti-

[1]Therefore the result of the analysis may not be applicable to certain WSN applications because the traffic pattern is usually sink-oriented in such applications.

nation. It is necessary to inspect that how the change of transmit power affects to the routing result. Considering such a grid network, point-to-point traffic happens randomly between any two nodes S and D. Here we denote the source and the destination nodes as $S(x_s, y_s)$ and $D(x_d, y_d)$, respectively. Note that $x_s, x_d \in [0, n-1]$, and $y_s, y_d \in [0, m-1]$.

If the transmit power is minimized, i.e., every node can only hear those nodes at its direct angles, the distance of the source and the destination can be given $D_{p1} = |x_s - x_d| + |y_s - y_d|$, here D_{p1} is the distance using power level 1. Without loss of generality, we set $(x_s, y_s) = (0, 0)$ and $(x_d, y_d) = (x, y)$, it can be rewritten as $D_{p1} = |x| + |y|$.

Since S and D are randomly selected, it is possible to derive the **expected distance** in such a network, denoted as

$$D^*_{p1} = E\{|x| + |y|\} = E\{|x|\} + E\{|y|\} \tag{5.5}$$

The random variables x and y for rows and columns are independent, therefore we derive the row expect $E\{|x|\}$ only. For a single row of nodes, the expected distance between the source and the destination is the average of the distances that the source node is fixed at a certain place for all the possible places:

$$E\{|x|\} = \frac{1}{n}\sum_{i=0}^{n-1}\frac{1}{n-1}\sum_{j=0, j\neq i}^{n-1}|i-j| = \frac{n+1}{3} \tag{5.6}$$

The detail derivation can be found in Appendix 13.

Thus the expected distance of a random source-destination pair in the network using power level 1 becomes

$$D^*_{p1} = \frac{n+1}{3} + \frac{m+1}{3} \tag{5.7}$$

If we increase the transmit power level, the network topology becomes more complicated. At this situation routing protocol plays very important role. It is possible to deploy a least-hop routing protocol that always selects the route with minimum hop count. For instances, routing protocols such as DSDV (Perkins & Bhagwat 1994) and AODV (Perkins & Royer 2001) are designed for finding a minimum hop route.

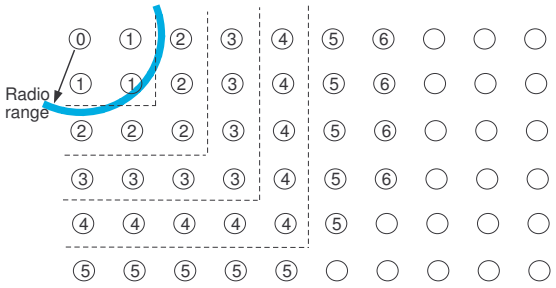

(a) Power level is 2

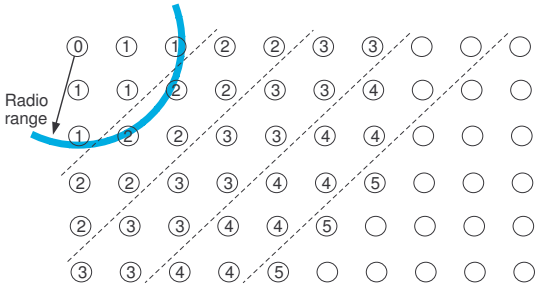

(b) Power level is 3

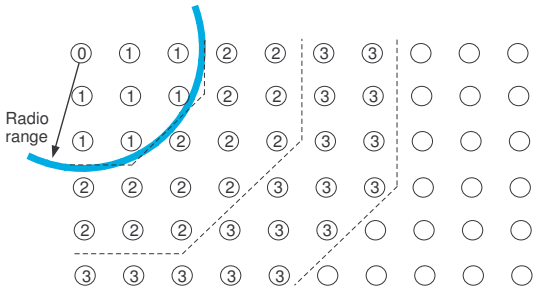

(c) Power level is 4

Figure 5.1: Number of hops to destination at different power levels

If we increase the transmit power so that a node can reach more nodes as shown in Figure 5.1, the expected distance between a random source-destination pair becomes

$$D^*_{p2} = \max\left\{\frac{n+1}{3}, \frac{m+1}{3}\right\} \tag{5.8}$$

$$D^*_{p3} = \left\lceil E\left\{\frac{|x|}{2}\right\} + E\left\{\frac{|y|}{2}\right\}\right\rceil = \frac{m+n}{6} \tag{5.9}$$

$$D^*_{p4} = \max\left\{\frac{m+1}{6}, \frac{n+1}{6}, \frac{m+n+2}{9}\right\} \tag{5.10}$$

According to the analytical results, we can compare the power-aware capacity of different transmit power levels, as shown in Table 5.1. Here we set the size of the network as $m = 10, n = 15$, the radio path loss factor $\alpha = 4$. For the radio ranges as $1, \sqrt{2}, 2$, and $\sqrt{5}$, the corresponding transmit power $P_{tx_i}, i \in (1, 4)$ are normalized to $0.1, 0.4, 1.6$, and 2.5, respectively. The receiver power consumption P_{rx} is normalized and fixed to be 1. This setting is based on the survey of power consumption of current WLAN products. The result shows that using power level 2 gives the best energy performance.

Table 5.1: Power-aware capacity

Level	$E\{D\}$	P_{tx}	C
1	9	0.1	0.101
2	5.33	0.4	0.134
3	4.5	1.6	0.085
4	3	2.5	0.095

Node density should also be considered because different transmit power levels should be set for different node densities. Figure 5.2 shows the comparison of energy consumptions over the expected distance route with different transmit power levels. For each individual density d, we set power level 1 to be 0.01, 0.05, 0.1, and 0.5 (very high, high, low, and very low), respectively, denoted as $P_{tx_{1,d}}, d \in [1, 4]$. $P_{rx} = 1$ and fixed for all the cases. It can be seen that when the node density increases, the energy consumption trends to decrease when we enlarge the radio range. Actually for the lowest density case $P_{tx_{1,4}} = 0.5$, the maximum power $P_{tx_{4,4}}$ is 12.5 times higher than that of receive power. This is not common in local ad hoc networks.

5.4 Random Distributed Network

In a randomly distributed ad hoc network, we need to find out the expected geometric distance between any two nodes and the expected hop distance.

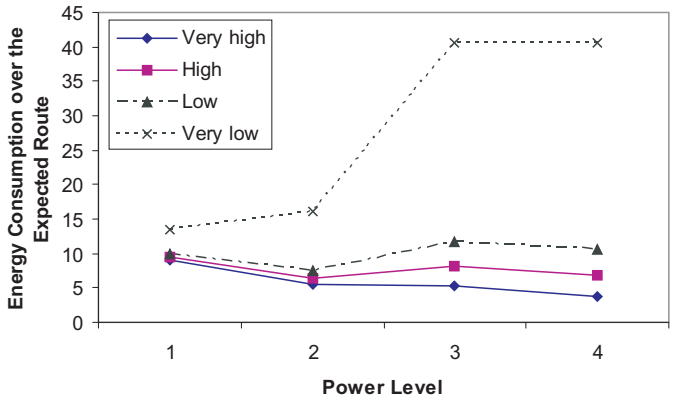

Figure 5.2: Energy consumption over the expected route in a mesh topology network with a scale of $m = 15, n = 10$ with different node densities

5.4.1 Expected Geometric Distance

between any two nodes randomly distributed within a unit square has been derived by (Weisstein 2005):

$$\begin{aligned}\mathcal{D}^* &= \underbrace{\int_0^1 \cdots \int_0^1}_{4} \sqrt{(x-u)^2 + (y-v)^2}\, dx\, du\, dy\, dv \\ &= \frac{1}{15}\left[\sqrt{2} + 2 + 5\ln(1+\sqrt{2})\right] = 0.521405433\ldots \end{aligned} \tag{5.11}$$

5.4.2 Expected Hop Distance

Suppose the transmit power can reach a distance of R and the node density is ρ, thus the number of neighbours is $\pi R^2 \rho$. We assume that the network is dense enough so that we can always find at least a single node from any given area. The Probability Density Function (PDF) of number of nodes at a distance of r is denoted as $p(r) = 2r/R^2$ if the nodes are uniformly distributed. By a reactive routing protocol such as AODV, for the source node, all its neighbours have the same chance to be selected as the next hop node. The expected distance of the hop from the source node to the **first** routing node is (Olafsson 2004)

$$D_1^* = \int_0^R r p(r) dr = \frac{2}{3} R \tag{5.12}$$

here D_1 means the distance for the first hop.

For an intermediate node, only those nodes that have not received a routing packet RREQ will be the next hop candidates, as shown in Figure 5.3. The expected value of $D_i, (i > 1)$ is

$$D_i^* = \frac{1}{A_s} \iint_{A_s} \sqrt{x^2 + y^2} dx dy \approx 0.7670R \tag{5.13}$$

here A_s is the area of the shadow region. In the figure, the current node has received a RREQ and starts to broadcast it. According to the AODV routing protocol, only those nodes in the gray area can be the next hop candidates.

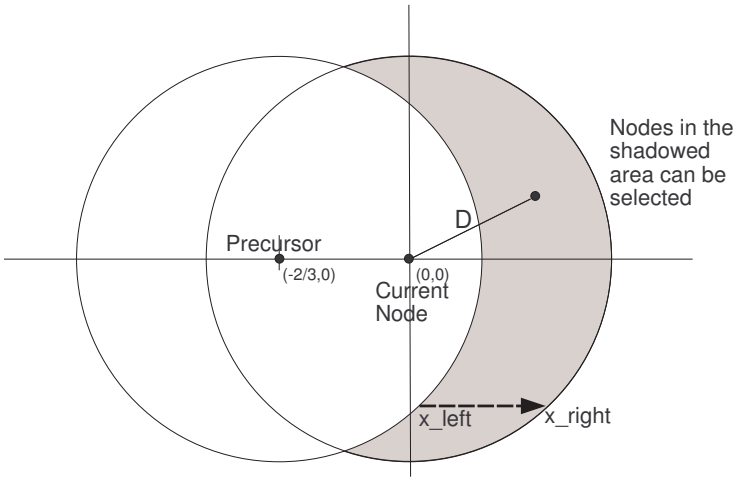

Figure 5.3: Routing progress of an intermediate node

Based on the previous discussions, we can find the expected route distance, i.e., the average number of hop count, in a random ad hoc network. Suppose we have a square area of $\mathcal{A}$, thus the average end-to-end distance $\mathcal{D}^* = 0.5214\sqrt{\mathcal{A}}$. With a minimum-hop routing protocol, we can derive the expected route distance in term of hop counts, denoted as:

$$D_{rand}^* = \frac{\mathcal{D}^* - D_1^*}{D_{i,i>1}^*} + 1 \approx \frac{0.5214\sqrt{\mathcal{A}} + 0.1003R}{0.7670R} \tag{5.14}$$

Thus the energy-aware capacity in a random topology ad hoc network can be evaluated by equation (5.1). This expression is the statistically **upper-limit** of the ad hoc energy-aware capacity, because we assume that the routing protocol can always find a minimum-hop path. The realistic situation is not as perfect as this assumption. However, when the node density is high and the expected hop

Table 5.2: Transmit power setting in simulation and the expected results

Level i	P_{tx_i}(mW)	R_i(m)	D_{rand_i}	$1/C_i$
-1	0.2	48.2	5.99	301.01
0	0.5	67.1	4.34	219.38
1	1	79.8	3.67	187.35
2	5	119.3	2.50	137.53
3	25	178.4	1.72	128.66
4	100	252.3	1.25	187.70
5	200	300	1.07	268.30

count is not big, the AODV routing protocol can approach to this limit, as we will see in the simulation section.

5.5 Simulation

AODV is deployed in our simulations. As mentioned, traffic load affects the AODV routing significantly because a node that has been suffered heavy traffic load has less chance to be selected anymore as a router, even though its location is very suitable. On account of this point, we apply our simulation with relatively light traffic, which usually happens in sensor networks.

The transmit power setting is refered to the Cisco Aironet 350 802.11 WLAN card (Cisco 2004). Here we set the maximum transmit power to be level 5 and it can cover 300m distance. However, in order to compare with some longer route distance $\mathcal{D}$, we set other two lower levels, denoted as 0 and -1. The path loss factor $\alpha = 4$. The settings and corresponding radio coverage R_i, expected route distance D_{rand} and the capacity $1/C_i$ are listed in Table 5.2. P_{rx} is 50mW for all the cases. 200 nodes are randomly distributed in a 400×400 m^2 square.

For each simulation 40 Constant Bit Rate (CBR) traffic connections are established randomly between two nodes. Each CBR link transmits 1 packet per second so that the entire network traffic is light. Mobility of nodes is ignored in our analysis and thus set to be 0 in the simulations.

The simulation results coincide nearly with our analysis. In Figure 5.4(a) one can see that route distance of simulation corresponds to our analysis, especially when the average hop count is less than 4. When the average hop count increases, which means the ratio $\mathcal{D}/R$ increases, there are more chances that a detoured route will

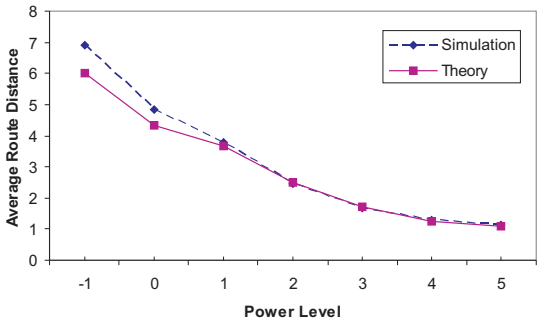

(a) Average route distance vs. the transmit power level

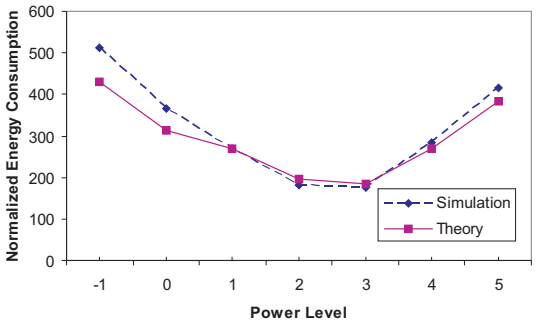

(b) Normalized energy consumption ($1/C$) comparison

Figure 5.4: Compare with Simulation Results

be established. Thus the simulations give longer hop count than that of the analysis. Figure 5.4(b) shows the energy performance comparison between theory and the simulation. The simulation results fit the theory well. It is interesting to see that at transmit power level 3, both give the best energy performance, while the expected route distance is around 2.

5.6 Concluding Remarks

In this chapter we analysed the energy performance of ad hoc networks that utilize transmit power control. We assert that minimizing the transmit power will not result to the best energy conservation, because the energy taken by receiving a packet is fixed at a single hop. When the transmit power decreases, the energy consumption taken by the receivers becomes more and more significant. In both

arbitrary and random node distributions we found this conclusion is true. To achieve the optimal energy performance, the average route distance should be kept as 2 or 3 hops with a moderate transmit power.

6 A POWER-AWARE ON-DEMAND ROUTING PROTOCOL

6.1 Introduction

Power control is an practical method for energy efficiency among the existing approaches. In CDMA cellular networks power control has very sophisticated implementation. In ad hoc networks because there is no infrastructure acting as coordinator and connection may occur between any two nodes in the network, power control is much more complex than that in cellular systems. In many works this issue has been addressed. In (Swetha et al. 2002), power control is demonstrated to increase traffic capacity of entire network, increase battery lifetime, and reduce the contention at the MAC layer. The authors further propose a power-control-enabled routing protocol for proactive routing schemes such as DSDV. In (Jung & Vaidya 2005) and (Agarwal, Katz, Krishnamurthy & Dao 2001), power control implementation on MAC layer has been proposed. The authors in (Park & Sivakumar 2002) asserted that the optimal transmission power is determined by the network load, the number of stations, and the network grid area. Based on this conclusion, they proposed two power control schemes: Common Power Control (CPC) for entire network scale and Independent Power Control (IPC) for hop-by-hop scale. (Doshi, Bhandare & Brown 2002) give energy efficiency comparison between multi-hop link and single hop link. The authors declared that an intermediate node acting as relaying device will decrease the energy consumption if its location is good. (Gomez & Campbell 2004) propose a viarable power control scheme so that a Minimum Spanning Tree (MST) is constructed for network connectivity. Some research focus on routing algorithm which considers battery residual of each node(Tan & Bose 2005).

(Gomez, Campbell, Naghshineh & Bisdikian 2003) proposed a power control routing algorithm called PARO for wireless networks. In PARO, the source node first uses maximum power to send data packet directly to the destination. Whereas

each node (between the S-D pair) enables *overhearing* to calculate the power consumption using a cost function as if the data packet is relayed by it. Then the best candidate will announce a *redirection* command to both the source and destination nodes to take the router role. This procedure is recursive until the cost function cannot be optimized anymore.

In this chapter we propose an energy efficiency Power-Aware Routing (PAR) protocol which can be adapted to the existing reactive routing algorithms such as AODV (Perkins & Royer 2001) and DSR (Johson et al. 2001). The protocol selects energy efficient route based on transmitter-receiver power adjustment when routing packet such as RREQ is propagated from source to destination nodes.

6.2 Hop-by-Hop Power Control

Hop-by-hop power control is proposed in (Bergamo et al. 2002) and (Doshi et al. 2002). This method requires that each node can put the transmit power level P_{TX}, at a suitable format field in the transmitted packet. It also requires that the radio receiver can measure the received signal strength, P_{RX}. With these power values, the node that has received the packet can estimate the link attenuation. In another word it can estimate the distance between the transmitter node and itself. Upon the received signal power, the node can adjust its transmission power to the remote node by:

$$P_{TX}^{*} = P_{TX} - P_{RX} + S_R + M \tag{6.1}$$

Here S_R is the minimum signal power required to correctly receive a packet. M is a power safety margin introduced to take into account channel and interference power level fluctuations. When a packet from this node is sent and received by the remote node, the remote node can do the same adjustment. This results in a close loop power control.

Here it arises a so-called *power imbalance* problem. We suppose that the ad hoc network follows IEEE802.11 MAC protocol (IEEE 1999), which uses RTS/CTS handshake to avoid collisions. If two nodes are transmitting a packet to their own destinations at the same time, one destination node may be interfered by another transmitting node which is not aware of this problem. This is illustrated in Figure 6.1: when node C has a packet to D, it broadcasts RTS packet and

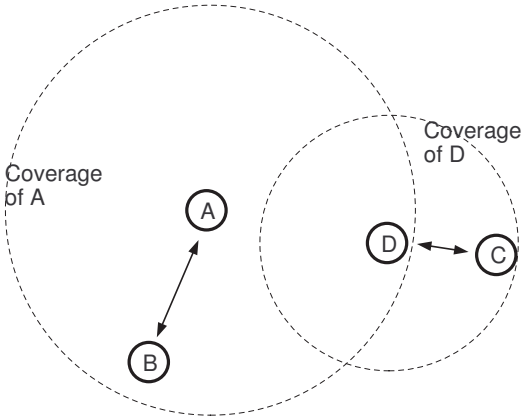

Figure 6.1: Power imbalance problem: when A is transmitting to B, it violates the communication between C and D.

D replies a CTS packet by adjusted power. This signal cannot be heard by A, because the distance between C and D is shorter than that between A and B. Thus both A and C transmit simultaneously and cause collision at D.

This problem can be solved by setting maximum power when transmitting RTS and CTS packets. That is, in Figure 6.1, when node D has received a RTS packet (which is sent with maximum power), it replies a CTS packet with maximum power. This will of course prohibit any possible transmission in its full power coverage. Node A will be notified and will not transmit during the time specified by the CTS from D. However, when we consider the situation given in Figure 6.2, this solution will prohibit the simultaneous transmission even they may not interfere each other.

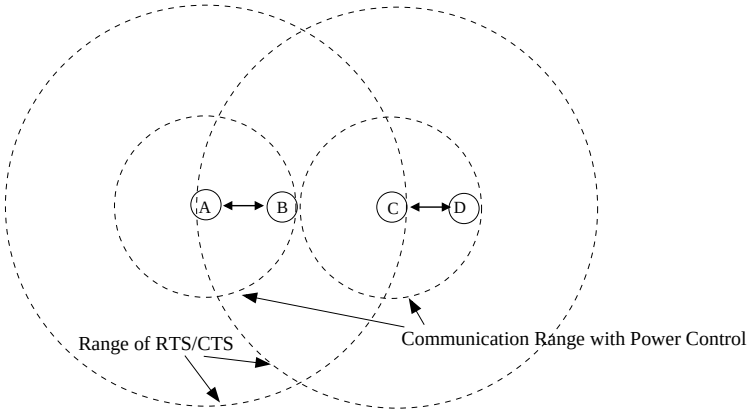

Figure 6.2: Simultaneous transmissions between A and B, C and D are possible, but prohibited by RTS/CTS

6.3 Power Control Routing

Based on the result of (Cano & Manzoni 2000) and related works, it shows that reactive routing protocols such as AODV and DSR give better performance than their proactive counterparts. Here we propose a power control routing scheme for reactive routing protocols.

We assume that a route in ad hoc networks is always a duplex link. All the nodes in the network have normalized the transceiver, i.e., with the same maximum transmit power and the same variation scale.

6.3.1 Uplink and Downlink Power Control

In AODV or DSR protocol, when a route is to be established, the source node initiates a *Route Request* (RREQ) packet, which is broadcast to all its neighbours. For power control issue, we assign each intermediate node two distinguish transmit power values for uplink $P_{TX_{up}}$ and downlink $P_{TX_{down}}$, respectively. For the source and the destination nodes, there is only one direction that either $P_{TX_{up}}$ or $P_{TX_{down}}$ is available. As depicted in Section II, when a node sends a packet, it embeds its transmitting power into the packet, which is RREQ at here. Because the source node doesn't know the location of its neighbours, it will broadcast the RREQ packet with maximum power. The nodes that have received the RREQ can adjust its uplink transmit power by equation (6.1).

The same broadcast will continue by the neighbours with maximum power until the RREQ packet reaches the destination. The destination node will send a *Route Reply* (RREP) packet to its uplink node, the same, with embedded transmit power data. The node that receives this RREP can now adjust its downlink transmit power by equation (6.1). This procedure can be illustrated by Fig. 6.3.

After a route has been established, equation (6.1) can be applied for both uplink and downlink power adjustment along the route when DATA packets and their ACK are exchanged hop-by-hop.

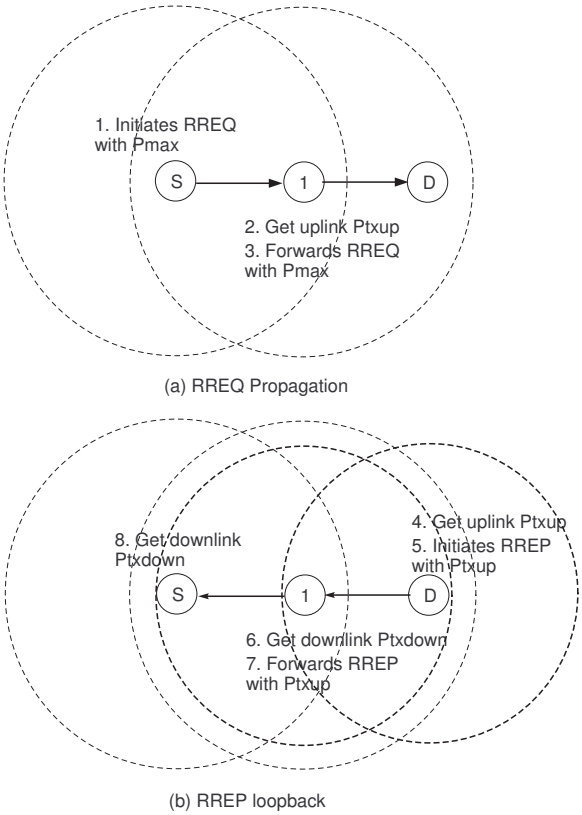

Figure 6.3: Route Establishment with Power Control

6.3.2 Energy Efficient Route Finding

When a RREQ packet is sent with maximum power as depicted previously, it is possible that several neighbours with different distance to the source will receive it. This may result to that a less efficient route will be selected, as shown in Figure 6.4.

In the figure, a route is to be established from nodes S to D. According to section 3.3.2, a moderate hop distance will have best energy efficiency, therefore the optimal route is S-1-2-3-D. However, S initiates a RREQ with maximum power; both nodes 1 and 2 will receive it. First there is a contention between node 1 and 2 to relay the RREQ. If node 2 gets the chance first, both nodes 3 and D will receive the RREQ and D will send RREP upon the reception immediately. Thus a less efficient route S-2-D is established. Actually this is true when original AODV or DSR is applied. On the other hand, if node 1 wins the contention and forwards the RREQ packet, both nodes 2 and 3 will receive it. In the case node 2 has already received the same RREQ once. It will discard the packet according to

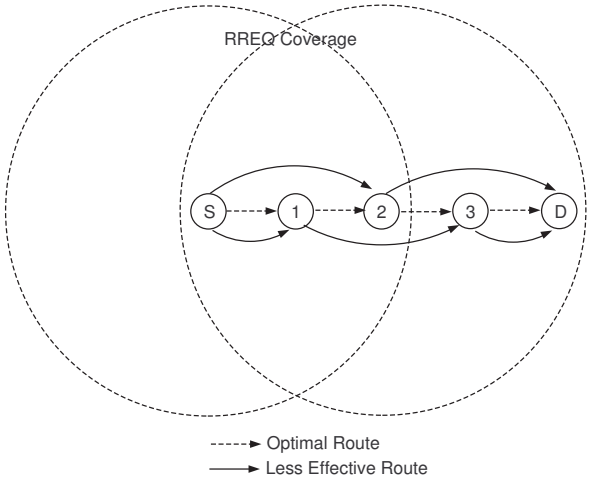

Figure 6.4: Route Selection with Maximum RREQ Power

AODV and DSR protocols. Now it is for nodes 2 and 3 to compete for the channel. We will get another less efficient route S-1-3-D if node 3 wins the contention.

In order to find the optimal energy efficient route, two rules are deployed. The first is that every intermediate node holds a transmission back-off interval according to the received RREQ signal power. As mentioned at beginning, we've assumed that all the nodes here have normalized transmitter power. Upon receiving a RREQ packet, it is possible for the node to estimate the distance between the uplink node and itself by radio propagation equation:

$$P_{RX} = \frac{KP_{TX}}{D^{\alpha}} \tag{6.2}$$

According to (Doshi et al. 2002), there exists an optimal distance D_{opt} by which the minimum hop-by-hop power consumption is achieved. We denote the received signal power as $P_{RX_{opt}}$ when D_{opt} is given by equation (6.2).

The back-off time is set according to the ratio of actual received signal power to $P_{RX_{opt}}$, denoted as:

$$T_{bk} = c\|P_{RX} - P_{RX_{opt}}\| \tag{6.3}$$

Here c is a constant. This rule will guarantee that a more energy efficient hop will be chosen. Apply this to Fig. 6.4, node 1 will send RREQ before node 2.

The second rule is about multiple RREQ receptions. If we look at Fig. 6.4 again, we will get node 1 to relay the RREQ first. Both nodes 2 and 3 will receive it, but node 2 has received one RREQ already. By original rule node 2 will discard the

second RREQ. Unfortunately this will result to route S-1-3-D selected. However, it is possible for node 2 to compare the received signal power of these two RREQ packets. If the condition satisfies:

$$\|P_{RX1} - P_{RX_{opt}}\| > \Delta + \|P_{RX2} - P_{RX_{opt}}\| \tag{6.4}$$

then the node that receives the new RREQ will replace the uplink node by the current one. Here P_{RX1} and P_{RX2} are the received signal power of previous RREQ and current RREQ, respectively. Δ is a safety margin to tolerate signal fluctuations. It means the node that generates the second RREQ is closer to the optimal distance. The node will replace the previous uplink node by the current one. Back to Fig. 6.4, if node 2 backs-off its RREQ, it will receive the second RREQ from node 1, with the signal power satisfying equation (6.4). Thus node 2 will replace the uplink node from S to 1. Because the second RREQ that node 2 received has better power condition to equation (6.3), node 2 will send the RREQ before that of node 3, which has received a RREQ from node 1 already. The same update will happen on node 3 thus the optimal energy efficient route S-1-2-3-D is established.

One situation needs to be considered, as shown in Fig. 6.5. In the figure, both nodes 1 and 2 are located far away from the source with about the same distance, they will back-off the relaying of RREQ by approximately the same T_{bk}. If we assume that node 1 wins the contention, it will send RREQ to 2 and 3. Node 2 will replace its uplink node from S to 1 because the later one has better energy performance according to equation (6.4). When node 2 broadcasts the RREQ, node 3 will replace its routing data because node 2 shows a better energy budget than that of node 1. Thus a less efficient route S-1-2-3-D is established.

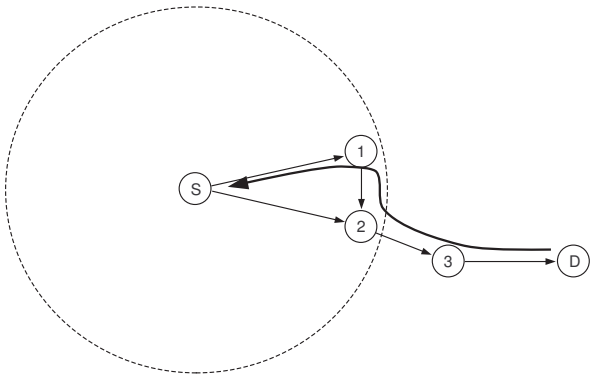

Figure 6.5: Less Efficient Route

This problem can be recovered by setting a simple rule: if the back-off interval T_{bk}

is expired, the node will drop any duplicated RREQ. We can see that the optimal route S-2-3-D will be selected as illustrated in Fig. 6.6.

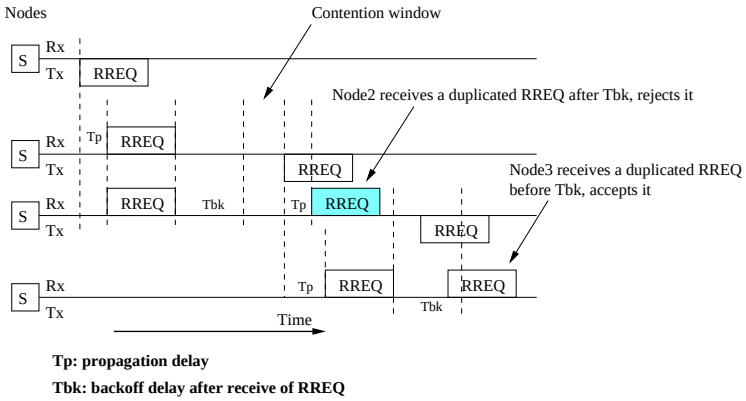

Figure 6.6: Contention window plays role to select route

6.3.3 Summary of Power Control Routing Protocol

Here we summarize our power control routing scheme:

1. Hop-by-hop power control is achieved by equation (6.1).
2. RTS/CTS handshake uses maximum power to avoid collisions.
3. RREQ is broadcast with maximum power.
4. An intermediate node backs-off RREQ packet. The back-off interval is proportional to the difference between the received signal power and an optimal value.
5. Upon receiving a duplicated RREQ packet, the node compares it with the previous one. If found it is better, it will update its routing table.
6. A node should drop all the RREQs that come after the back-off interval.

6.4 Energy Efficiency Analysis and Simulation Results

The power control routing scheme proposed at here cannot increase the network capacity because maximum power is used in RTS/CTS handshake. This is neces-

sary to avoid collisions. However, the scheme can select an energy-optimal route based on any reactive routing protocol. Meanwhile, a moderated transmitter power reduces the interference to other receiving nodes thus will improve the reception quality. By this means it increases the network throughput because the rate of retransmission is reduced. A back-off of RREQ packet forwarding is introduced, proportional to the difference between the received signal power and the optimal one. This will increase the route establishment latency. However, when the node density is high, this is not a problem. The routing latency in a dense network becomes lower because the back-off delay T_{bk} approach to zero if there are always nodes available at optimal distance. In original AODV, all the nodes in the radio coverage of a transmitting node receive the RREQ and all will start channel contention. In our scheme, this is scattered by the distance equation (6.3). If the density of network is properly high, there are always nodes located at the proper distance from the RREQ-source node and these nodes will start contention to relay RREQ earlier than other nodes. It means that fewer nodes will join the contention thus latency is reduced.

6.4.1 Simulation Environment

A simulation model is setup for the scheme described above. We compare the energy efficiency performance of our algorithm with other three schemes: the original AODV, AODV using MAC-layer power control(Jung & Vaidya 2005), and PARO described in Sec. 6.1. Mobility is set as random walk with moving speed between SPEEDMIN to SPEEDMAX m/sec. After the arrival of a destination, a node will stay there (pause) for a random time from PAUSEMIN to PAUSEMAX seconds and then randomly select another destination and moving speed. Traffics are generated as *Constant Bit Rate* (CBR) with 512 bytes user data in each packet. Every traffic link will transfer 1000 packets at a rate of 4 pakcet/sec. The simulation time is 250sec.

For the power control, the transmitter power level is rectified into 4 stages: 1 (level 4), 0.5 (level 3), 0.2 (level 2), and 0.1 (level 1). We set the radio path loss factor $\alpha = 4$ and assume 200m can be covered by the maximum power (level 4), and receiver sensitivity is -96dBm, antenna gain $K = 1$. Thus by the power levels we set, the radio coverage radius are 200m, 158.74m, 119.96m, and 92.83m, respectively.

The results are given in the following figures.

In this model we don't consider the energy consumptions taken at MAC and network layer, such as RTS/CTS handshakes, broadcasting of RREQ and replying RREP, etc, because the protocols been examined here all use maximum power for them and result in identical power consumption.

6.4.2 Simulation Results and Discussion

6.4.2.1 Route Length and Energy Efficiency

An example of the routing results by the three protocols is given in Fig. 6.7, in which AODV gives the shortest path (5 hops) from the source node (ID=24) to the destination node (ID=03), meanwhile PARO produces the longest path (8 hops), and PAR has moderate hop count (6 hops). Fig. 6.8 shows the statistics of route distance of 100 randomly selected source-destination pairs. It can be seen when the network scale (node number) increases, all the three routing algorithms have longer route distance. Among them PARO gives longest route distance, AODV gives the shortest, and PAR's is slightly higher than AODV, and both are 50% shorter than PARO. This is because PARO uses a very different mechanism, which is not based on RREQ flooding, to explore then energy optimal route.

6.4.2.2 Power Consumption and Standard Deviation

Fig. 6.9 shows the result of average energy drain of different scenarios. We can see that when packet receiving energy consumption is not considered, AODV with MAC power control, PARO, and PAR all exhibit significant energy reduction from AODV, whereas PARO is the best. This is due to the fact that PARO's *redirection* algorithm does not consider receiving energy cost at all. However, when the receiving energy is considered, PAR becomes the most energy-efficient and PARO becomes the worst except original AODV. This result supports the statement in Chapter 3 that energy consumption during receiving is not neglectable.

Fig. 6.10 shows the average route establish time, which is counted from the RREQ broadcasting from the source node to the time the RREQ comes back. Since PARO does not use RREQ/RREP flooding, and the final route establishing time is dependent on data packet generate rate as each new data packet may trigger

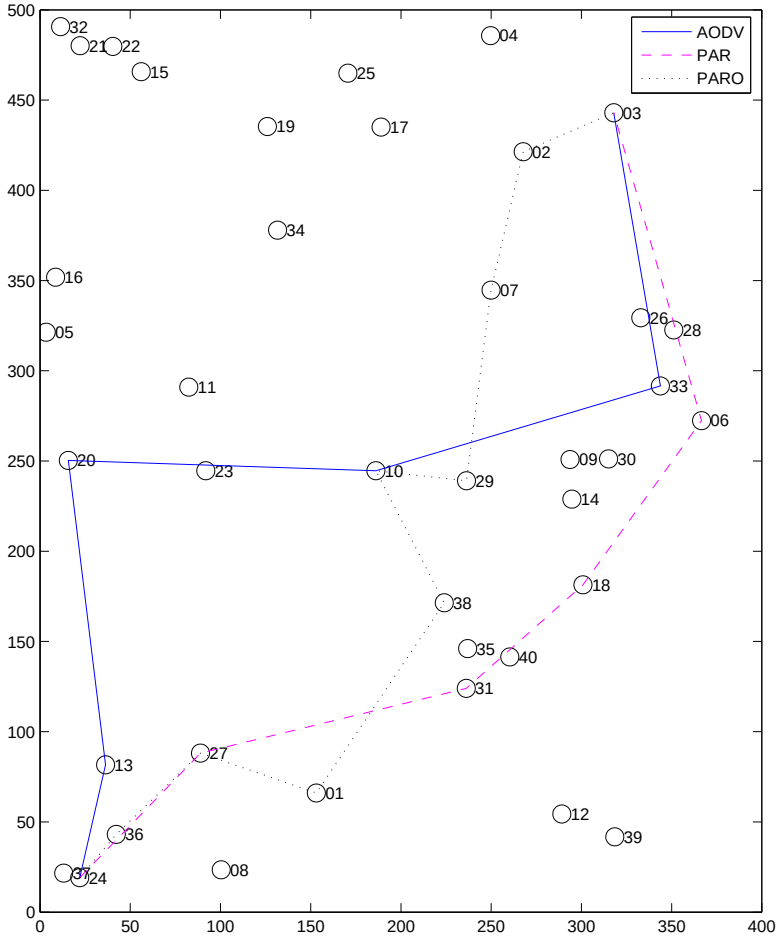

Figure 6.7: A typical result from three routing protocols

a redirection, we do not compare it in our simulations. From the figure one can see that the route establish time monotonically increases with the network scale for both protocols, and PAR's time is 30% higher in a small network, and up to 100% higher in a large network, than that of AODV. This is caused by RREQ back-off at the intermediate nodes.

6.4.2.3 Link Stability

When a node involved in a route has moved out of the radio coverage of precursor node, a link break occurs. A new route establishment approach is triggered by the precursor node sending *Route Error* RERR packet. Frequent link breaks degrade

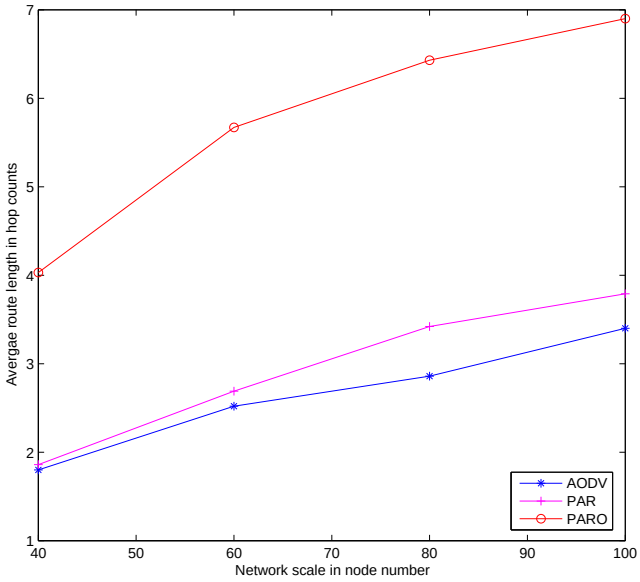

Figure 6.8: Average route distance in hop counts

the transmission performance because they cause both transmission delay and extra overheads. Fig. 6.11 shows the simulation results of link break counts of different scenarios. We have set a moderate mobility of network with randomly 1-10m/s moving speed. In our protocol, since it selects the nodes with a distance around 100m as optimal next-hop candidates, the link break is significantly less than that of the original AODV. PARO has best link stability in small scale networks. However, when the network scale increases, it exhibits a deteriorated performance. This is due to the reason that PARO produces extremely long route in large scale network thus the accumulated hop-by-hop break probability is significantly increased.

6.5 Concluding Remarks

In this chapter we have demonstrated our approach to energy conservation for ad hoc routing and compared its performance with other solutions. In a reactive routing protocol, it is possible to select a more energy efficient route by inspecting the hop-by-hop transmitting and received power when route request packet is broadcast throughout the network.

With MAC layer power control, a significant amount of energy can be saved

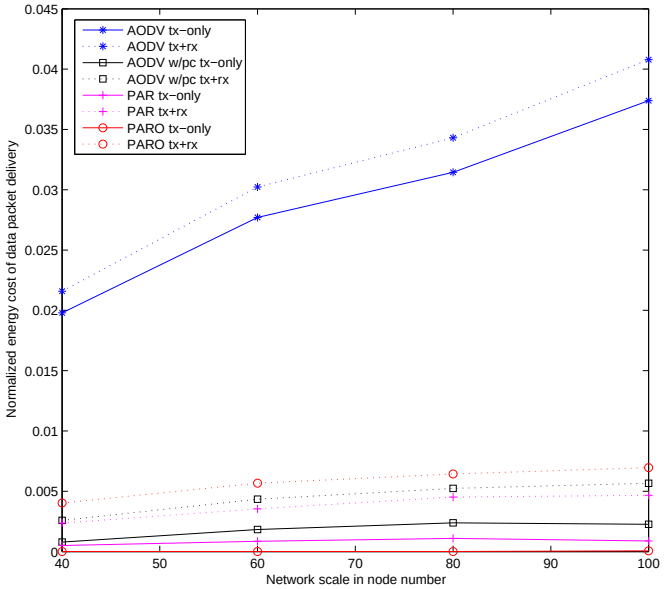

Figure 6.9: Energy cost of packet delivery

compare to that non-power-control scheme. With power-aware routing protocol presented in this paper, we obtain even better energy conservation. In our protocol, since a long hop is trend to be divided into shorter multihops, more nodes are involved into the network activity evenly. This makes energy drain even in the network and increase the overall network lifetime.

With proper distance of a hop, the link can endure more node mobility and the probability of route broken is reduced. This will increase the transmission performance and reduce the network overhead.

The power control routing scheme we proposed here is simple to be implemented on any reactive ad hoc routing protocol, even though we deployed AODV in our simulation. The scheme also requires that transmitter power scalable. This is not a technique problem because there are products available for this purpose.

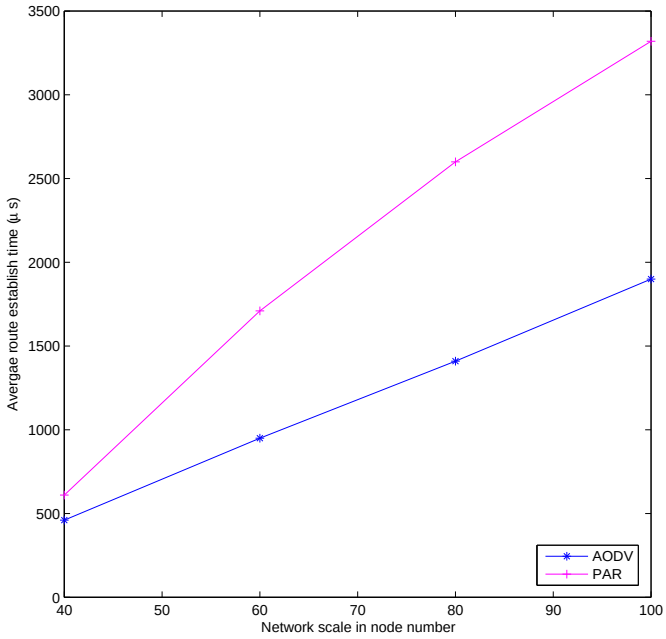

Figure 6.10: Average route establish time (AODV and PAR only)

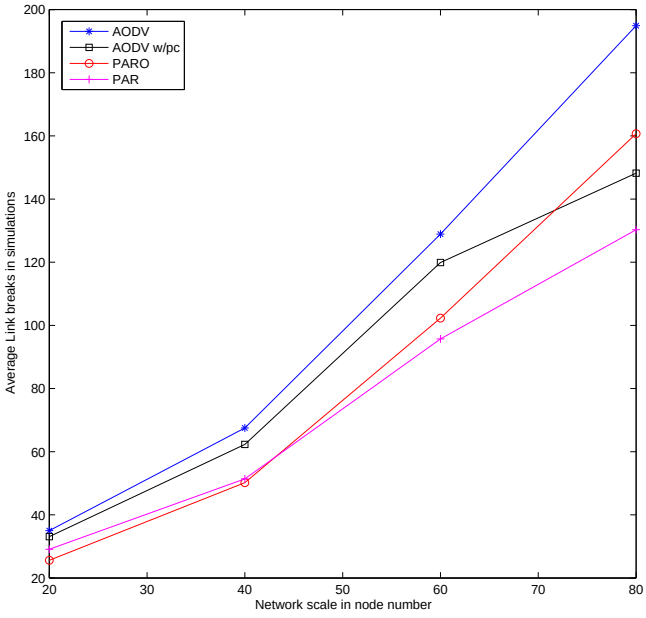

Figure 6.11: Link stability statistics

7 POWER-AWARE ROUTING TO COPE WITH COMMUNICATION GRAY ZONES

7.1 Introduction

Communication Gray Zone (CGZ) problem was discovered in (Lundgren, Nordström & Tschudin 2002). (Kim, Lee, Kwon, Lee & Choi 2007) have also reported that gray zones exist in carrier sensing and packet reception from their IEEE802.11a testbed measurement results. A CGZ in ad hoc network is defined as an area in which data messages can not be exchanged although the HELLO messages indicate neighbor reachability, as shown in Figure 7.1. A node in CGZ suffers very high packet drop rate.

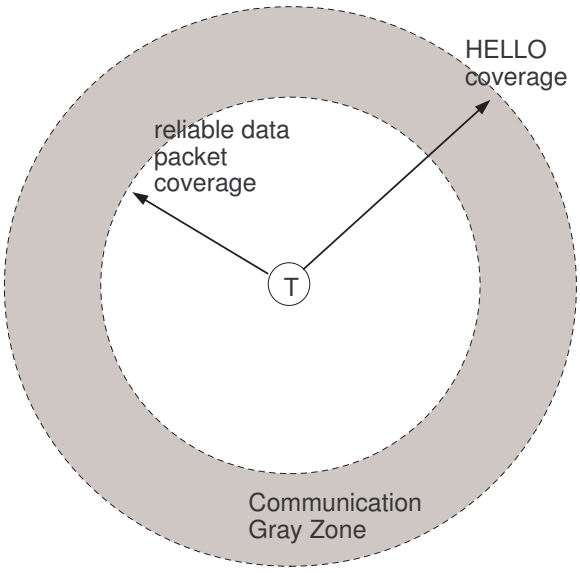

Figure 7.1: Communication Gray Zone

The CGZ problem comes with reactive routing protocols such as AODV (Ad hoc On-Demand Distance Vector). AODV relies on neighbor sensing to keep track of those nodes which are used as relay points for data transmissions in a multihop path. To achieve this, AODV uses periodic HELLO messages. The

communication gray zones are caused by the different properties between HELLO and DATA packets. The reasons are:

- Different Transmission Rate - control messages are sent at a basic bit rate while data packets are usually at higher bit rates. Transmission at lower bit rates is more reliable than that at higher rates.

- No Acknowledgements - Receiving a broadcast HELLO message doesn't mean that transmissions are reliable in the opposite direction.

- Small Packet Size - Control messages are shorter than data packets, thus are less prone to bit errors.

- Fluctuating Links - At the transmission borderline, communication tends to be unreliable. A successful HELLO receive doesn't mean that consistent communication is also possible.

In (Lundgren et al. 2002), some methods are proposed to eliminate the communication gray zone, including 1) exchanging neighbor sets, 2) N-consecutive HELLOs, and 3) SNR (Signal-to-Noise Ratio) threshold for control packets. Among them the SNR threshold method achieves the best performance. However, the experimental scenario they deployed was relatively simple. (Aguero, Galache & Munoz 2009) recently analysed the relationship between Signal-toNoise Ratio (SNR) and Frame-Error Rate (FER) of IEEE802.11 at different transmitting bit rate and proposed an SNR-AWARE DSR protocol to cope with the problem. In this chapter we deploy a modified Power-Aware Routing (PAR) protocol as depicted in Chapter 6, in which the nodes in CGZ will not be selected as routing devices. The protocol also enables the nodes keep monitoring the link quality through a route. When the node is moving into a gray zone, a new route-establishment procedure will be invoked to prevent the CGZ phenomenon.

The solution proposed in this chapter is based on the reports and analysis from MANET. However, CGZ is a common phenomenon in all wireless communication systems if the facts listed above present. In recent work the idea has been borrowed to solve link stability problem in IEEE802.15.4 sensor networks in Cinet. We have observed a significant packet delivery ratio improvement.

7.2 Power-Aware Routing Protocol

7.2.1 Range of Gray Zones

The actual shape of CGZ is usually an irregular circular area around a transmitting node due to the variation of co-channel interference and geographical environment of the network. For this reason we select the signal-to-noise ratio as measure to detect the gray zone. It is also possible to use bit error rate (BER) or packet error rate (PER) as measurement, as it can be shown that BER/PER are monotonous functions of SNR. The current 802.11 hardware measures the link quality in terms of SNR(YDI-Wireless n.d.).

In (Clark, Leung, McNair & Kostic 2002), the authors found that the BER and PER of IEEE802.11b radio link are approximately inverse-proportional to the receive SNR. They also inspected the BER and PER of IEEE802.11b at different bit rates. To achieve the same PER, 1Mbps (Barker-1 modulation) rate requires approximately 4dB lower E_b/N_0 than that of 11Mbps (PBCC-11 modulation). Think of the radio power attenuation formula Eq. 6.2 wherein α is the path loss factor varying from 2 to 5 in different environments, the range of 11Mbps rate is from 63% to 83% of that of 1Mbps for a 4dB gap.

The PER results given in (Clark et al. 2002) were measured on a fixed packet length, which is 1000 bytes. To find the effect of packet length, we deployed a MATLAB Wireless LAN toolbox (CommAccess 2003) to check the PER for different packet lengths and bit rates. In this MATLAB simulator, we set the DATA packet 512 bytes and the HELLO packet 50 bytes. The simulation shows that an approximately 4dB SNR reduction will make the PER of HELLO packets equal to that of DATA packets. This result coincides with that of (Clark et al. 2002).

Datasheet of Cisco Aironet 350 WLAN PC card (Cisco 2004) also gives a hint to estimate the range of CGZ. Table 7.1 shows the transmission ranges at 1 and 11Mbps, respectively for both indoor and outdoor environments. These results were measured under the normal data packet transmission. The range of CGZ is around 60% for both indoor and outdoor environments.

In (Dominique & Guerin-Lassous 2003), IEEE802.11 throughput was measured over distance. With a full range of 150 meters, the throughput of UDP transmis-

Table 7.1: Cisco A350 radio range

Rate	Indoor	Outdoor
1Mbps	107m	610m
11Mbps	40m	244m

sion dramatically decreases beyond 75-90 meters. This indicates that the CGZ is about 40-50% of the full range.

Based on the previous results, we found that the range of gray zone seems relatively large. Later in our simulation, we will set rest 40% of radio coverage to be gray zone. In another word, we define *Communication White Zone* (see Figure 7.1) that has a radius $D_{WZ} = 0.6D_{\max}$.

7.2.2 PAR Protocol to Cope with CGZ

The PAR protocol basically consists of two parts: hop-by-hop power control and energy-efficient gray-zone-avoiding routing. Hop-by-hop power control is achieved by the way that the transmitter power P_T can be embedded into a packet to let the downlink node to adjust uplink power P_T^* by Eq. 6.1.

Here we summarize the PAR protocol given in Chapter 6 with new features to cope with CGZ.

1. Hop-by-hop power control. At MAC layer, RTS/CTS handshake uses maximum power to avoid collisions. Such a handshake also results to a close loop power control using Eq. (6.1) so that the DATA packet can be transmitted at a proper power level.

2. RREQ is broadcast with maximum power. Thus upon the reception of a RREQ, the node is able to calculate the *hop weight* by $W_h = |P_r - P_{opt}|$. Here P_r is the received power and P_{opt} is the ideal power that the transmitting node locates at *optimal distance* D_{opt}. D_{opt} depends on the gray zone range. We set $D_{opt} = 0.5D_{\max}$.

3. An intermediate node i accumulates the *hop weight*, denoted as $\sum_i W_{h_i} = W_{h_i} + \sum_{i-1} W_{h_i}$ and puts it into the outgoing RREQ. Upon the receiving of a duplicated RREQ, the node compares the new W'_{h_i} with the previous one. If it is found that $W'_{h_i} < W_{h_i}$, the node will update its routing table.

4. A Gray Zone Alarm (GZA) RERR is issued when a node which is already using maximum transmit power has detected several consective reception failures. A failure is detected when the result of Eq. (6.1) is greater than a threshold, denoted as

$$P_T^* > P_{GZA}. \tag{7.1}$$

5. When a DATA packet is to be transmitted, the RTS/CTS handshake will give the transmitting node possibility to estimate the required transmit power and adjust the power accordingly.. If it is found that current power level is not enough for a secured transmission, the node will increase the power until it uses the maximum power.

7.3 Analysis and Simulation Results

The PAR scheme deployed here can select an energy-optimal route based on any reactive routing protocol. A moderated hop distance will less likely lead to gray zone phenomenon. Meanwhile, a moderate transmit power will reduce the interference to other nodes thus improve their reception quality. It means that the network throughput is increased because the rate of retransmission is reduced.

7.3.1 Simulation Environment

A simulation model is setup for the gray zone problem described above. Different scenarios in respect of node density, node mobility, and network scale are simulated. We compare three different routing schemes: the original AODV, the AODV with control packet SNR threshold (noted as AODV-th hereafter), and the PAR protocol with gray zone features. The second scheme is one of three schemes proposed in (Lundgren et al. 2002) with the best link performance. Here control packets include HELLO, RREQ, RREP, RERR, and MAC layer control packets such as RTS/CTS/ACK. In our simulator, The SNR threshold is set for AODV-th that DATA packets and control packets can be received at the same distance, i.e., only those nodes within the range that DATA packet can be reached are regarded as network neighbours.

Nodes are set to move in a rectangular area in random waypoint model. Traffics are generated as *Constant Bit Rate* (CBR) with 512 bytes user data in each packet.

Every traffic link will transfer 100 packets at a rate of 4 pakcets/sec. 10 CBR links are established.

The radio transmit power is rectified into 6 stages. This is based on the Cisco A350 datasheet as shown in Table 7.2. We assume 200m can be covered by the maximum power (level 6). Thus radio coverage radii of other levels can be determined by Eq. (6.2), as shown in Table 7.2. We set $D_{WZ} = 0.6D_{\max}$, i.e., for the power level 6 with a coverage of 200m, range between 120m and 200m is regarded as gray zone. The optimal distance is set within the range between power level 1 (63.25 m) and 2 (94.57 m).

Table 7.2: Available transmit power settings (from Cisco Co. Ltd.)

Level	**Power**	**Range**($\alpha = 4$)
1	1 mW (0 dBm)	63.25 m
2	5 mW (7 dBm)	94.57 m
3	20 mW (13 dBm)	133.75 m
4	30 mW (15 dBm)	148.02 m
5	50 mW (17 dBm)	168.18 m
6	100 mW (20 dBm)	200 m

7.3.2 Simulation Results and Discussion

7.3.2.1 Packet Drop Rates

Fig. 7.2(a) shows the packet drop rates among three schemes in different scenarios: node densities, mobilities, and network scales. Both AODV-th and PAR have very low packet drop rate. When the network scale increases, the average hop count of routes increases, therefore it can be observed that drop rate increases for all the three schemes. However, the increment of PAR and AODV-th is less significant than that of AODV. The packet drop rates are stable in respect of node density for all the three schemes. When mobility increases, both AODV-th and PAR have increased drop rate while AODV doesn't show big change.

7.3.2.2 Link Stability

In PAR, since the nodes at a moderate distance are more likely to be selected, the link break probability is significantly less than that of the original AODV.

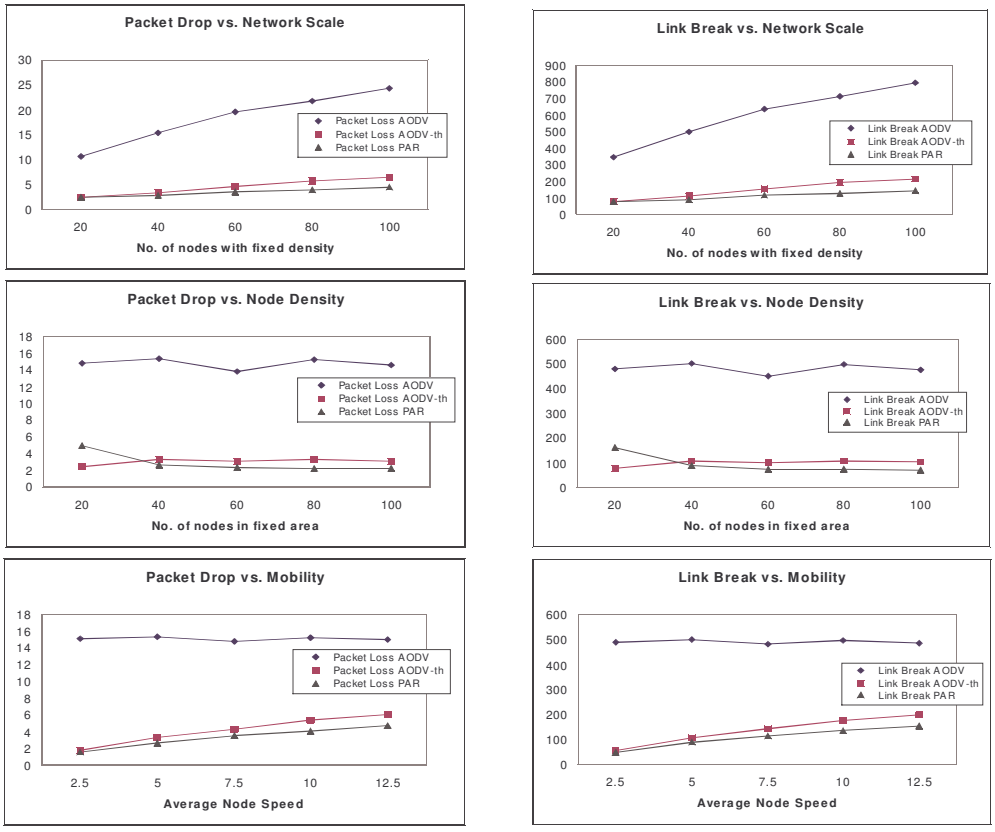

(a) Packet Drop Rates (b) Link Breaks

Figure 7.2: Packet Drop Rate (a) and Link stability (b)

Fig. 7.2(b) shows the simulation results of average link break counts in different scenarios. In all the cases PAR and AODV-th show very low link break compare to AODV; When the node mobility and the network scale increase, AODV's link break increment is the most significant. These figures correspond to those packet loss figures.

7.3.2.3 Energy Consumption and Standard Deviation

Figure 7.3 shows the result of total energy drain. In all the cases AODV-th consumes much more energy than that of AODV and PAR. When the network scale increases, all the schemes show an increment of energy consumption, because the average hop count increases. Among them the increment of AODV-th is more significant. It seems that node density and mobility do not affect the energy consumption of all these three schemes. The disadvantage of AODV-th and AODV routing can be explained as: AODV-th tends to select nodes that are too close to

the precursor, while AODV tends to select nodes in a gray zone.

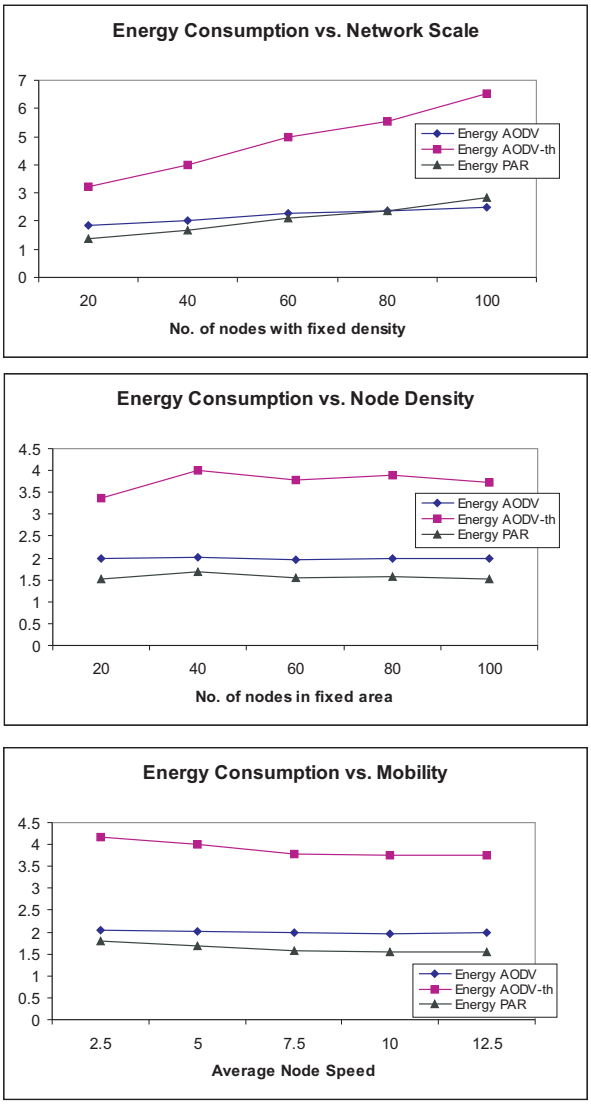

Figure 7.3: Average Energy Drain

Another important metric is the standard deviation of energy drain. A network with more even energy drain among the nodes has longer network lifetime (Cho & Kim 2002, Jäntti & Ki 2005). Figure 7.4 is the standard deviation of energy drain when the node density increases. It shows that PAR gives the least standard deviation of energy drain among these three schemes while AODV-th performs the worst.

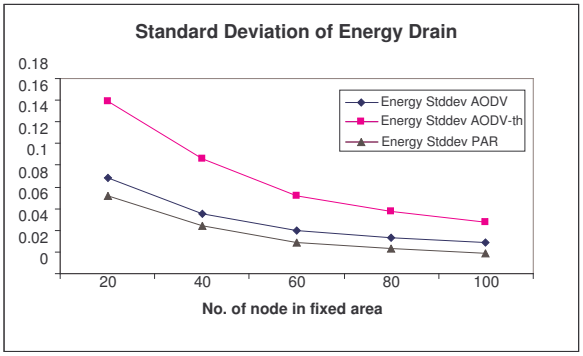

Figure 7.4: Standard Deviation of Energy Drain

7.4 Cinet Implementation Results

We adopted this idea in Cinet Sync2Sink protocol. The Cinet Sync2Sink protocol applies a global synchronization protocol described in Chapter 9. When the SYNC frame is broadcasted, which is similar to RREQ broadcasting in AODV or DSR, each node receives a new global timestamp. In the meantime each node is able to estimate the link quality to the node who sends the SYNC frame[1]. A threshold of LQI or RSSI has been selected to select the upstream nodes as relays to the Sink.

We set up a network with 9 routing nodes and 5 noise sensor nodes in our laboratory. According to (Srinivasan & Levis 2006, Maheshwari, Jain & Das 2008) and a number of related works, an LQI threshold $LQI_{th} > 90$ or equivalently $RSSI_{th} > -60$dBm indicates a Packet Reception Ratio (PRR) 90% or higher.

Fig. 7.5 shows the data frame delivery ratio when the hop count to sink is increased. Note that $LQI_{th} = 0$ indicates a non-Link-State routing protocol. It can be seen that at $LQI_{th} = 90$ the PRR hits the maximum value in multihop scenario, which improves PRR by 10% comparing with that of $LQI_{th} = 0$. A low LQI threshold results in that the network has less number of hops from the sink to the most remote nodes, but the radio the link goodput is poor due to the long distance of the hops. On the other hand, a high LQI threshold gives good radio performance, but a remote data packet has to be relayed by more routers back to the sink, and it also aggravates the hidden node problem(Bachir, Barthel, Heusse & Duda 2005).

[1]IEEE802.15.4 MAC layer is able to report the Link Quality Indication (LQI) or Receive Signal Strength Indication (RSSI) to upper layer.

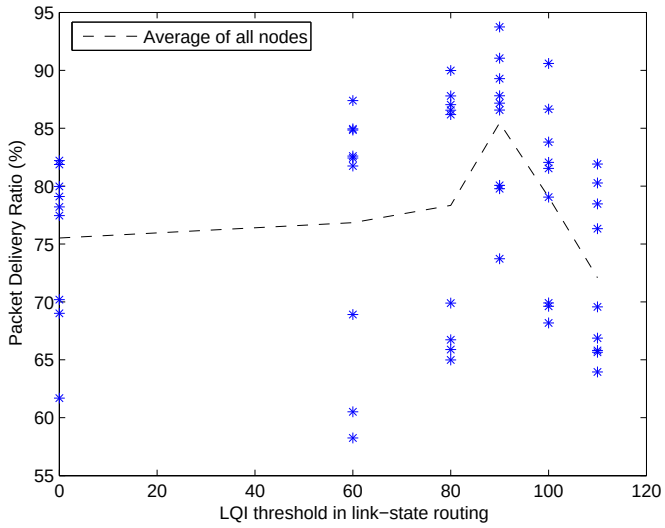

Figure 7.5: Cinet testbed throughput result using grayzone elimination

7.5 Concluding Remarks

With PAR protocol we deployed and modified in this chapter, we obtained significant reduction of packet drop rate and link breaks, which is usually caused by the communicaton gray zones. With proper distance of a hop, a link can endure more node mobility, and the probability that a route breaks decreases. This will increase the transmission performance and reduce the network overhead. AODV-th also gives good link stability and small packet drop rate. The disadvantage of AODV-th is that, since there is no power control routing, a hop distance tends to be very short compared to the utilized transmit power level, it decreases the energy performance.

In PAR protocol, since a long hop is trend to be divided into shorter multihops, more nodes are involved into the network activity evenly with proper transmit power. This makes even energy drain in the network and thus increases the overall network lifetime.

8 LINK-STATE CLUSTERING ALGORITHM AND ENERGY PERFORMANCE STUDY

8.1 Introduction

MANET can be categorized into two types depending on the features of wireless devices: homogeneous and heterogeneous. In a homogeneous ad hoc network every mobile device has the same amount of resources such as radio capacity, battery energy, transmission rate, etc.; while in a heterogeneous ad hoc network mobile devices have different amount of resources. Furthermore, MANET can be also classified as peer-to-peer (i.e., flat) networks or hierarchical (i.e., clustered) networks.

Most of ad hoc routing protocols such as DSDV, AODV, and DSR are designed for flat networks. Research shows that when the network scale becomes large, these protocols generate significant routing overhead and finally make the network performance unacceptable (Cano & Manzoni 2000, Das, Perkins & Royer 2000, Perkins & Royer 1999). For this reason, clustered ad hoc networks are considered to be better solutions for large scale ad hoc networks (Xu & Gerla 2002, Cai, Lu & Wang 2003). Clustering is especially attractive for heterogeneous networks, since high capacity nodes are natural candidates for clusterheads.

Clustering algorithms can be classified into two categories: clusterhead-based and non-clusterhead-based (Cai et al. 2003). In (Hou & Tsai 2001), it is shown that clusterhead-based schemes outperform non-clusterhead-based scheme in term of reducing the traffic overhead for large-scale ad hoc networks. Also in a heterogeneous ad hoc network, it is convenient to construct a clusterhead-based network due to the different capacities of the nodes. There are also researches related to the clustering algorithm of non-uniformly distributed ad hoc networks (Kawadia & Kumar 2003). More general clustering discussions can be found in (Ramathandran, Kapoor, Sarkar & Aggarwal 2002) and (Chen, Liestman &

Liu 2004).

In this chapter we introduce a clustering algorithm suite, which can be applied to both heterogeneous and homogeneous ad hoc networks. The clustering algorithm is based on the radio link state between the clusterheads and slaves therefore we denote it as "Link State Clustering Algorithm (LSCA)".

8.2 LSAC for Heterogeneous Networks

8.2.1 System Model

We assume such a heterogeneous ad hoc network, in which there exists two kinds of nodes: Heavy-weight Nodes (HN) and Light-weight Nodes (LN). HNs have higher battery capacity than that of LNs. A HN has two stages of transmit power (and the radio range): the higher one P_{Tx_h} used for inter-cluster and the lower one P_{Tx_l} for its slaves. All the nodes use IEEE802.11-like CSMA/CA MAC protocol. This assumption is an abstract model of practical ad hoc networks, such as a network that contains both Personal Data Assistants (PDA) and laptops, where PDAs are regarded as LN and laptops as HN. Furthermore, we can clusterize any heterogeneous ad hoc network in a way that all the mobile nodes with their **battery capacity** E_b greater than a **threshold** E_{bth} as HN and those with battery capacity less than E_{bth} as LN.

8.2.1.1 Inter-cluster and Intra-cluster Traffic

A clusterhead is dedicated to both inter-cluster and intra-cluster traffic. A way to distribute the radio resource for these two types of traffic must be considered. It is possible for clusterheads to use different radio interfaces (i.e., different frequencies) or to use different time intervals to avoid the inter- and intra-cluster traffic collision. However, to use different radio interfaces requires more complexity of the nodes, and the energy consumption is higher. Thus we choose the second way and assume that clusterheads are synchronized.

All the nodes, HNs and LNs, are uniformly and randomly distributed. Mobility is considered in this model.

8.2.2 Clustering Algorithm

The clustering algorithm is described as follow:

1. Each HN will always act as a clusterhead, which contains a predetermined **Cluster ID** (CID) and a **Slave Table** (ST). The CID will be broadcast and shared by all its slaves.

2. A HN periodically broadcasts **BEAcon for Clustering** (BEAC) containing its CID with transmit power P_{tx_l}. The period to broadcast is T_{BEAC}, which can be either fixed or variable.

3. A LN should always be a slave of one and only one HN. If no BEAC is heard, the LN marks itself as Orphan node and keeps listening to the radio channel.

4. **Cluster Forming** A LN sets itself as clusterless when it is powered on, i.e., CID=UNKNOWN. Upon the reception of the first BEAC, the LN marks itself as a LN of the corresponding HN and sends back a **Beacon Reply** (B_REP). The HN will add it to ST. The LN also records the SNR of the received BEAC, denoted as Γ. Γ represents the **link state**.

5. **Cluster Updating** If a LN has received a new BEAC from another HN, it will compare the link state with the previous one. If $\Gamma_{new} > \Gamma_{old} + \Delta$, it updates its HN by sending two packets: a B_REP to inform the new HN, and a **Slave Cancel** (SCAN) to inform the old HN to remove it from the slave table. Here Δ is chosen large enough to prevent the link fluctuating.

This algorithm does not require any change of 802.11 firmware, i.e., MAC layer and lower protocol stack. A BEACON frame is simply a broadcasting frame containing the information described in this section.

Since this algorithm lets the slave nodes monitor the link state to its clusterhead for cluster updating, we denote it as **Link-State-Aware Clustering** (LSAC). This clustering algorithm is fully distributed. An example of LSAC heterogeneous clustering can be seen in Figure.8.1.

If a LN needs to send packets to another node, it will first forward the packet to its clusterhead. The clusterhead will first check its ST that whether the destination node is in the table. If not, it will deploy a routing protocol amongst

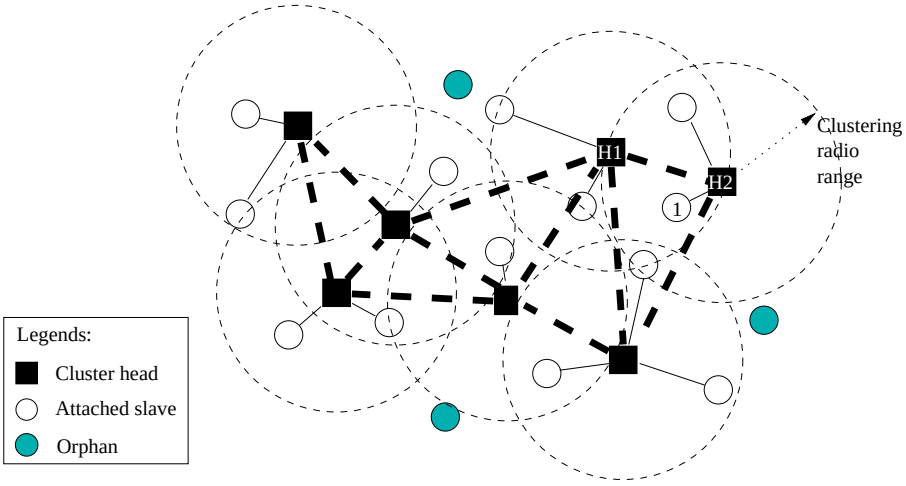

Figure 8.1: An example of heterogeneous LSCA.

the clusterheads to find a route to the destination. Because the number of nodes involved into routing dramatically decreases, so does the overall routing overhead.

8.3 Performance Analysis

8.3.1 Cluster head population

One of the most important metrics of wireless ad hoc networks is the network connectivity. In a clustered ad hoc work described in section 8.2, the network connectivity consists of two parts:

1. the connectivity of clusterheads, which is a flat ad hoc subnet, and
2. the coverage of clusterheads should cover the whole service area, i.e., every slave node should in the radio range of at least one clusterhead.

(Younis & Fahmy 2004) proved that in HEED if $R_t \geq \sqrt{5}(2 + 1/\sqrt{2}))R_c \approx 6R_c$, the cluster heads are connected, where R_t denotes the inter-cluster communication radius and R_c denotes intra-cluster communication radius. (Lin & Tsai 2006) has proved that a lower bound $R_t \geq (1+\frac{\sqrt{26+16\sqrt{2}}}{4})R_c \approx 2.75R_c$ is sufficient for cluster head connectivity.

In (Santi & Blough 2002, Koskinen 2004, Yu & Li 2003, Olafsson 2004, Gupta & Kumar 1998, Bettstetter 2002) and a number of related researches, the connec-

tivity of flat ad hoc networks is investigated in terms of network scale A, number of nodes N, and radio radius r. As claimed in (Yu & Li 2003), in order to keep a probability that every node is connected to the whole network no less than 90%, the node density must not be less than 2.5 node per unit area if all nodes have unit radio radius ($r = 1$). In (Bettstetter 2002), a lower bound of uniformly distributed random network connectivity is given. Gupta & Kumar (1998) asserted that that if n nodes are placed in a disc of unit area in $\Re^2$ and each node transmits at a power level so as to cover an area of $\pi r^2 = (logn + c(n))/n$, then the resulting network is asymptotically connected with probability one if and only if $c(n) \to +\infty$. Penrose (1997) has shown that the longest edge M_n of a minimum spanning tree of n points randomly distributed in unit area satisfies

$$\Pr(n\pi M_n^2 - \log(n) < b) = e^{-e^{-b}} \tag{8.1}$$

Hence, by setting $r = \sqrt{(b + \log(n))/n\pi}$, the connectivity probability becomes $e^{-e^{-b}}$. Now it would be easy to compare how much more power would be needed to keep the clusterhead based backbone network connected with the same probability as the flat network:

$$R_{flat} = \sqrt{(b + \log(N))/N\pi} \tag{8.2}$$

$$R_{cluster} = \sqrt{(b + \log(N_H))/N_H\pi} \tag{8.3}$$

For the second question, we suppose a uniformly distributed random ad hoc network in an area of A. Let $F(r)$ denotes the Cumulative Density Function (CDF) of distance r between two randomly selected points. Indeed $F(r)$ is a function of node density ρ, denoted as (Bettstetter 2002)

$$F(r) = 1 - \exp(-\rho\pi r^2) \tag{8.4}$$

The probability that a slave node hears at least one cluster head is then

$$\begin{aligned} \Pr(r) &= \Pr\left\{\min_i d_i \le r\right\} = 1 - \Pr\left\{\min_i d_i \ge r\right\} \\ &= 1 - \prod_i \Pr\{r \le d_i\} = 1 - (1 - F(r))^{N_H} \end{aligned} \tag{8.5}$$

here N_H is the number of cluster heads. This is called **local connectivity** of the network (Olafsson 2004). Thus the probability that all LNs are locally connected,

denoted as $\Pr_{all}$, is

$$\begin{aligned} \Pr_{all} &= \Pr\{(\text{All LNs are connected})\} \\ &= \left[1-(1-F(r))^{N_H}\right]^{N_S} \end{aligned} \tag{8.6}$$

N_S is the number of slaves.

Through the above discussion we can find out the suitable number of cluster-heads with the given radio range and node density.

8.3.2 Overhead Analysis

Overheads in a clustered ad hoc network consist of two types: clustering overhead and routing overhead. Here we compare the energy consumption taken by the clustered network proposed with flat ad hoc networks using typical reactive routing protocol such as AODV.

In a flat network using AODV, routing is a procedure of flooding RREQ packets. To estimate the energy consumption taken by one routing procedure from node S to node D, we have

$$E_{AODV} = \sum_{i,i\neq D}(E_{tRREQ} + \sum_{j\in N_i} E_{rRREQ}) + E_{RREP}. \tag{8.7}$$

here E_{tRREQ} stands for the energy of broadcasting RREQ at each node except the destination D. E_{rRREQ} is the energy consumed by a neighbor node of i for receiving the RREQ and N_i is the neighbor set of node i. When the RREQ message reaches the destination node D, D will send a RREP back to S by recuring the path. From the equation we can see that for each RREQ broadcast, there are multiple receptions of it. This is called **overhearing**. The transmission of RREP is point-to-point. Thus in a large scale ad hoc network if every node has a big number of neighbors, energy taken by delivering RREP is usually negligible comparing with that of broadcasting RREQ. Equation (8.7) shows that the energy taken by flooding RREQ consists of two parts: sending and receiving RREQ. In a fully connected network, a RREQ will be received by all the neighbours of the sending node and result in multiple RREQ receptions (overhearing), therefore energy cost of receiving is much higher than that of sending.

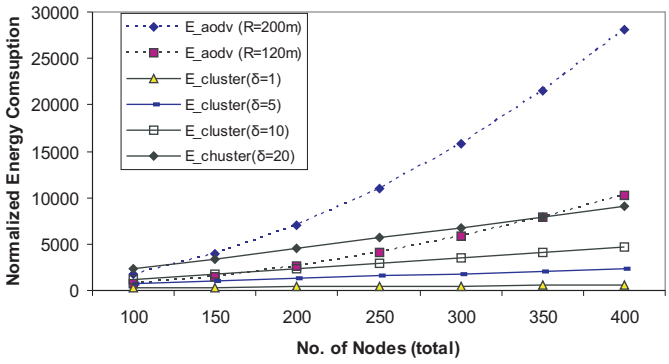

Figure 8.2: Analytical Overhead Energy Consumption Comparison

Let's suppose that in the network there are $N(N \gg 1)$ nodes, equation (8.7) becomes

$$\begin{aligned} E_{AODV_N} &= \sum_{1}^{N-1}(E_{tRREQ} + \overline{N}E_{rRREQ}) + E_{RREP} \\ &\approx N(E_{tRREQ} + \overline{N}E_{rRREQ}) \end{aligned} \tag{8.8}$$

Here $\overline{N}$ is the expected number of neighbors of the network, denoted as $\overline{N} = \frac{N\pi r^2}{\mathcal{A}} - 1$.

From above analysis we can find that in a dense flat network using AODV, the energy consumption of routing overheads follows $E_{AODV} \propto \Theta(N^2)$, if A, r are fixed.

To model the overhead cost of a clustered network, one must also consider the energy consumed by clustering activities. Thus we introduce a metric—the ratio of routing events λ_r and clustering event λ_c, denoted as

$$\delta = \frac{\lambda_c}{\lambda_r} \tag{8.9}$$

δ stands for the average number of clustering events between any two routing events, thus we can derive the energy cost of clustered routing:

$$\begin{aligned} E_C &= E_{AODV_{N_c}} + \delta E_{cluster} \\ &= E_{AODV_{N_c}} + \delta N_c(E_{tBEAC} + \overline{N}_s E_{rBEAC}) \end{aligned} \tag{8.10}$$

here $N_c, \overline{N}_s$ are the numbers of HNs and average slaves of one HN, respectively.

Table 8.1: LSAC Simulation Settings

Area	600m x 600m
No. of Nodes	50 to 300
No. of HNs in Clustered mode	30
AODV mode Tx power	800mW
Cluster mode HN to HN Tx Power	800mW
Cluster mode HN to LN Tx Power	300mW
Rx Power in all cases	400mW
AODV mode radio range	200m
Cluster mode HN to LN radio range	120m
Mobility	2.5m/s, waypoint
Traffic amount	40 random CBR
Simulation time	50sec.
Re-clustering interval	3sec.
Media Access Control	IEEE 802.11
Radio path loss factor (α)	4
Bit rate	2 Mbps

Figure 8.2 shows the energy cost of overheads for different scenarios in a square area of $\mathcal{A} = 600 \times 600m^2$. In the figure, we present two flat AODV results with node radio range of 120m and 200m, respectively. For the clustered model, the radio range between HNs is 200m and between HN and LN is 120m. Four different clustering rates δ are given. We can see that when δ is less than 10, the clustered model outperforms flat AODV in most cases. Nevertheless, $\delta = 1$ is enough for accurate routing. It seems that reducing the radio range of a flat network will result in less overhead energy consumption. However, this will make two problems worse: 1) increase the number of hops thus increase the end-to-end transmission delay, and 2) increase the hop count will make the connections less stable, thus result in more re-routing procedures, which also consumes more energy.

8.4 Simulation and Result Analysis

Simulation environment settings are as shown in Table 8.1. Figure 8.3 shows the overall energy cost of some flat AODV and clustered modes in different node populations. Please note that y-axis is in logarithm scale. It can be seen that when the network scale is not big (i.e., 50 nodes), the clustered mode does not give advantages in term of energy consumption. As the network scale grows, clustered modes show no significant energy drain increment, but flat networks

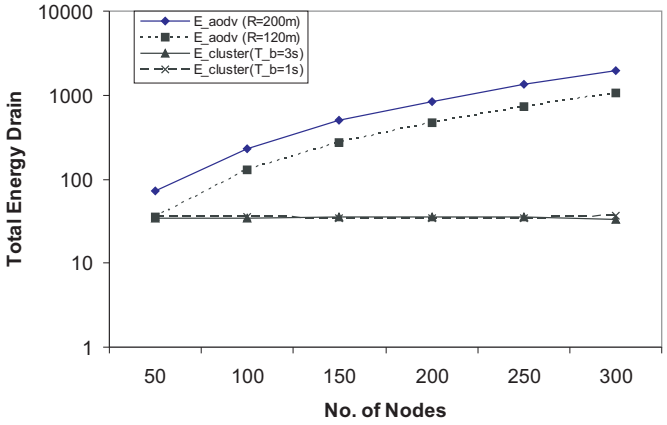

Figure 8.3: Energy Consumption Comparison

energy consumption increases dramatically. Since in all the scenarios the traffic amount is constant, we can assert that in a large-scale flat ad hoc network, the energy consumed by routing overhead is dominating. On the other hand, a large-scale clustered network gives much better and stable energy performance. When the number of network nodes increases, energy taken by routing/clustering slightly increases.

8.5 LSAC for Homogeneous Networks

The LSAC algorithm given in Section 8.2 is designed for heterogeneous ad hoc networks, in which the nodes are pre-determined to be HNs or LNs. Also, the population of HN is pre-deterministric according to the service area. However in many cases, the total number of nodes and the size of service area are unknown, or nodes are homogeneous that we cannot pre-determine that which nodes will act as clusterheads. In this section, we propose a modified LSAC, denoted as **LSAC-ho**, which can be applied to homogeneous ad hoc networks.

In order to select clusterhead, we suppose that every node holds a budget variable for clusterhead election. The budget can be its battery residual, or elapsed time it has been acting as a clusterhead, etc. Every node has two transmission power levels: the higher one is used to communicate with other clusterheads when it is acting as a clusterhead. There are 3 issues need to be considered: cluster forming, clusterhead re-electing, and clusterhead canceling. Following rules are given:

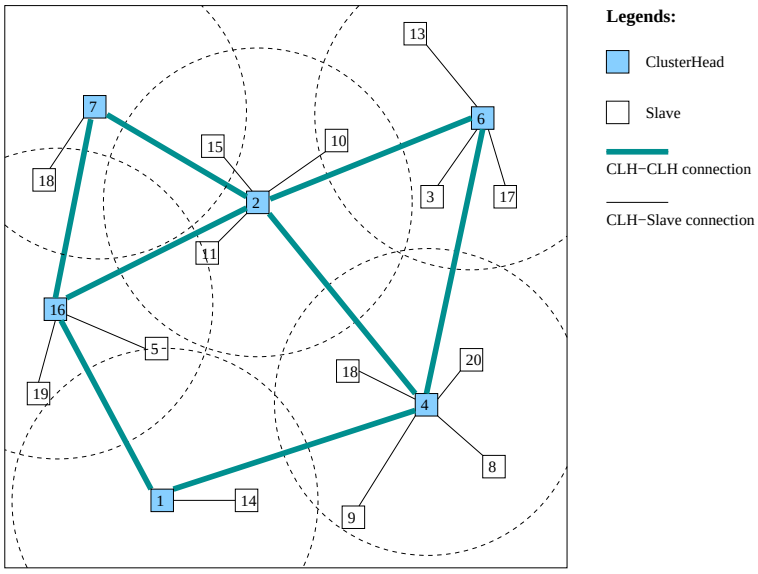

Figure 8.4: Dynamic cluster forming scenario (The number on each node is the time sequence that the node comes to alive)

1. **Cluster Forming** When a node is powered-on, it marks itself clusterless and sets up a random waiting timer T_w and starts to monitor the radio channel for BEAC. We set $T_w > T_{BEAC}$ so that a node has higher priority to be a slave of its nearby clusterhead. If no beacon is heard within T_w, the node mark itself as a clusterhead. Once a node is notified as clusterhead, it sends a BEAC immediately.

2. **Clusterhead Re-electing** A slave embeds its budget γ_b in B_REP packets. If a node is set as clusterhead, it starts a timer T_h for acting as clusterhead. When T_h expires, it selects the node that has highest γ_b as the next clusterhead and sends it a packet to notify it.

3. **Clusterhead Canceling** If a clusterhead hears a BEAC from another clusterhead, it will set itself as a slave and send a B_REP to the other cluster head.

A cluster forming example is illustrated in Figure 8.4. A state transition diagram is shown in Figure 8.5. The cluster forming phrase is asynchronous and dynamic so that a new node can easily join to an existing network or two subnetworks can merge together seamlessly. Here we deploy the battery residual as the metric to initiate clusterhead re-electing. However, in a sensor network, if the devices are too simple to retrieve this information, a random selection is acceptable.

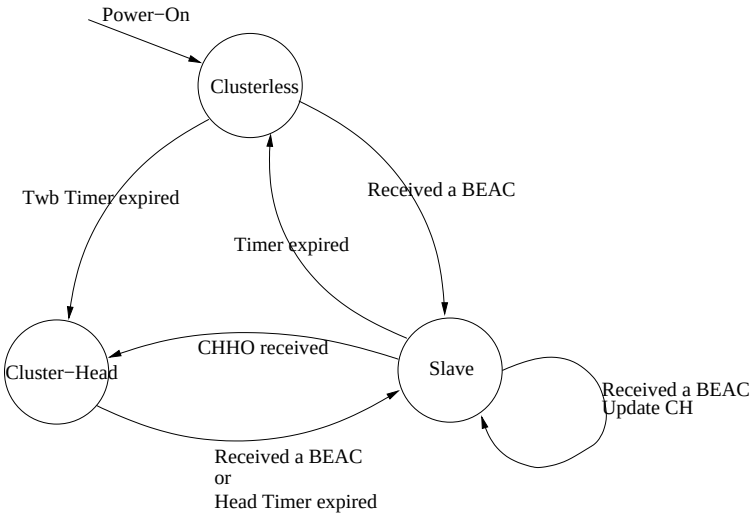

Figure 8.5: State Transition of LSCA-ho

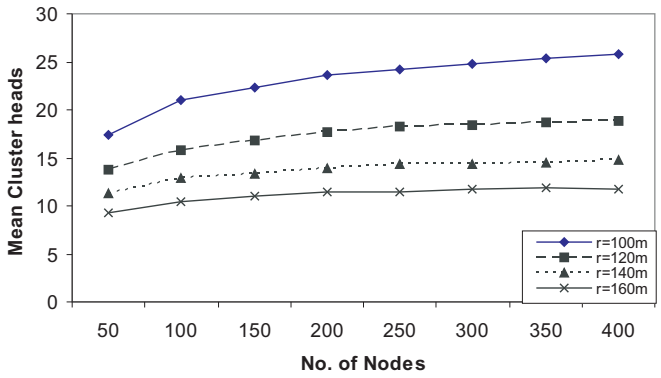

Figure 8.6: Simulation results: Mean number of clusters

LSAC gives very good scalability in term of clusterhead population. Figure 8.6 shows the simulation results of average number of clusterheads when total number of nodes varies. Different intra-cluster radio ranges are presented. We can see that as the number of nodes grows, the number of clusters converges to a upper-limit. An empirical formula can be drawn from our simulation results:

$$N_H \approx 2.4A/\pi r^2 \tag{8.11}$$

Figure 8.7 shows the comparison between the simulation results and Equation (8.11).

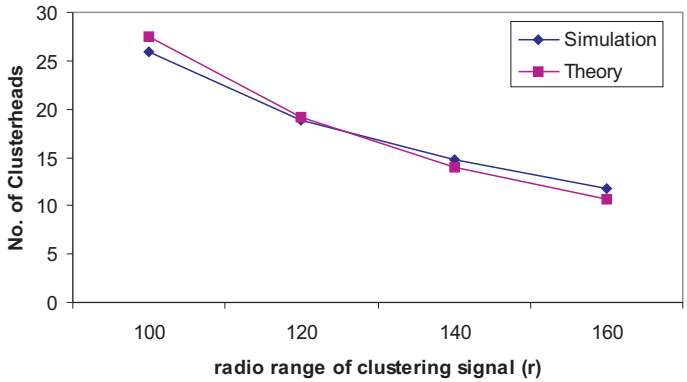

Figure 8.7: Comparison of clusterhead population bewteen simulation and Equation (8.11) at 400 nodes in 600x600 m^2.

8.6 Radio Resource Distribution

In section 8.2 we discussed the radio resource assignment for intra- and inter-cluster traffic. In case a time-division based assignment is deployed, we need to consider the durations dedicated to intra-cluster traffic and inter-cluster traffic.

Let's assume that every node, includeing clusterheads and slaves, generates $\bar{\alpha}$ traffic by average. If the nodes are normally distributed, the average traffic generated by a cluster is

$$\overline{\mathcal{T}} = \bar{\alpha}(\frac{N_S}{N_H} + 1) \tag{8.12}$$

The overall traffic generated by all the nodes is

$$\mathcal{T} = \bar{\alpha}(N_S + N_H) = \bar{\alpha}N \tag{8.13}$$

The generated traffic is delivered through a clusterhead backbone. The number of clusterheads involved depends on the route distance. In Chapter 4, we found a first order approximation of mean hop count of a flat ad hoc network using reactive routing protocol in term of network area A and radio radius R, depicted as equation 5.14.

If the network is symmetric, i.e., all the nodes have the same amount of data to each other. Thus the time duration ratio between inter-cluster traffic and

intra-cluster traffic is

$$\eta = \frac{\mathcal{T}_{inter}}{\mathcal{T}_{intra}} = \frac{(\mathcal{D}+1)\mathcal{T}}{\sum_i \overline{\mathcal{T}}} = \mathcal{D}+1 \tag{8.14}$$

8.7 Concluding Remarks & Future Work

In this chapter we proposed a clustering algorithm based on the link state between clusterheads and slaves. This algorithm can be applied to both pre-determined heterogeneous networks (LSAC-he), and homogeneous networks construct a virtual backbone (LSAC-ho). We inspected the routing and clustering overhead of our algorithm and compared it with that of a flat reactive ad hoc network. The simulation results show that the overhead energy consumption of a flat ad hoc network is a dominating factor of overall energy drain. By the implementation of our clustering algorithm, routing and clustering overheads cost becomes very small. For a homogeneous ad hoc network, it is still possible to apply our clustering algorithm. Simulations show that our algorithm is scalable.

We used a NS-2 based simulator with some prelimilary results of energy efficiency. Research in the near future will focus on the following topics:

1. End-to-end packet delivery delay. On one hand, a packet may travel through more nodes in clustered mode because all the packets must pass through clusterhead(s). On the other hand, because of the synchronization and less network overhead, a clustered network may have less radio interference than that of a flat counterpart.

2. Mobility impacts. Most of the overhead in clustered networks is caused by beacon broadcastings and receptions. A proper rebroadcasting period of beacon depends on the mobility of the nodes. An optimal rebroadcasting period is desired to minimize the clustering overhead when the connectivity of the network is kept.

3. Comparison with other types of clustering algorithms.

9 A GLOBAL SYNCHRONIZATION SCHEME FOR CLUSTERED SENSOR NETWORKS

9.1 Introduction

Synchronization is an important issue for many applications in MANET and WSN. A synchronization scheme helps the nodes coordinate the transmission/reception of data, avoid collisions, analyse and track events correctly, and perform a more efficient sleeping policy for energy saving. Especially for energy efficiency in WSN, many works have been conducted to this issue: Gao, Niu & Yang (2009) applied a global synchornization scheme to periodically put the sensor nodes into sleep and claimed the network lifetime increase from 22 hours to 20 days on an IEEE802.15.4 platform. Chalhoub, Guitton, Jacquet, Freitas & Misson (2008) proposed a MAC scheduling algorithm based on synchronization for IEEE802.15.4 tree-based WSN to save energy. They claimed that 33% energy can be saved by applying the scheme in NS-2 simulations. Slama, Jouaber & Zeghlache (2008) proposed a distributed TDMA algorithm for WSN in which global synchronization is achievable, and by simulations they found the network lifetime is prolonged in terms of running time comparing to previous works.

Synchronization in wireless ad-hoc/sensor networks can be done either globally (i.e., all the nodes in the network agree a common clock time) or locally (i.e., a set of nodes geographically located close agree a common clock time). On the other hand, synchronization can be also classified as external (i.e., there is an external clock reference such as GPS) or internal (i.e., nodes agree a common clock among themselves). In (Elson & Römer 2002), the authors claim that energy efficiency, scalability, robustness, and ad hoc deployment are the key principles of time synchronization design in wireless sensor networks.

In wireless ad-hoc/sensor networks, synchronization is usually performed by passing a time-stamped message to the nodes that need to be synchronized. Two basic

ways can be used to perform synchronization between two nodes: *sender-receiver synchronization* and *receiver-receiver synchronization*. In sender-receiver synchronization a pair of nodes adjust their clock by exchanging a synchronization frame (e.g., NTP in (Mills 1994)); in receiver-receiver synchronization two or more receivers adjust their clock by receiving a (broadcast) synchronization frame from a common reference node (e.g., RBS in (Elson, Girod & Estrin 2002)).

Authors in (Li & Rus 2004) proposes a global clock synchronization scheme that a time-stamped message is passed through a loop of nodes. The scheme can be applied to both flat topology and clustered topology. They implemented Research of (Elson & Estrin 2001) deals with synchronization problem in a way called *post-facto* sychronization. In post-facto scheme, the synchronization is proceeded after some nodes in the network have detected an event. Post-facto synchronization is more energy efficient comparing to the traditional ones.

Authors in (Ganeriwal, Kumar & Srivastava 2003) proposed a global synchronization protocol denoted as TPSN—Time-sync Protocol for Sensor Networks. In TPSN, first the network runs into a "level discovery phase" by a root node broadcasting *level-discovery* message. Once the level-discovery phase is done. The whole network is synchronized by sender-receiver pair-wise synchronization initiated by the root node. However, this scheme will encounter heavy collision of level-discovery messages when the node density increases, because level-discovery messages are broadcast. (Sommer & Wattenhofer 2008) implemented one-hop TPSN using their Tinynode platform, which has XE1205 RF module, and achieved an average of 191.54μs synchronization error.

Most of these synchronization schemes rely on direct physical layer operatibility, i.e., the timestamp can be directly inserted into the outgoing frame during the transmission and arrival of a frame can be captured by hardware interrupt when the frame is being received(Maróti, Kusy, Simon & Lédeczi 2004, Elson & Estrin 2001, Elson et al. 2002, Ganeriwal et al. 2003). For example (Maróti et al. 2004) implemented their Flooding Time Synchronization Protocol (FTSP) onto Mica2 moto platform which operates a separated RF module of 433MHz. (Cox, Jovanov & Milenkovic 2005) adopt the FTSP to an IEEE802.15.4 platform, but synchronization function still relies on a separated RF module Chipcon CC2420, which is able to capture the time when Start-of-Frame Delimiter (SFD) is being received. However, the sensor nodes are trend to have higher integration, smaller size, thus lower energy cost and fault rate. Direct hardware access may

not available in the future. For example, Jennic JN5139 is a new IEEE802.15.4-compatible platform shipped with a single chip(Jennic Co. Ltd. 2006).

Moreover, most of the above proposals do not consider the sleeping of sensor nodes and assume that the sensor node clock is always running after synchronization. In fact, most sensor platforms employ sleeping mode to save energy, and during the sleep a node usually runs on a much slower crystal with much higher drift, compared to that during the normal mode. For example when a Cinet node goes to sleep, it is operated by a 32kHz ceramic oscillator, instead of the 7.3728MHz crystal oscillator in running mode. Some applications even employ "deep sleep" mode, in which the node will loss all the RAM data.

On the other hand, due to the scalability problem of large scale sensor/ad-hoc networks, it is desired to organize large-scale networks into clustered architecture. A clustered ad-hoc/sensor network can greatly reduce the network overhead cost in routing and medium access control (Xu & Gerla 2002, Cai et al. 2003).

In this chapter a global synchronization scheme for clustered ad-hoc/sensor networks is proposed. The clustering protocol is a cluster-head-based scheme and cluster forming (cluster head election) is proceeded by beacon broadcasting periodically sent by cluster heads. The proposed synchronization is globally initiated by a default cluster head called *synchronizer* and spread out through the cluster heads in the network. Synchronization is periodically repeated in order to cope with node mobility and clock driftings. The protocol only assumes a CSMA/CA MAC layer as fundamental and no direct hardware access is necessary. Compatibility with IEEE802.15.4 is discussed later in the chapter.

The rest of the chapter is organized as follows: Section 9.2 describes the global synchronization scheme. A brief introduction of random competetion clustering using link state is given in this section as well. Section 9.3 gives performance analysis of our scheme. Time accuracy of the scheme is also discussed. Section 9.4 presents the settings and results of simulation. Section 5.6 concludes the paper.

9.2 Synchronization Scheme

The synchronization scheme proposed in this paper is based on the LSCA—*Link State Clustering Algorithm* proposed in Chapter 8(Gao & Jäntti 2006*b*). Since

LSCA is based on random competetion, it clusterizes a network within $O(1)$ time, thus a fast and simple scheme. Link state monitoring results in a high stability for cluster maintenance (Gao & Jäntti 2006*b*).

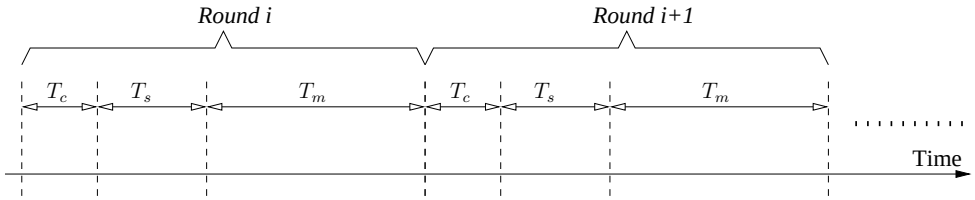

Figure 9.1: Network timing of LSCA

To enable the global synchronization, the network periodically runs in round, with each round three phases: re-clustering phase (with time T_c), synchronization phase (with time T_s), and operating phase (with time T_m), as shown in Fig. 9.1.

Once the network is clustered, it runs into the synchronization phase. Our synchronization scheme is receiver-receiver-based. In order to synchronize the whole network, a *network synchronizer* (denoted as *S-node*) is introduced. The S-node is a cluster head by default. To guarantee this, the CSMA/CA back-off of S-node in C-phase is set to zero so that it will always win the contention.

9.2.1 Global Synchronization Scheme

After a clustering phase, the S-node starts to broadcast a *Synchronization Beacon* (SB) using inter-cluster communication power P_H. A SB frame is marked as $\mathrm{S}(l, \tau_d)$, where l is called *synchronization layer* (for the S-node $l = 0$) and τ_d is a random differ time as a number of time slots. We set $0 \leq \tau_d \leq W_s$, where W_s is the duration of *synchronization window* (SWIN). Each time slot interval, denoted as t_s, is set long enough so that the radio propagation time t_p is negligible, i.e., $t_p \ll t_s$.

The cluster heads of the first synchronization layer that have received $\mathrm{S}(0, \tau_d)$ will align their clock to start next SWIN at the same time as they know τ_d from the received SB. Again, each cluster head differs the rebroadcasting of SB by a random time τ_d. The SB sent by the i-th layer cluster heads is marked as $\mathrm{S}(i\%N + 1, \tau_d)$, where N is a constant that prevents co-channel interference. Typically $N = 3$ or 4.

An illustration of this synchronization scheme is shown in Figure 9.2. The idea of

random delay of SB is similar to CSMA/CA, in which a random backoff is used to avoid collision. For example in Figure 9.2, nodes 1 and 2 ($l = 1$) will likely broadcast SB at different time slots, thus collision of SB on node 3 is avoided. The idea that the cluster heads having received a SB frame will be aligned to start next layer synchronization is similar to IEEE 802.11 DCF function (IEEE 1999), in which *network allocation vector* (NAV) is used to align the neighbouring nodes for the next channel contention.

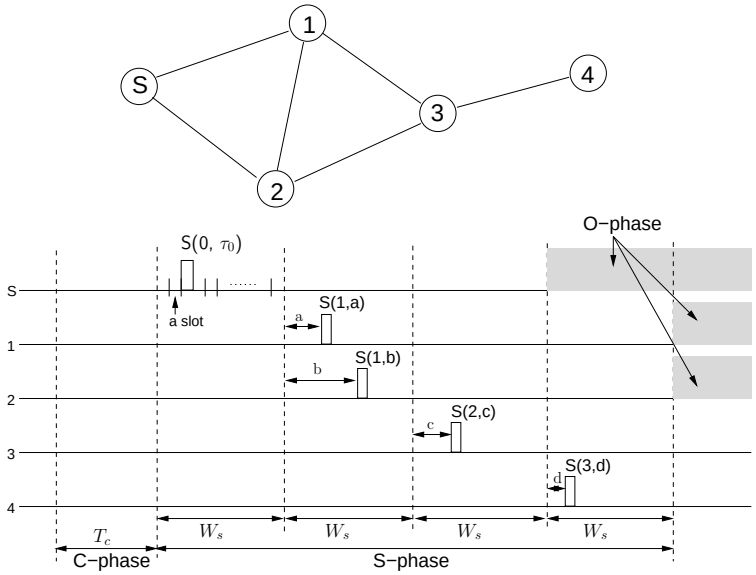

Figure 9.2: Synchronization scheme for beacon-based clustering (only CLHs are shown in the figure)

A cluster head may not be synchronized due to the collision of SB frames. In this case, the cluster head will run in unsynchronized mode until it receives a SB in next round. However, the probability that a cluster head runs in unsynchronized mode is very small, as analysed in Section 9.3.

9.2.2 Network operation

A sychronized cluster head starts O-phase to maintain the cluster by sending CB frames after $N \times W_s$ time, as shown in Figure 9.2. Between two consecutive CB frames the time is equally divided into a number of windows. Here we still use W_s as window duration so that the synchronized cluster head can coordinate with each other. CB frames sent by a synchronized cluster head is now denoted as $\text{CB}(i, \tau_d)$, where i is the synchronization layer of the cluster head and τ_d is the random delay in term of t_s. The random delay of CB is used to avoid collision

on those slave nodes that can hear CB frames from different cluster heads at the same synchronization layer.

A slave node that has received a CB$(i, *)$ should keep awaken in next W_s for the case that CB$(i+1, *)$ may be heard. Because the cluster heads are synchronized in layers, CB$(i, *)$ should always come before CB$(i+1, *)$. This is illustrated as an example in Figure 9.3, in which CH_i^1 and CH_i^2 are two i-th layer cluster heads, and CH_{i+1} is a $i+1$-th layer cluster head.

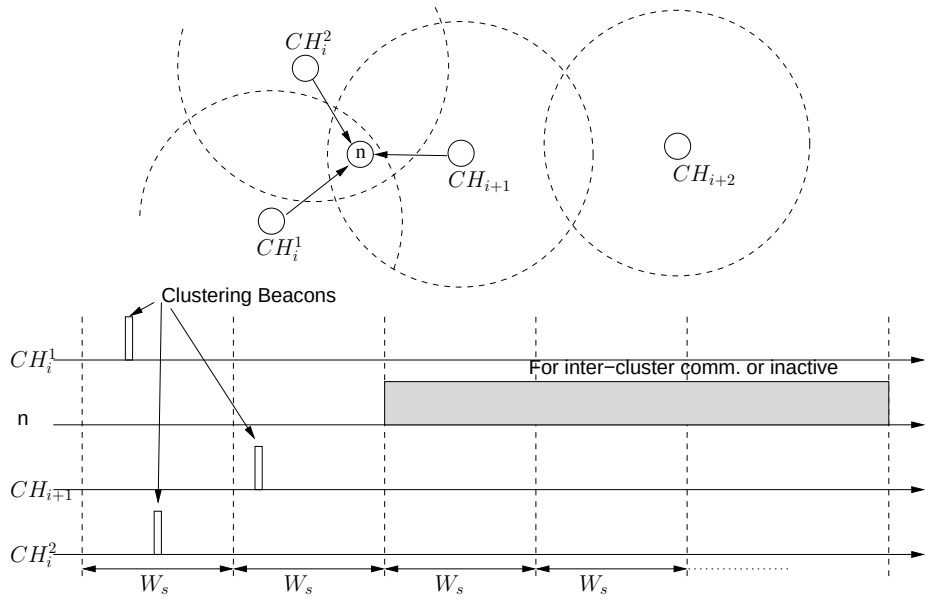

Figure 9.3: The slave node n can receive CB from cluster heads at same and/or different layers without collision.

O-phase duration is $M \times N \times W_s$, where M, denoted as *O-phase duration*, is an integer constant dependent on the nodes' clock precision and network topology change caused by mobility.

9.3 Analysis

9.3.1 Synchronization Accuracy

In Section 9.2.1 it is mentioned that the signal propagation time t_p is negligible, i.e., $t_p \ll t_s$. If $t_s = 1ms$, which is close to the slot duration defined in IEEE

802.15.4 standard[1], and usually the radio range of sensor nodes is shorter than 200m, we have the radio propagation time $t_p = \frac{200}{3\times10^8} = 0.67\mu s$, which is much less than t_s. This synchronization scheme can make the network synchronized at 1ms level.

Nowadays for embedded sensors, the clock accuracy is achieved to 10^{-6} (Römer 2001). It means that the clock drifting of two sensor nodes is around 60μs after one minute. If in O-phase it is chosen $M = 100$ and $N = 4$, then synchronization will be re-proceeded after $M \times N \times W_s = 6.4$ seconds. Our synchronization scheme keeps an accuracy of 1ms level, which is much greater than the clock drifting in 6.4 seconds.

9.3.2 Synchronization probability

The synchronization scheme proposed in this chapter gives high probability to synchronize the whole network, because only cluster heads are involved in synchronization phase. Furthermore, each cluster head will have maximally 6 neighbouring cluster heads (as the optimal case in cellular system). The synchronization phase is initiated from the S-node, therefore these neighbouring cluster heads will belong to different synchronization layers on a planar area[2].

Suppose that there are n i-th layer cluster heads neighbouring to an unsynchronized cluster head. The probability that this node will be synchronized is: at least one i-th layer cluster head sends SB in a time slot different from other $n-1$ cluster heads, denoted as

$$\Pr(n, W_s) = \begin{cases} \frac{\sum_{k=1}^{n} (-1)^{k+1} P_k^n C_k^{W_s} (W_s - k)^{n-k}}{W_s^n}, & W_s \geq n \\ \frac{\sum_{k=1}^{W_s} (-1)^{k+1} P_k^{W_s} C_k^n (W_s - k)^{n-k}}{W_s^n}, & W_s < n \end{cases} \tag{9.1}$$

It can be seen that the probability a cluster head to be synchronized is very high as $W_s \geq n$ holds. With $W_s = 16$ and $n = 6$, $\Pr(6, 16) = 0.9966$. Figure 9.4 shows $\Pr(n, W_s)$ at different n and W_s.

[1]In IEEE 802.15.4 15ms time is equally divided into 16 slots between two consecutive CBs. A beacon frame takes one slot.

[2]The case that all the neighbours belong to the same synchronization layer happens when the network is deployed on the surface of a sphere. The cluster head on the opposite pole to the S-node may encounter such a case.

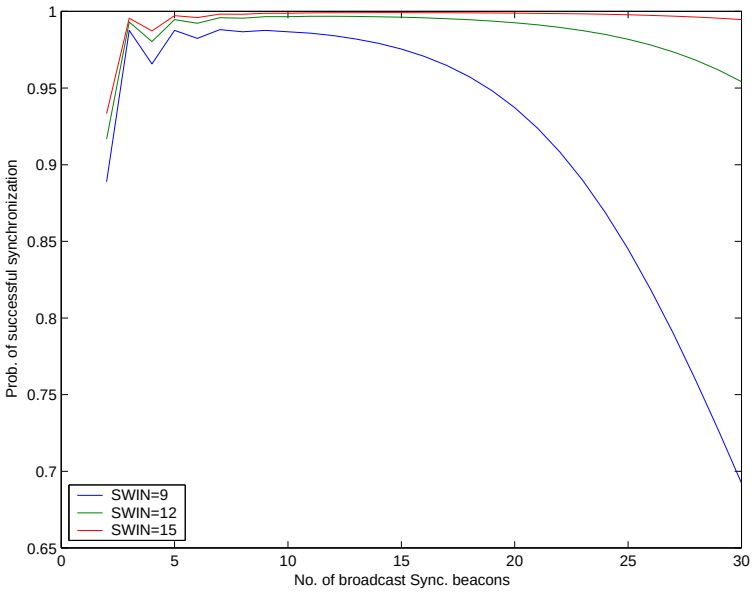

Figure 9.4: The probability of receiving an SB without collision

9.4 Simulation Results

We set a simulation scenario of 200 nodes uniformly and randomly distributed in a square of 600×600 sq.meters. Mobility is considered and a random way-point model is deployed with a nonzero minimum speed. The total simulation time is 300 sec. and statistics are collected every 10 sec. We set t_s = 1ms, T_c = 1sec, W_s = 16, N = 4, and M = 100 as default. The default value of beacon range R_b = 100m and inter-cluster communication range R_c = 200m.

Since in LSCA, mobility of nodes will make a cluster head (except the S-node) be canceled by hearing a CB from another cluster head and join the second cluster as a slave, and a slave node may rise up to be a cluster head when it doesn't hear CB for a certain period, the number of unsynchronized cluster heads will increase as mobility increases. Figure 9.5 shows the population of unsynchronized cluster heads at different mobility settings. From the figure one can see that the chance that most cluster heads are synchronized is rather high.

To cope with the increasing unsynchronized cluster heads caused by mobility, a shorter O-phase duration is desired. Figure 9.6 shows the population of unsynchronized cluster heads as M increases. Figure 9.7 shows the ratio of collided S-frames to the total number of sent S-frames. From the figure we can also assert that the main fact that causes cluster heads unsynchronized is mobility, because

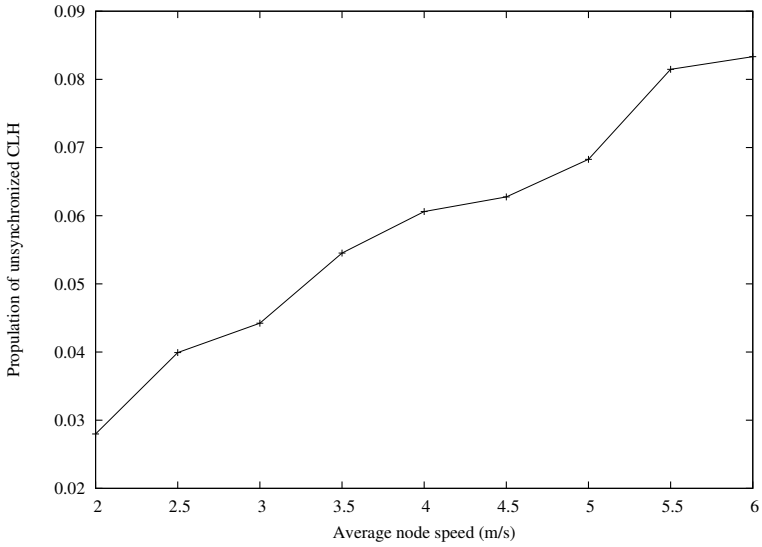

Figure 9.5: Population of unsynchronized cluster heads vs. mobility

the ratio of collided S-frames is independent of M and node speed.

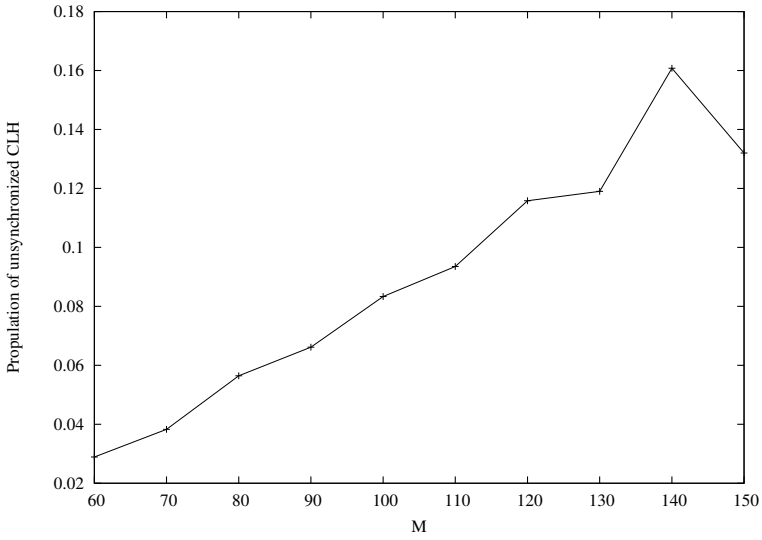

Figure 9.6: Population of unsynchronized cluster heads vs. M (average node speed: 6m/s)

9.5 Testbed Implementation

We implemented our synchronization scheme on Cinet testbed, which is an IEEE 802.15.4 platform using ATmel128L controller and CC2420 RF module. In the

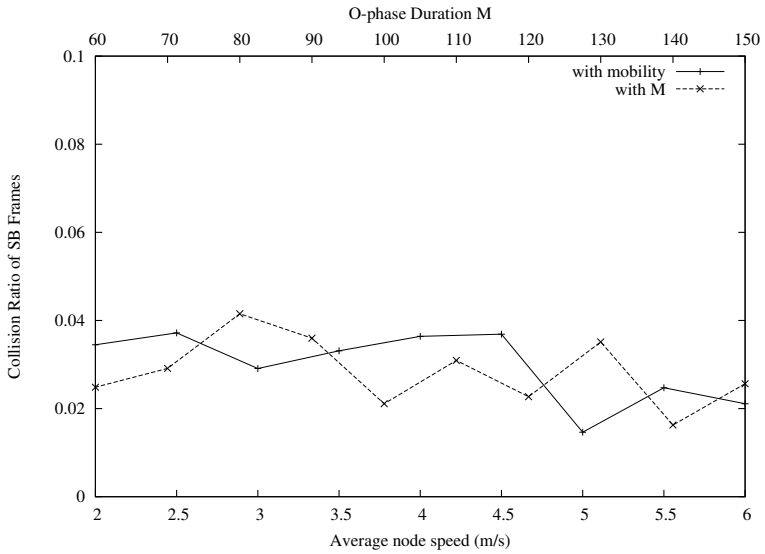

Figure 9.7: SB collision ratio statistics at different M and mobility settings

testbed 10 nodes are deployed as cluster heads[3], and they are arranged 1 to 3 hops away from the S-node. The sink node is allocated as S-node and periodically broadcasts SYNC frame every 5 seconds. The SYNC frame contains following data:

1. Sink Address: 2 bytes IEEE802.15.4 short address
2. Sequence number: 1 byte, incremented by SINK at each round
3. Next Sync Time: 4 bytes integer in milliseconds, indicating next SYNC broadcasting time

Once a cluster head has received a SYNC, it will send a SYNC-ACK frame back to SYNC in O-phase. By counting the throughput of SYNC-ACK we will have the statistics of synchronization efficiency. The SYNC-ACK contains the clock drift of the node so that the accuracy of synchronization is evaluated.

9.5.1 Synchronization performance

Fig. 9.8 exposes the mean clock drift before the next SYNC frame arrives to each node. One can see that the average of clock error for all the nodes at

[3]Due to the shortage of nodes, we do not have slave nodes in the test. Anyway this does not vary the results.

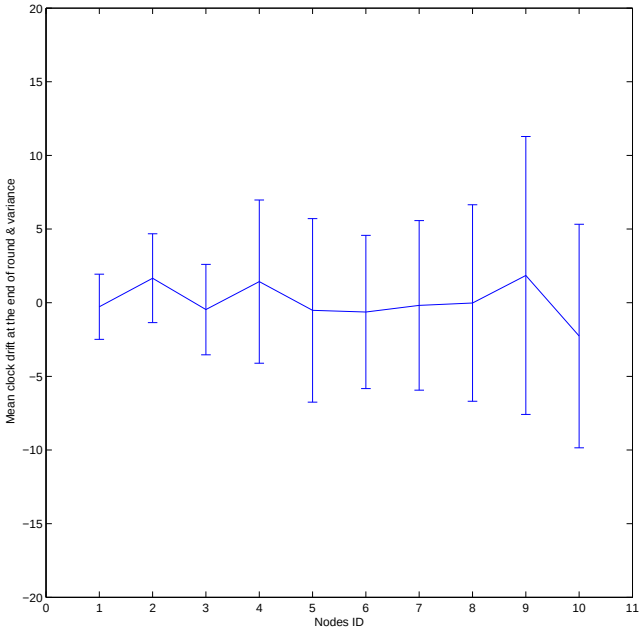

Figure 9.8: Clock drift of the nodes at end of each synchronization phase

different layers is small with only some drifting from each node. The driftings of each node is caused by the node's oscillator which has relatively constant skew during the test time. However, the first layer nodes (ID=1,2,3) have least variance comparing to the third layer nodes (ID=8,9,10). This is due to the fact that the time uncertainty caused by channel access (which is only from the S-node indeed) at the first layer is much smaller than the nodes at deeper layers. Note the time unit in the Figure is in milliseconds, this magnitude is much higher than that of theory (1ms) is due to the timer interrupt of ATmega128L is probably blocked by other interrupts such as radio communication interrupt.

Fig. 9.9 shows the reception goodput of SYNC-ACK packets. Clearly the first layer nodes have best goodput and the furthermost nodes (layer 3) have the worst. As explained in this chapter, a node with more upper-layer neighbors has lower chance to be synchronized. Layer 3 nodes unfortunately have more upper-layer neighbors than that of layer 1 nodes, which have only the S-node. Another reason causing the goodput deterioration is the SYNC-ACK packets from remote nodes have to travel through longer, thus have higher chance to be lost or dropped.

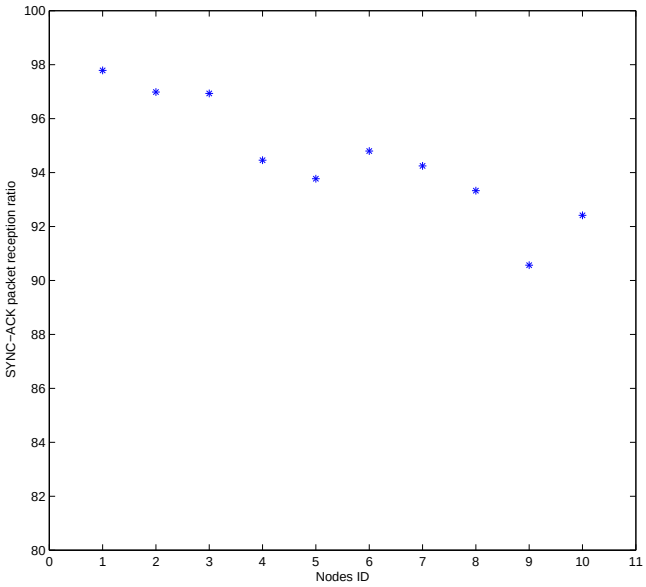

Figure 9.9: The reception goodput of SYNC-ACK

9.5.2 Energy performance

Energy performance is tested by putting the nodes (except the Sink, which is always main-powered) into sleep mode. As shown in Section. 3.2.4, wireless devices consume very tiny energy when the radio transceiver is turned off. And no node should transmit when its neighbors are all sleeping.

9.5.2.1 Coping with Clock Drift

Usually the drifting of a crystal oscillation is called PPM (Portion per Million), denoted as p. We also assume that all the nodes are running at the same clock rate, denoted as R MHz. The maximum drifting between arbitrary two systems will be:

$$\Delta T = 2 \times p \times \mathbf{T}/R \tag{9.2}$$

where $\mathbf{T}$ is the synchronization period.

In an energy-efficiency oriented sensor network sleeping cycle is usually the dom-

Table 9.1: Energy drain and synchronization performance

Node no.	$T_{slp}/\mathbf{T}$	Mean Current (mA)	SYNC-ACK goodput (%)
1	0 (no sleep)	43.1	100
2	0.990	2.54	100
3	0.992	2.31	99
4	0.994	2.18	56

inating factor in $\mathbf{T}$, i.e., $T_{slp} \gg T_c \approx T_s \approx T_m$, equation (9.2) becomes:

$$\Delta T \approx 2 \times p \times T_{slp}/R \tag{9.3}$$

All the nodes that have received a SYNC frame should then set their sleep timer by $T_{slp} = \mathbf{T} - T_c - T_s - T_m - \Delta T$.

9.5.2.2 Energy Efficiency Bound

Energy efficency is defined as the ratio of the time the network is in sleep mode versus the overall time. We have:

$$\eta_e = \frac{T_{slp}}{\mathbf{T}} = \frac{\mathbf{T} - T_c - T_s - T_m - \delta}{\mathbf{T}}$$

Subsititute ΔT from equation (9.3) and let $T_{slp} \to \infty$:

$$\eta_e \approx 1 - \frac{2p}{R} \tag{9.4}$$

This indicates that the energy saving is only dependent on the accuracy of clock oscillations throughout the whole network if sleep time is set long enough.

9.5.2.3 Experiment Results

We set up a network with 1 sink and 4 nodes. Node 1 is always on and other 3 nodes use different T_{slp}. The average current drain of each node in one synchronization cycle is shown in Table. 9.1. In the experiments we set $\mathbf{T} = 10s, T_s = 50ms, T_m = \mathbf{T} - T_s - T_{slp}$. During the sleep, a node runs on a 32.768kHz external ceramic clock which has ±50ppm in specification. This means that there are maximum $2 \times 50 \times T_{slp}/32.768/1000$ time skew between any two nodes. Taking $T_{slp} \approx \mathbf{T}$, it gives 30.5ms time skew at worst in 10 seconds. The result from node

2 shows that the syncrhonization scheme can save up to 99% of energy without loss of performance. As T_{slp} increases, the probability of missing SYNC frame becomes higher. Especially for node 4, because the η_e (0.994) is very close to the theoretical limit (0.9969 from Eq. 9.4), the perfomance deteriorates dramatically.

9.6 Concluding Remarks

In this chapter we proposed a global time synchronization scheme for clustered wireless ad-hoc/sensor networks. The synchronization is proceeded right after the cluster-forming phase and continued by network operation phase. In order to cope with mobility of nodes and clock drifting, synchronization must be periodically repeated. Because only cluster heads are involved in the synchronization and a collision-avoidance mechanism is introduced when broadcasting synchronization frames, this scheme presents a high probability that the whole network is synchronized.

10 LOAD BALANCED AODV — AN IMPROVEMENT OF PERFORMANCE AND FAIRNESS

10.1 Introduction

An ad-hoc wireless network consists of a set of wireless nodes that want to communicate with each other (in packet-switching format) without infrastucture (i.e., base stations). To achieve this, a distributed routing protocol is necessary in case that the radio signal of a source node cannot reach the destination node directly. The source node has to send packets to some other nodes in between and let these nodes relay the packets to the destination. Basically there are two types of routing protocols: proactive and reactive. A proactive routing protocol tries to update the network topology all the time so that every single node has complete up-to-date network topology. When a routing request initiated, the source node is able to find a route from its topology table. On the contrary, a reactive routing protocol tries to find a route on fly when there is a traffic request at source node. To achieve this, the source node broadcasts a route request packet. It is shown that reactive routing protocols perform better than proactive ones in terms of connect times and throughput (Dyer & Boppana 2001).

Amongst the existing reactive routing protocols, AODV (Perkins & Royer 2001) is one of the most interested. AODV is a distributed protocol based on distance vector algorithm, which tries to find a route with shortest distance vector. When a source node has packet(s) to a certian destination to which the source node does not have a route, the source node broadcasts a RREQ (Route REQuest) packet to all its neighbors. Upon the receive of RREQ, each intermediate node first looks up its own route table in cache; if the destination node address is not in the table, the intermediate node re-broadcasts the RREQ and regards the node that sends this RREQ as its precedor. This procedure continues until the RREQ reaches the destination node. The destination node sends RREP (Route REPly) upon

receiving the first arrivel RREQ. Each intermediate node forwards the RREP to its precedor until the RREP arrives at the source node. Meanwhile, each node (including the source node) having received the RREP establishes a route entry in its route table. A route entry contains the destination node address, next hop node address, and a TTL (time-to-live) that this entry will expire. In AODV, HELLO messages are periodically sent in order to maintain a *neighbor table* and keep link information up to date.

However, in a practical ad-hoc network, because of high mobility and random distribution of nodes (e.g., viechles distributed along roads), and edge effect, some factors casue AODV does not always find an optimal route. For example, nodes geographically located in the center of a network may already have undertaken excessive routing task; nodes that have big number of neighbors may potentially have excessive routing traffic. Therefore, load balancing routing has attracted researchers and some recent works can be found in (Lee & Gerla 2001, Hassanein & Zhou 2001, Ganjali & Keshavarzian 2004, Bisnik, Abouzied & Busch 2006, Song, Wong & Leung 2004).

In this chapter we propose a new scheme that simply utilizes AODV routing parameters, including route table size, freshness of route entries, and neighor table size, to achieve better throughput and QoS performance comparing with original AODV. The scheme requires slight modification of AODV protocol, and mobile nodes using our scheme can work together with those nodes using original AODV. Simulations based on NS-2 (Fall & Varadhan 2003) show significant QoS improvement.

The rest of the chapter is organized as follows. Section 10.2 explains the motivation of our research and explores the related work. Section 10.3 depicts the parameter control algorithm based on AODV. Section 10.4 presents simulation environment, scenarios, and the results of comparison. Section 10.5 concludes the discussion.

10.2 Motivation and Related Work

An example of wireless ad-hoc network is shown in Fig 10.1. In the network node A wishes to establish a route to D. Two possible pathes exist (i.e., A-E-D and A-B-C-D). According to the distance vector algorithm, AODV will pick the path

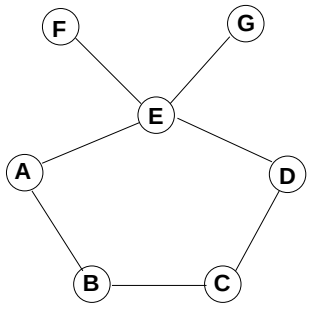

Figure 10.1: An exmaple network

A-E-D. However, in case of another traffic may have been setup between F and G, node E will have excessive routing load if A-E-D is selected. A more desirable path in case is A-B-C-D. This is often referred to as "load balancing problem".

Authors in (Lee & Gerla 2001) proposed a dynamic load-aware reactive routing protocol for ad hoc networks. In this scheme, each intermediate node counts the pending packets in its outgoing buffer and accumulates this information to the re-broadcasted RREQ. The distination node compares the arrived RREQ packets from different routes and selects the one with minimum path load. However, this scheme only counts the outgoing buffer size at each node, and does not consider potential traffic (e.g., when a network has just started operation, the buffer is empty for all the nodes). Another disadvantage of such a scheme is that a destination node has to wait for all the possible coming RREQs. In order to do this, the destination node starts a waiting timer for RREQs. However, the timer duration is dependent on the network size, which is usually unknown before the network is deployed (scalability problem).

In (Song et al. 2004), a load-balance-oriented on-demand routing protocol is proposed for wireless ad-hoc access networks (i.e., some nodes act as Internet gateways and all other mobile nodes communicate with these nodes directly or indirectly). The authors propose an grouping algorithm based on AODV so that the routing load is balanced by evenly distributed source nodes into a number of groups. Basically this is a load-balanced clustering algorithm. It requires that the gateway nodes must have more radio/battery resources than other nodes.

The authors in (Hassanein & Zhou 2001) considerred the geographical information into load-balancing routing. The authors propose a Load-Balanced Ad-hoc Routing (LBAR) with which a route with *minimum cost* will be selected. The cost of a route is an accumulated value summed by the number of active paths in

each intermediate node and traffic interference (denoted as the number of active paths of a neighboring node) given by the node's neighbors. The traffic interference is the sum of all the active path of a node's neighbors. The same, it is the destination's duty to select a route that comes with minimum accumulated cost so the scalability problem exists. The protocol has to periodically exchange traffic interference information between neighbors thus generates more network overhead comparing to AODV and DSR.

Our work aims to design a load-balancing routing protocol without modification of routing packet format of AODV, and the scheme should apply available information that is present in AODV so that routing overhead will not be increased.

10.3 AODV with Parameter Control

In this section we illustrate our load-balanced AODV scheme. A source node here performs the same as original AODV, i.e., it broadcasts a RREQ when it has some data for an unknown destination. For each intermediate node that has recieved a new RREQ (that is, the sequence number is greater), we control the route finding procedure of AODV using following parameters:

1. L_{rt}: the size of routing table of this node.
2. Δt_i: the life time that the i-th entry of the routing table, denoted as $\Delta t_i = t_e^i - t_0$, where t_e^i is the expiration time of this route entry and t_0 is the current time that the node is processing the RREQ.
3. N: the size of neighbor table of this node (i.e., the number of neighbors).
4. p: a scaling factor, $0 \leq p \leq 1$.

For each non-duplicated new RREQ, the node calculates the *cost function* using following formula:

$$C = k \left[pN + (1-p) \sum_{i=1}^{L_{rt}} \Delta t_i \right] \tag{10.1}$$

The cost function is used as differ time to re-broadcast the RREQ. k is a constant to scale the differ time in proper range. By this mechanism, the first copy of RREQ

that arrives the destination node has the *minimum accumulated cost*. Note that in our scheme there is no need to change the format of AODV routing packets (RREQ, RREP, RERR, and HELLO), thus giving possibility that in a network nodes may use either original AODV and load-balanced AODV. This design gives more flexibility.

As illustrated in Figure 10.1, node E is located at the center of network with the largest number of neighbors ($N = 4$). A better route for A and D communication is to avoid using E, in case of either a route F-E-G has been already established or will be established in future.

A delayed re-broadcasting of RREQ seems to result in a longer route establish time. However, the delay gives a diversity of radio channel occupation thus alleviates the *routing storm effect*(Tseng, Ni, Chen & Sheu 2002), which is caused by simultaneous broadcasting of RREQ when a route-finding procedure is going on. In (Trung & Kim 2002), the authors proposed delay of RREQ based on the battery residual, in order to provide more energy-efficient routing.

The scaling factor p in equation (10.1) can be used to adapt traffic mode of communications. For long-term traffic such as CBR or high volume TCP/FTP communications, a route may be used up to the end of its life time. In this case p should be small to let L_r and Δt_i as dominating factors. However, for burst-like communications such as sensor data transmission and email delivery, p should be large because an established route is used only for short time communication even though the life time of the route is much longer. Actually, if changing RREQ format is possible, we can let the source node specify p because it is aware of traffic volumn of the incoming communication.

10.4 Simulation and Analysis

We simulate our scheme using ns-2 with both static and mobile scenarios: a 5×5 grid static network and a 50-node mobile network in $1000 \times 1000m^2$. We establish 10 CBR connections and randomly select source-destination pairs in both scenarios. The details of simulation settings can be seen in Table. 10.1. The packet rate of CBR varies from 1 to 11 packets per second to emulate light to heavy traffic environments, respectively. All the links are generated in first 10 seconds and the total simulation time is 250 seconds.

Table 10.1: Load-Balanced AODV Simulation Settings

Simulation time	250 sec.
No. of nodes	25 (grid), 50 (mobile)
macType	IEEE 802.11
ifqType	Queue/DropTail/PriQueue
ifqLen	variable (50 default)
antType	Antenna/OmniAntenna
propType	Propagation/TwoRayGround
channel	Channel/WirelessChannel
Traffic type	CBR
No. of CBR links	10
CBR generate rate	variable (1-11pkt/sec)
Packet size	512 bytes
scaling factor p	0.5

We inspect following metrics and compare them with original AODV:

1. Delivery ratio $\mathcal{R} = \frac{n_r}{n_s}$, where n_r and n_s are the numbers of received and transmitted (traffic) packets, respectively.
2. Average end-to-end delay $\mathcal{D} = \frac{\sum_{n_r} \tau_i}{n_r}$, where τ_i is the end-to-end delivery delay of packet i.
3. Average jitter $\mathcal{J} = \frac{\sum_{n_r} |\tau_{i+1} - \tau_i|}{n_r}$.
4. Energy efficiency, in terms of mean energy consumption and its standard deviation.

In the following plots our scheme is indicated as L-AODV (denoted as Load-balanced AODV).

Figure 10.2 shows the comparison of packet delivery ratio at different CBR packet rates. When the network traffic is light ($\leq$2 packets/second), AODV and our scheme perform identically. However, when the traffic becomes heavier, our scheme outperforms AODV with approximately 10% increment. Especially at CBR rate of 4pkt/sec, the difference hits the highest point at 18%. In Figure 10.3 one can see the improvement of end-to-end delivery delay of data packets. At a medium traffic volume (4 packet/second), our scheme outperforms AODV most significantly. As the traffic grows, both schemes converge their end-to-end delay. Figure 10.4 shows the arrival jitter of the two schemes. Once again, at light traf-

fic volume (≤ 2 packets/second) both schemes exhibit low jitter, and our scheme gives less jitter than that of AODV when traffic becomes heavier.

We can see from the comparisons of packet delivery ratio, end-to-end delay, and jitter, our scheme has significant performance improvement at 4pkt/sec CBR rate. The reason can be explained as follow: when the traffic is light, the radio channel is not crowded even AODV establishes most routes through the center of network, therefore both AODV and AODVM perform very good; when the traffic increases, the relaying nodes at center of the network becomes congested in AODV but our scheme tries to balance the load using detoured routes thus gives the most significant improvement; when the traffic becomes excessive, the whole network becomes congested thus the difference of between AODVM and AODV is less significant.

Figure 10.5 illustrates amount of routing overhead packets (i.e., RREQ, RREP, RRER, and HEllO). There is not a big difference between these two schemes.

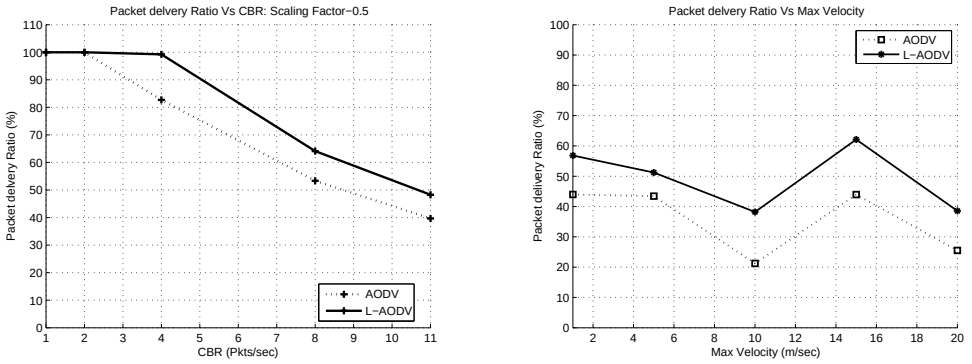

(a) Grid network (b) Mobile network at CBR=4pkt/sec

Figure 10.2: Comparsion of packet delivery ratio

Because the network traffic load is balanced in L-AODV, communications between each individual pair gain more fairness in term of end-to-end delay. Figure 10.6(a) shows the comparison of average end-to-end delay of each individual source/destination pair at traffic load of 4pkt/sec in the grid network simulation.

With L-AODV, nodes in a network are involved into network activity with an more evenly-distributed manner. This gives fairness in term of energy consumption. Figure 10.6(b) shows the energy residue and standard deviation of AODV and L-AODV at different interface queue lengths after 250 seconds of simulation in the grid network simulation.

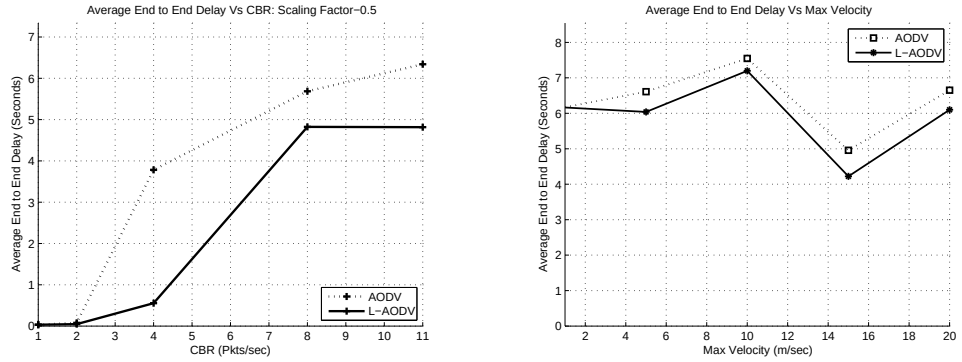

(a) Grid network (b) Mobile network at CBR=8pkt/sec

Figure 10.3: Average end-to-end delay of data packets

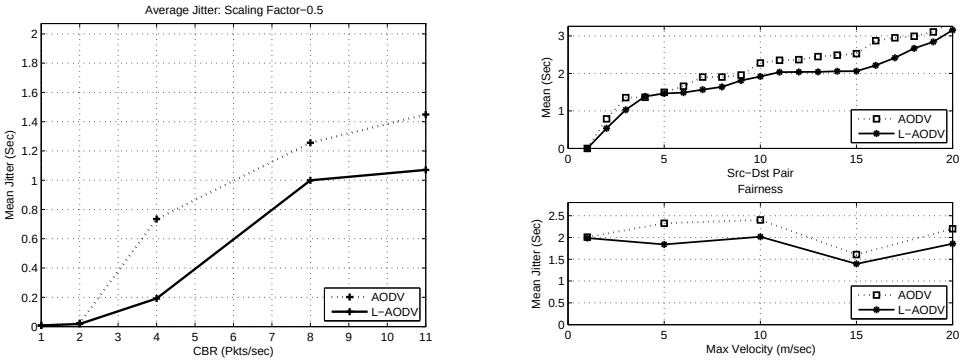

(a) Grid network

(b) Mobile network (up: Jitters per source destination pair statistics; down: Jitters at different mobility)

Figure 10.4: CBR jitter comparison

10.5 Concluding Remarks & Future Work

In this chapter we proposed a modified AODV routing protocol (L-AODV) that can improve packet delivery ratio, end-to-end delay, packet arrival jitter by balancing the routing load at route establishment phase. The proposed scheme utilizes some routing parameters that are already available in AODV to establish routes which can balance the load throughout the whole network. NS-2 simulation results proved the advantages of our scheme by comparing with original AODV. In a low traffic load network, L-AODV does not exhibit advantages over AODV; when the network traffic increases, AODV puts excessive load on the nodes located at the center of network thus the QoS performance is significantly worse than that of L-AODV, because L-AODV tries to find a route with less traffic between the source and destination.

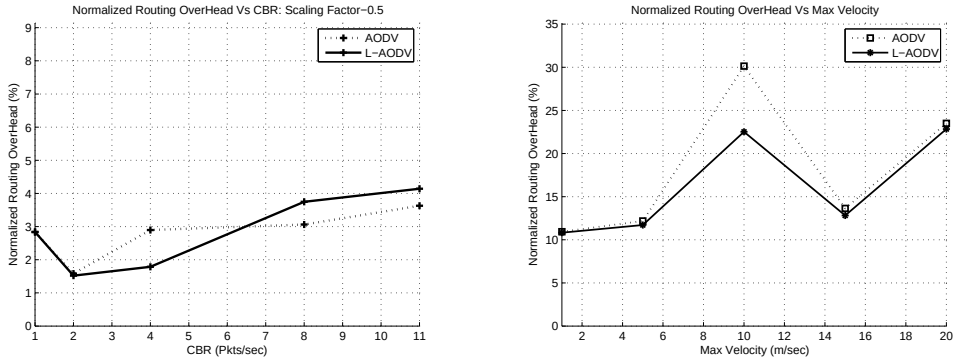

(a) Grid network (b) Mobile network

Figure 10.5: Normalized routing overhead comparsion

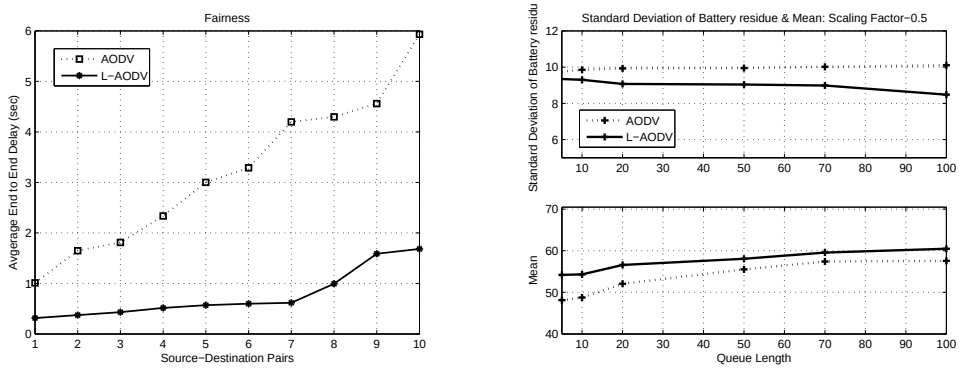

(a) Comparison of end-to-end delay (b) Energy residue and standard deviation at different IFQ buffer length

Figure 10.6: Fairness and Energy Efficiency

We are still working on this scheme. There are a number of issues pending:

1. We are going to implement traffic volumn of each link and this will affect the scaling factor p as discussed in the paper.

2. An alternative solution to improve the performance of delivery is to balance the load using multipath routing. Since AODV by nature will send multiple RREP back to the source node. It is possible to use all the established paths and send packets depending on the load of each path.

11 LOCALIZED MULTIPLE NEXT-HOP ROUTING PROTOCOL (LMNR)

11.1 Introduction

Wireless packet-switching network routing protocol has been an intensive research topic in recent years. Basically there are two types of routing protocols in aspect of the number of paths selected: single-path routing and multi-path routing. Multipath routing is considered to be more able to tolerate link failures, especially when the mobility of network nodes is relatively high.

Using multipath to deliver the packets has advantages in energy efficiency: Baek & de Veciana (2007) claimed that the network lifetime is prolonged by balancing the traffic using multipath proactive routing; Popa, Raiciu, Stoica & Rosenblum (2006*a*) demonstrated that energy could be saved by reducing the congestion effects; energy can be also saved by reducing the communication overheads because a multipath routing scheme is usually more robust in link failure.

Most of the multi-path routing schemes presented are either targeted to find a number of *disjoint* routes or energy efficient routes (Ganesan, Govindan, Shenker & Estrin 2001, Li & Cuthbert 2004, Popa, Raiciu, Stoica & Rosenblum 2006*b*). In these schemes, traffic load is either distributed or sent on the best (e.g., most energy-efficient, best in QoS, etc.) path. In the first case, i.e., distributing load on multiple paths, the destination node has to cope with synchronization of arrival packets. Choosing the best path could avoid synchronization issues, but the process could easily drain out battery in the participating nodes because the source node continuesly uses the path until the link breaks (due to the node mobility or death).

In this chapter we propose a new multipath routing scheme. We classify all the paths between a source-destination pair in to two types: I) node disjoint paths, and II) local paths (to the next hop). Instead of sending packets parallely using type-I paths, we use single route between source and destination, but can be

adjusted locally by type-II paths. The novelty of our scheme is that the source and intermediate nodes are given liberty to choose from multiple local paths to the destination based on a cost function. This will reduce delay caused by global re-routing procedure and increase the network performance. We demonstrate our scheme by extending Ad-hoc On-demand Distance Vector (AODV)(Perkins & Royer 2001) routing protocol, exploring the HELLO messages in AODV to update cost of each indivisual node. Based on this idea, hereafter we call our protocol Localized Multiple Nexthop Routing Protocol (LMNR).

11.2 Description of LMNR

11.2.1 Modified AODV Scheme - Reverse Routing

As AODV retricts intermediate nodes to have single route to the destination[1], this will decrease the link stability and thus the delivery performance is degraded. We modify the route discovery process to incorporate multiple routes: when an intermediate node j receives another copy of RREQ from the same source, it will check the hop count to the source[2]. If the new RREQ has a smaller hop count (i.e., shorter distance to the source node), it updates the route entry as original AODV does; if it has equal hop count as the one(s) in route table, node j simply adds a new route (multipath to source). The algorithm is given in details in Listing 11.1.

Listing 11.1: RREQ Processing at Intermediate Node(s)

```
Receive RREQ(hc, sn, prc, src, dst)
   hc:  hop count to source
   sn:  sequence number
   prc: Predecessor who sends this RREQ
   src: Source addr
   dst: Destination addr
BEGIN
```

[1]In a reactive routing procedure such as AODV, a Route REQuest (RREQ) packet is broadcast by a source node which does not know a path to a destination node. Upon receiving a RREQ, an intermediate node establishes a temporal route entry in its routing table. Duplicated RREQ from the same source node will be ignored. The temporal route entry will be either confirmed when the node receives a Route REPly (RREP) from the destination, or expired when time out.

[2]In a RREQ message a *hop count* field is initialized as 0 by the source and incremented by each intermediate node.

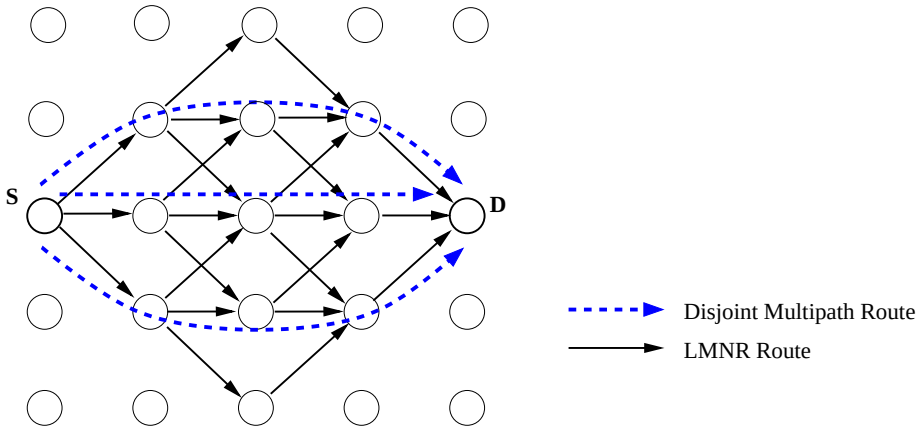

Figure 11.1: An example of local-multipath routing result in 5×5 grid network

```
IF(exist RouteEntry to src in RouteTable)
   IF(hc > RouteEntry.hc)
      Drop RREQ;
   ELSE IF(hc == RouteEntry.hc)
      IF(prc != RouteEntry.prc)
         Add a new entry;
      ELSE
         Drop RREQ;
   ELSE
      Replace RouteEntry with new one;
      Forward the RREQ;
ELSE
   Add a new entry;
END
```

The destination node follows the same principle as intermediate nodes: it sends out RREP to all RREQ's it receives except the ones coming with larger hop count. An intermidiate nodes upon receiving a RREP multicasts it to all its predecessors (established during the RREQ processing phase) in its route table.

By this mechanism, alternate (and equal hop count) paths at each intermediate nodes for one source-destination communication pair will be found. With the knowledge of the routes each intermediate node can now avoid using (next-hop) nodes which have higher cost function, without increasing the number of hops to the destination. An example of LMNR result is given in Figure 11.1.

11.3 Local Path Selection by Periodic Updates

Once the route-establishment procedure is completed, source-destination pair and the intermediate nodes involved will select a single path amongst all the available (local) multipaths. However, dynamic adjustment should be considered so that the intermediate nodes either shall not drain out all their energy, or alleviate and balance the routing load. For this purpose we modify the AODV neighbor table, and introduce a new metric *Node Cost* (NC), which is put into neighbor table.

Actually the node cost function can be choosen from the following metrics (or a combination of them). First it can be a congestion measurement which is proportional to the MAC layer contention (backoff) window (CW) size, if IEEE 802.11(IEEE 1999) CSMA/CA is applied. It is denoted as

$$NC_i = CW_i/CW_{max}. \tag{11.1}$$

NC can also be a measure of network layer information, for example, the outgoing queue buffer occupation ratio:

$$NC_i = Q_i/Q_{max}, \tag{11.2}$$

or simply the packet leaving rate at the network layer queue:

$$NC_i = 1/\mu_i. \tag{11.3}$$

If AODV routing protocol is applied, NC can be a measure of routing table size and freshness of route entries:

$$NC_i = \sum_{k=1}^{K_i} \Delta t_k, \qquad \Delta t_k = t_e^k - t_0 \tag{11.4}$$

where K_i is the size of routing table (number of entries) of node i, t_e^k is the k-th entry's expiration time, and t_0 is the current time.

Using AODV HELLO message, which is periodically sent by all the nodes, NC can be exchanged so that a predecessor can dynamically select its next-hop node which has the least cost function.

It is possible that for a given intermediate node all of its next-hop nodes may

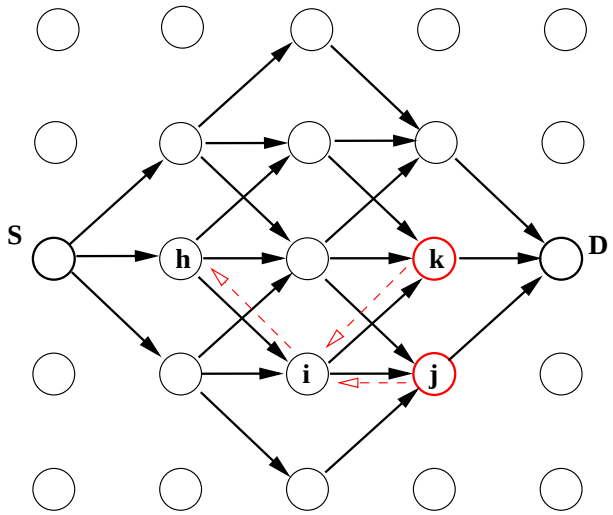

Figure 11.2: Back-propagation of LMNR

have very high cost. To cope with this problem, a back-propagation mechanism is introduced. The back-propagation logic can be described as: if node i sees that all its next hop nodes' cost function (NC) are greater than a threshold, say ψ, node i will back propagates this status to its predecessor so that its predecessor is able to give up using this path. In Figure 11.2, node i will inform node h if both nodes k and j have cost function greater than the threshold.

11.4 Simulation: Parameters & Results

We simulate our scheme by modifying AODV routing protocol in ns-2 (Fall & Varadhan 2003). We compare LMNR with original AODV in end-to-end delay, jitter, packet delivery ratio, and network overhead ratio. 10 Constant Bit Rate (CBR) traffic flows are generated and sources and destinations are randomly selected. Packet generating rate starts from 1 packet/sec to 15 packet/sec to simulate different traffic loads. Equation (11.4) is applied. Aother settings are the same as those in Table.10.1.

Fig. 11.3 shows a routing example of the two protocols we have compared. In the figure the dotted blue path is the result of AODV, and dotted magenta lines are the links utlized by LMNR.

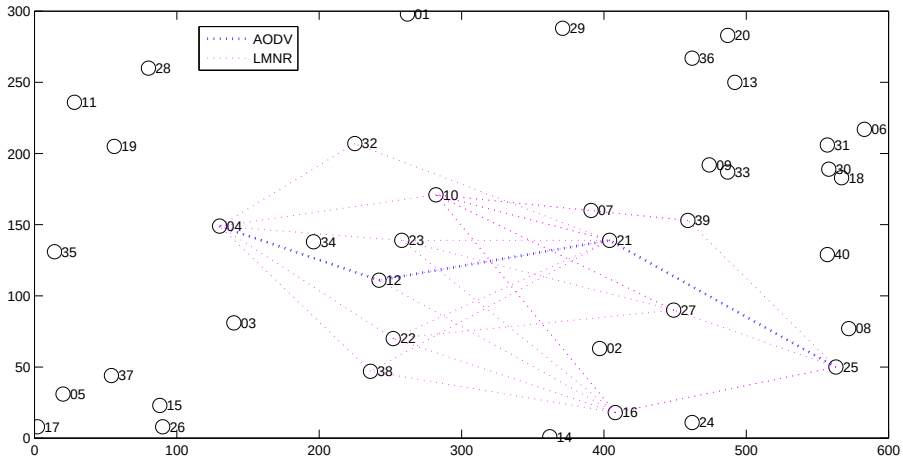

Figure 11.3: Routing result of LMNR and AODV

11.4.1 Throughput Performance

Figure 11.4(a) shows the comparison of end-to-end delivery delay between ADOV and LMNR. It can be seen that at low traffic load (i.e., 1-2 packet/second CBR), AODV and LMNR perform very similar, because such a traffic load does not jam the radio channel and links are stable. As the taffic volumn increases, LMNR outperforms AODV significantly, because selecting a local next-hop candidate takes much less time than that of re-establish a new end-to-end route. When the traffic volumn becomes overwhelmning, the delay in LMNR also increase because all the links are jammed.

Figure 11.4(b) shows the packet delivery ratio of LMNR and AODV. The same as the end-to-end delivery delay, LMNR performs better at moderate CBR rate. At both low and high traffic volumn AODV does not exhibit performance disadvantage.

Figure 11.4(c) gives the jitter measurement of CBR. There is a clear reduction of jitter in LMNR comparing to AODV. A small jitter is important in real-time wireless sensor/actuator networks because in which most control algorithms are based on a synchronous arrival of sensed data.

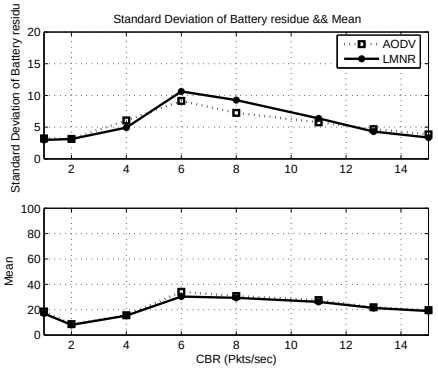

(a) End-to-End Delivery Delay Comparison

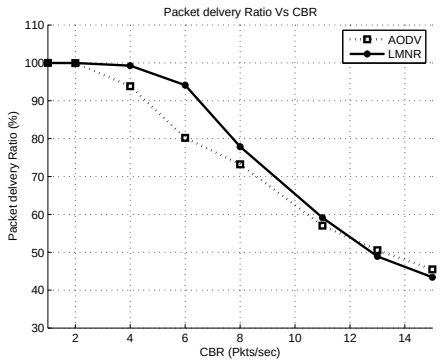

(b) Packet Delivery Ratio Comparison

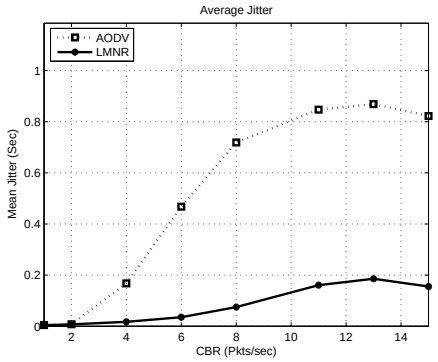

(c) Jitter Comparison

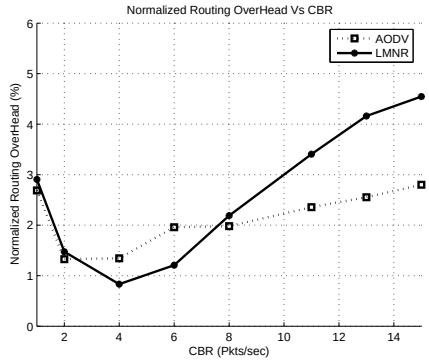

(d) Routing Overhead Comparison

Figure 11.4: LMNR Simulation Results

In Figure 11.4(d) we can see the routing overhead ratio of LMNR and AODV. At moderate traffic volumn, the routing overhead generated by LMNR is only 60% of that by AODV. This is caused by local next-hop selection does not require any extra routing overhead. It is also observed that at this traffic range LMNR reaches its lowest overhead ratio. At low traffic, periodical next-hop updating of LMNR does merely give more overhead but not any benefit to packet delivery. At high traffic, since the whole network is jammed and LMNR local selection fails. This will turn the nodes to use original AODV route re-establishment eventually.

11.4.2 Energy Efficiency Performance

Fig. 11.5 shows the average node battery residual after each simulation. It can be seen that at low traffic volumne, LMNR outperforms AODV definitely. As the traffic load increases, the whole network is more engaged in communications and battery residual drops, and LMNR trends to have no further energy efficiency

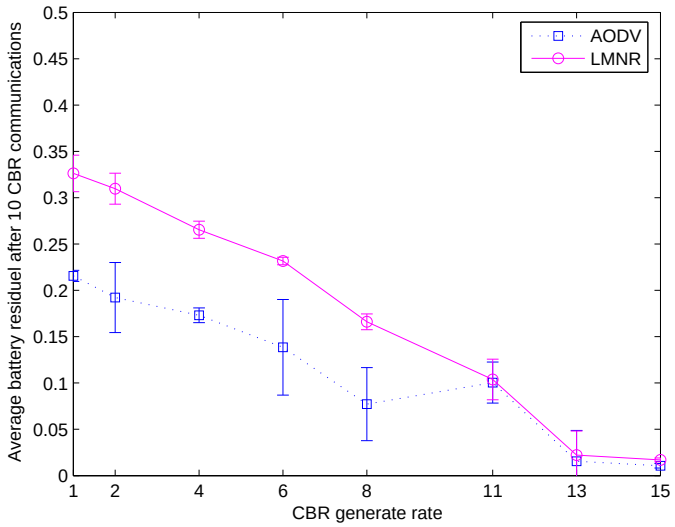

Figure 11.5: Battery Residual after all communications

versus AODV. However, due to the routing traffic distribution feature of LMNR, the variance of battery residual is much smaller than that of AODV in all the cases as the errorbars indicated in the figure. This means LMNR network will have longer life time than that of AODV even the average battery residuals are identical.

11.5 Conclusion

In this chapter we proposed a multipath routing protocol (LMNR) which establishes a end-to-end route by dynamically selecting optimal local paths. The NS-2 simulation results show that the proposed protocol gives more robustness to wireless packet networks. From the simulation results we can conclude that LMNR is suitable for the wireless networks that have moderate traffic volumn in term of packet delivery goodput and energy efficiency.

12 SELF-ORGANIZATION IN WIRELESS CELLULAR NETWORKS – TWO-HOP TWO-SLOT CDMA UPLINK MULTI-CELL CONSIDERATIONS

12.1 Introduction

In broadband CDMA cellular networks, a critical problem is cell planning, i.e., to find suitable location for base stations so that the inter-cell interference can be minimized. At a starting stage, as the network is supposed to support few users, base stations are scattered and cell planning problem is trivial. As the number of users increases, so does the demand for network capacity. Cell splitting is applied to increase the network capacity when initially the base stations are sparsely distributed. However, 1) the cost of infrastructure increases when more base stations are deployed; 2) base station placement becomes more difficult as the cell radius is getting smaller; and 3) splitting cells introduces more frequent handovers and will eventually surpass the network processing capability. Multihop cellular system is desirable when these problems emerge (Lin & Hsu 2000, Wu, Qiao, De & Tonguz 2001, 3GPP 1999, Zadeh & Jabbari 2001*a*). A multihop cellular system has advantages in terms of energy reduction and capacity enhancement.

In (Yamamoto & Yoshida 2004), a two-hop uplink model using Frequency Division (FD) is proposed for CDMA cellular system. A mobile node may send data to an intermediate node, which acts as a repeater, instead of communicating to the base station directly. A repeater can transmit and receive simultaneously using two sets of antennas (as well as two frequency bands). The authors analyse the capacity of such a network and assert that the inter-cell interference is reduced and thus the network capacity can be increased. However, duel-mode terminals working at different frequencies are required in such a network.

Authors of (Zadeh & Jabbari 2001*b*) inspect the performance of a multihop CDMA

cellular system with cellular overlay (which is done by deploying wireless routers in a large cell). The characteristic function of interference has been analyzed using moment expansion. They conclude that power consumption is highly decreased when more routers are deployed.

A proposal of integrated Cellular and Ad-hoc Relay (iCAR) network is presented in (Wu et al. 2001). In such a network a number of relaying nodes working in ad hoc mode are deployed by the cellular operator to relay the traffic to the base stations. Each node, including user terminals and relays, has two interfaces for directly cellular communication and relay communication respectively. Authors proof that the network capacity is increased in term of reducing the call block rate.

In (Radwan & Hassanein 2006) a numerical analysis is given for multihop CDMA uplink. The authors claim a increase of capacity both in simultaneous calls and overall data rate at base station when multi-hop is deployed. However, the analysis is focused in a single cell and inter-cell interference is ignored. Also, the way of implementing power control, especially between mobile nodes, is not mentioned in the paper.

In this chapter we propose a simple multihop scheme for uplink communications of packet-switch CDMA cellular networks. In such a cellular network each cell is concentrically divided into two areas: the inner area that is close to the base station and the outer area to the boundary of the cell. Mobile nodes far away from the base station will deliver their packets to those are in the inner area, and the inner area nodes will relay the packets for the outside nodes and, of course, transmit their own packets to the base station. Besides the simplicity of implementation, the advantage of this scheme is that the mobile nodes need only one aerial interface, whereas in most previous discussions two individual antennas are required for relaying mobiles/nodes.

The novelty of our proposal comparing with other multi-hop solutions can be listed as

1. Less Overhead: the proposed scheme doesn't require any extra radio band for relaying data, and no routing protocol is needed;

2. Less Infrastructure: no fixed relaying nodes are required, the relaying function is performed autonomously and automatically by the mobile nodes in

the network;

3. Simplicity: since no extra routing protocol and infrastructure are needed in this scheme, there is no need for mobiles to bear a heavy, complex protocol stack.

It is worth noting that this scheme can be extended, i.e., the hop number can be more than two. However, the analysis of capacity and details of implementation for more hop numbers is not covered in this paper. In order to keep the analysis and implementation simple, we consider only two-hop scheme here.

The rest of this chapter is arranged as follow: Section 12.2 describes the modeling of our scheme. We give analysis of the throughput of the proposed scheme and compare it to single-hop CDMA system in Section 12.3 for the case that mobile nodes use constant transmit power, and similar comparison is given in Section 12.5 for the case that power control is applied. Sections 12.4 and 12.6 present the simulation settings and results for the constant transmit power case and power control case, respectively. Section 12.8 concludes the work.

12.2 System Model

We assume a packet-switching variable spreading factor direct sequence CDMA (VSF-DS-CDMA) cellular system in which the mobile nodes are aware of the distance to the base station[1]. All the cells are the same in size with radius R. A cell $\mathcal{A}$ in such a system is divided into two concentric areas: the outer area from which the distance to the base station is larger than aR and the inner area from which the distance is less than and equal to aR (denoted as $\mathcal{A}_O$ and $\mathcal{A}_I$, respectively and $\mathcal{A}_O + \mathcal{A}_I = \mathcal{A}$), where $a \in (0, 1)$ is called *2-hop splitting factor*. We normalize the cell radius $R = 1$ for simplicity. In the first stage of analysis, we assume that all the mobile nodes use a fixed transmission power P. We consider an interference-limit system. Consequently, an arbitrarily located receiver sees constant interference power I which depends only on the node density ρ and P, i.e., $I \propto \rho P$.

The system is supposed to be synchronized, i.e., communications are divided into

[1]In practice, this can be achieved by measuring the Received Signal Strength Indication (RSSI) of a downlink pilot channel.

time slots. The synchronization can be simply achieved by listening to periodic broadcasting of synchronous pilot beacon from base stations. We propose a "Two-Hop Two-Slot" (2H2S) uplink scheme as following:

1. All the mobile nodes in $\mathcal{A}_O$ transmit packets at odd-numbered slots; and all the mobiles nodes in $\mathcal{A}_I$ transmit packets at even-numbered slots;
2. A node in $\mathcal{A}_O$ sends its packets to a certain nearby node in $\mathcal{A}_I$. The nodes in $\mathcal{A}_I$ act as relays for the outer nodes.

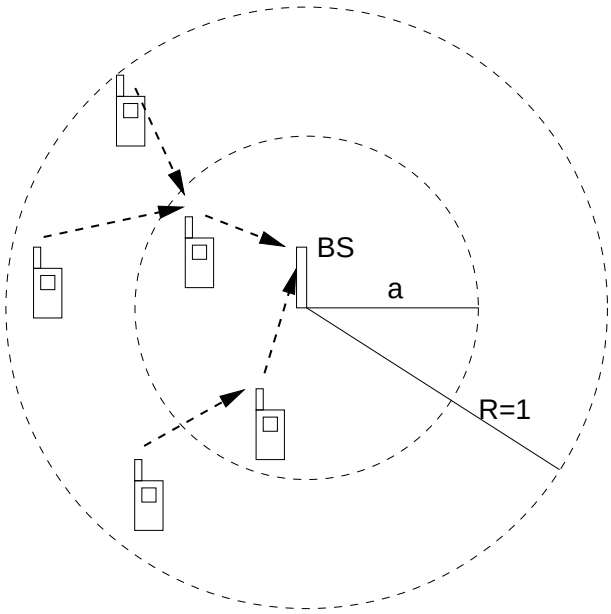

Figure 12.1: A cell of 2H2S CDMA cellular system

Figure 12.1 illustrates the mechanism of 2H2S.

12.3 Capacity Analysis – Fixed Power Transmitters

Due to the symmetry of cellular pattern, we consider the uplink capacity of one cell according to the co-channel interference from its first tier neighboring cells. The capacity of one uplink communication i can be expressed as

$$r_i(x_i) = \frac{WP}{\gamma(\sum_{j \neq i} I_j + \nu)} x_i^{-\alpha} \tag{12.1}$$

where x_i is the distance between the mobile node i to its base station, α denotes the path loss factor, W is the chip rate (bandwidth), P is the transmission power, γ is the required SINR ratio for correct reception, and I_j denotes the co-channel interference, which consists of both intra- and inter-cell interference, ν denotes the noise, which in an interference-limit system can be negligible.

We assume all the mobile terminals are uniformly and independently distributed (i.i.d.) in the geographical area, and the node density is denoted as ρ. Based on this assumption, we treat the intra- and inter-cell interference as two statistical constants.

12.3.1 Single-hop (i.e., Conventional CDMA)

In a single-hop CDMA cellular system, all the mobile nodes send packets to the base station directly. Modulation and coding are kept constant and data rate is controlled simply by varying the spreading factor. A node in position $0 < x \leq R \equiv 1$ achieves uplink data rate:

$$r(x) = \begin{cases} \frac{WP}{\gamma(I_a+I_b)} x^{-\alpha} & 1 \geq x \geq x_m \\ r_m & 0 < x < x_m \end{cases} \tag{12.2}$$

where $x_m = \left(\frac{WP}{\gamma(I_a+I_b)r_m}\right)^{1/\alpha}$ which indicates the distance boundary that a node can achieve maximum data rate r_m, and r_m is the maximum rate restricted by modulation and coding at the radio interface, I_a and I_b are intra- and inter-cell interference, respectively. Due to the orthogonality of CDMA, I_a and I_b are considered as statistical constants, denoted as

$$I_a = \iint_{\mathcal{A}} P\rho p(d) d^{-\alpha} d\mathcal{A} \tag{12.3}$$

$$I_b = 6 \iint_{\mathcal{B}} P\rho p'(d) d^{-\alpha} d\mathcal{B} \tag{12.4}$$

where $\mathcal{A}$ is the cell we are concerning, $\mathcal{B}$ is one of the 6 first tier co-channel cells of $\mathcal{A}$, p and p' are the probability distribution of mobile nodes to the base station of $\mathcal{A}$ in cell $\mathcal{A}$ and cell $\mathcal{B}$, respectively. For the first-order approximation, we treat the cells as perfect circles with $R = 1$, and the distance between two neighboring base stations is therefore $\sqrt{3}$ (suppose the reuse factor K=1 in CDMA), thus we

have

$$I_a = \rho P \int_0^{2\pi} \int_0^1 2\pi r^{1-\alpha} dr d\phi,$$
$$I_b = 6\rho P \int_0^{2\pi} \int_0^1 2\pi r (r^2 + 3 - 2\sqrt{3} r \cos(\pi - \phi))^{-\frac{\alpha}{2}} dr d\phi$$

where $p(r) = 2\pi r$ is the expected node number at distance of r within the cell $\mathcal{A}$, and $p'(r) = \sqrt{r^2 + 3 - 2\sqrt{3} r \cos(\pi - \phi)}$ is the expected node number at distance of r within the cell $\mathcal{B}$, respectively. Fig. 12.2 shows the idea of the upper equation.

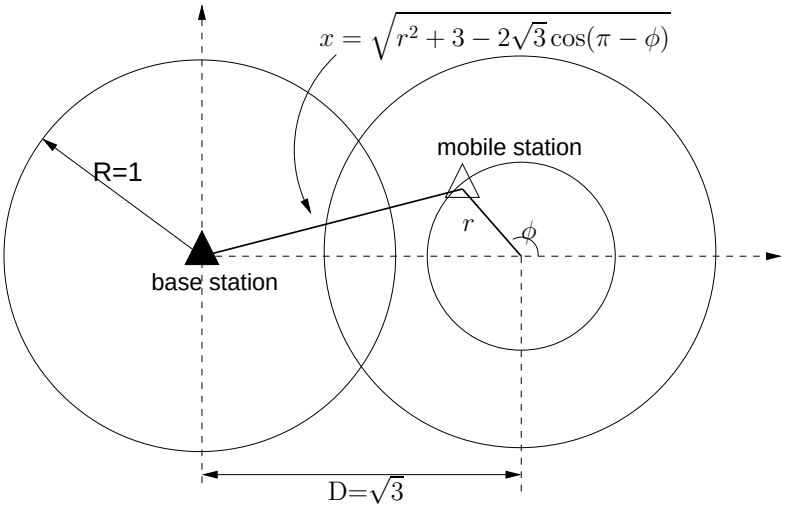

Figure 12.2: Uplink co-channel interference (suppose reuse factor $N = 1$ in CDMA).

According to Equ. (12.2), the overall capacity of single-hop CDMA is then

$$\Gamma_{cdma} = \frac{1}{\mathcal{A}} \iint_{\mathcal{A}} p(x) r(x) dx \tag{12.5}$$

Here we treat the path loss factor α as an integer for integral simplicity.

12.3.2 2-hop 2-slot

Since in 2H2S scheme, the throughput of uplink communication at the base station happens every two time slots, Thus the overall uplink throughput of 2H2S observed at base station is the even-number slot throughput Γ_e divided by 2. We have

$$\Gamma_{2h2s} = \Gamma_e / 2 \tag{12.6}$$

In an even-numbered time slot, only the mobile nodes in $\mathcal{A}_I$ transmit to the base station, thus the interference that a receiver sees becomes $I' < I$. $I' = I'_a + I'_b$ is related to the splitting factor a, denoted as

$$I'_a = a^2 I_a \tag{12.7}$$

$$I'_b = 6 \iint_{\mathcal{B}'} P\rho p'(d) d^{-\alpha} d\mathcal{B}' \tag{12.8}$$

where $\mathcal{B}'$ is the inner circle area $\mathcal{A}_I$ of a neighboring cell $\mathcal{B}$.

The achievable data rate becomes

$$\tilde{r}(x) = \begin{cases} \frac{WP}{\gamma(I'_a + I'_b)} x^{-\alpha} & x \geq \tilde{x}_m \\ r_m & x < \tilde{x}_m \end{cases} \tag{12.9}$$

where $\tilde{x}_m = \left(\frac{WP}{\gamma I' r_m}\right)^{1/\alpha}$.

Consider the case $a > \tilde{x}_m$, i.e., cell size is big or equivalently I is large ($x_m < \tilde{x}_m \ll 1$), an interference-dominating system, Γ_e is derived as

$$\Gamma_e = \frac{1}{A_I} \iint_{A_I} p(x)\tilde{r}(x) dx \tag{12.10}$$

12.3.3 Numerical Analysis

First we demonstrate that the throughput of 2H2S is greater than that of single-hop CDMA with a suitable splitting factor $a \in (0, 1)$.

When the cells are geographically divided into two transmission areas, both intra- and inter-cell interference are reduced. The intra-cell interference is reduced due to the reduction of number of transmitters because only inner-area mobiles are involved in interference counting; the inter-cell interference is reduced due to 1) the reduction of the number of transmitters in the co-channel cells, and 2) the transmitters are located in $\mathcal{A}_I$ of co-channel cells thus giving less interference than the case that there are transmitters located in both $\mathcal{A}_I$ and $\mathcal{A}_O$. Figure 12.3 gives a numerical comparison according to equations (12.5) and (12.10). One can see from the figure that when the splitting factor $a \in (0.15, 0.4)$, the 2H2S scheme outperforms single-hop CDMA.

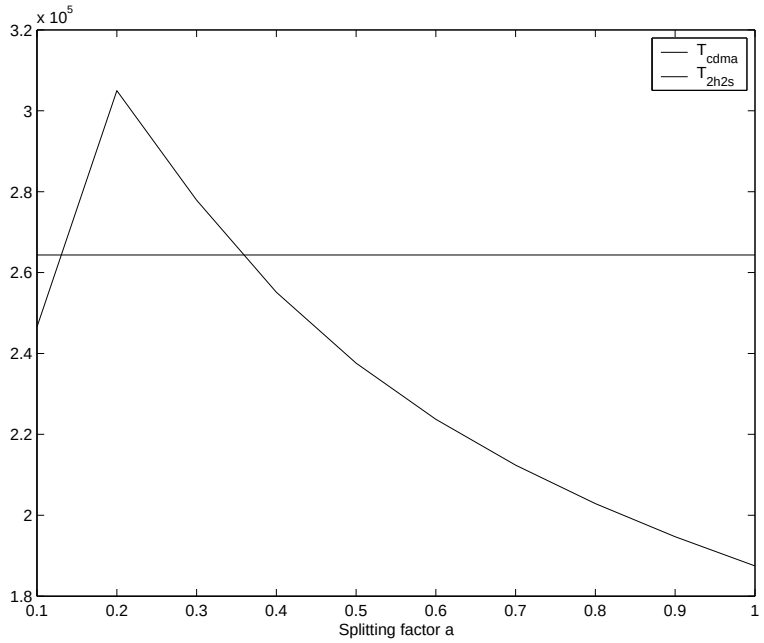

Figure 12.3: Comparison between Γ_{cdma} and $\Gamma_e/2$. Parameters are chosen as $W =$ 1.25MHz, r_m=5Mbps, $\alpha = 3$, $\rho = 100$, $P = 0.1$W.

12.3.4 Relay Selection

A mobile node in $\mathcal{A}_O$ can estimate the distance to the mobiles that are in $\mathcal{A}_I$ in even-numbered time slots (when the inner nodes are transmitting to the base station). A triangular relay selection scheme is implemented to let a mobile in $\mathcal{A}_O$ to select a relaying node in $\mathcal{A}_I$ as follows: Let $\mathcal{R}$ denotes the set of mobiles in $\mathcal{A}_I$ as relay candidates and the distance from each relay to the base station is $d_i, (i \in \mathcal{R})$. For a transmitting node j in $\mathcal{A}_O$, it has distance to each relaying node denoted as d_{ij}. We choose the relay node based on

$$\arg\min_i = \min\{qd_i + (1-q)d_{ij}\} \qquad i \in \mathcal{R} \tag{12.11}$$

where $q \in [0, 1]$ is a scaling factor.

This relay selection scheme requires the knowledge of inner-cell terminal locations. There are several ways to obtain it: 1) Once again, this can be obtained from the estimation of RSSI when the inner-cell terminals are communicating with the base station in odd-numbered slots. 2) All the nodes are equipped with a GPS device so that they can give out their geographical location in each outgoing frame to base station, other nodes can get this data by overhearing the packets.

Table 12.1: Simulation Settings (*$p_0 = 0.7, p_1 = 0.1, p_2 = 0.05$, refer to Figure 12.5)

Simulation time	300(sec.)
Cell radius R	1000(m)
Path loss factor α	4
Slot duration τ	10(ms)
P	0.1(W)
Bandwidth W	1.25(MHz)
Noise N_0	10^{-12}(W)
Packet size L	10(bit)
Minimum rate r_{min}	1(kbps)
a	varying
q	0.5
No. of nodes N	20, 50
Mobility mode	directional random walk*
Average node speed	varying

12.3.5 Fairness

If we assume that each node in the cell generates the same amount of traffic as other nodes, one constrain given here is that Γ_e should carry the traffic for both the nodes in $\mathcal{A}_O$ (denoted as Γ_o) and themselves. Since nodes are uniformly distributed, the traffic generated from $\mathcal{A}_I$ and $\mathcal{A}_O$ are proportional to a and $1-a$, respectively. This gives the constrain that

$$\Gamma_e \geq \frac{1}{1-a}\Gamma_o \tag{12.12}$$

12.4 Simulation of Fixed Power Transmitters

A MATLAB simulator is deployed and settings of simulation are given in Table. 12.1. In the simulator, 7 cells consist of a multiell environment as shown in Figure 12.4, in which the inner-area nodes are represented by a red circle and outer-area ones are represented by a blue one. We consider the throughput of the central cell due to the symmetry of the network. The nodes in other cells act only in interference calculations. We compare the throughput of 2H2S with pure CDMA by inspecting the time span of delivering 5000 packets from each of N mobiles to the base station.

For each time slot, the number of packets η_{ij} that can be delivered from node i

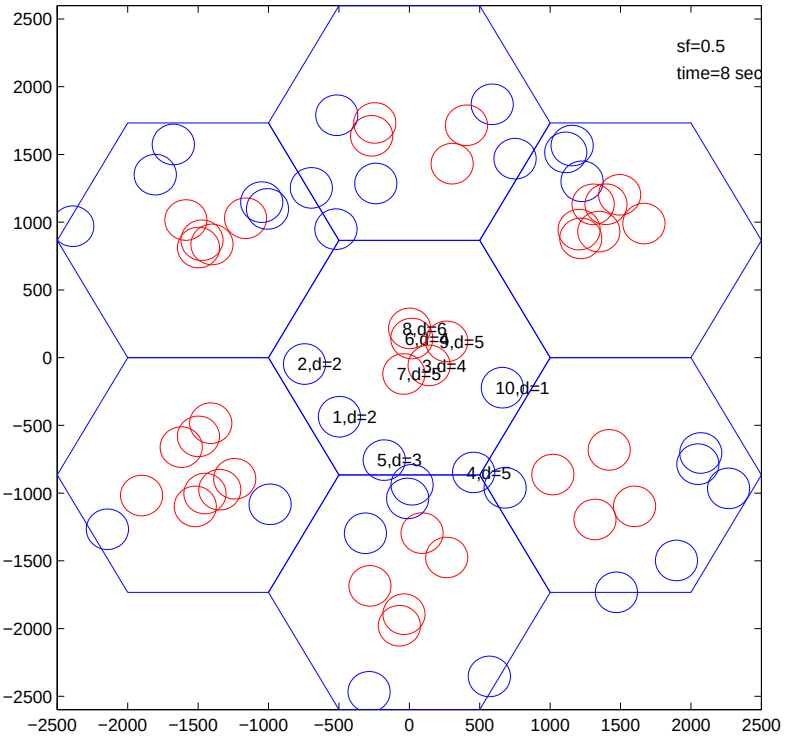

Figure 12.4: Simulation environment. The nodes in $\mathcal{A}_I$ are marked in red color. In the central cell, the nodes are marked by their (ID,direction) couple.

to j is dependent on 1) the maximum data rate r_m, if it can be reached, or 2) the instantaneous $C = W \log_2(1 + SINR_{ij})$, if the outgoing queue is long enough, or 3) all the outgoing packets in the transmitter's queue if the instantaneous capacity can carry all of them, denoted as

$$\eta_{ij} = \min \left\{ \frac{r_m \tau}{L}, \left\lfloor \frac{W \log_2(1 + SINR_{ij})}{r_{min}} \right\rfloor, q_i \right\} \tag{12.13}$$

where $\frac{r_m \tau}{L}$ is the number of packets can be delivered using maximum rate, $\lfloor . \rfloor$ denotes floor operation, r_{min} is the minimum data rate, i.e., one packet transmitted in one slot, q_i is the queue size of transmitter i. $SINR_{ij}$ is defined as

$$SINR_{ij} = \frac{g_{ij} P}{\sum\limits_{k,k \neq i} g_{kj} P + \nu}, \text{ with } g_{ij} = d_{ij}^{-\alpha} \tag{12.14}$$

The directional random walk mobility scheme (Cai et al. 2003) with border wrap-

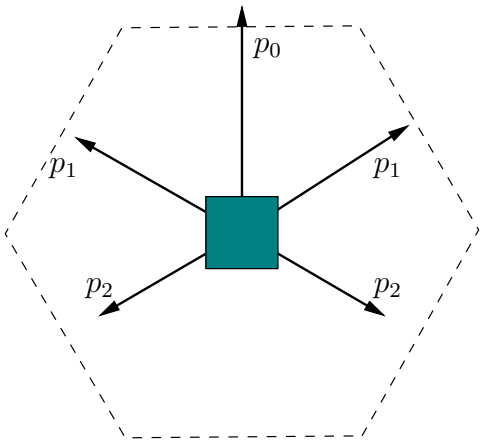

Figure 12.5: Directional random walk mobility scheme

around (i.e., a torus area) is shown in Figure 12.5. A node at each moment has 5 possible directions to move, with each direction a different probability. We have $\sum_i p_i = p_0 + 2p_1 + 2p_2 = 1$, where $p_0 = \max\{p_i\}$ denotes the moving direction that is randomly selected when the simulation starts. And other possibilities give fluctuation of the movement. Each cell is a torus area so that a node moves out from its cell will appear (move in) from the opposite side of the same cell.

Figure 12.6 shows the comparison of 2H2S with single-hop CDMA at different N and average node speeds (with splitting factor $a = 0.3$). Our scheme outperforms the single-hop CDMA with 50% of delivery time under different mobility circumstances. One can also see that the delivery time shrinks as the mobility increases. This is a well proof of the conclusion of "mobility increases the capacity of ad hoc networks" in (Grossglauser & Tse 2002).

Different values of a results to different delivery performances, as shown in Figure 12.7. If we consider the system throughput as the inverse of delivery time, this figure matches well with the numerical result shown in Figure 12.3. When a is too small, it is becomes difficult for the mobiles in $\mathcal{A}_o$ to find a relay; when a becomes large, then most mobiles are acting as relays but there is not much traffic coming from the outside area $\mathcal{A}_o$ for relaying, thus resulting in a waste of bandwidth. Indeed, when $a = 1$, the performance of 2H2S become 50% of single-hop CDMA system.

In single-hop CDMA with out power control, a major problem is fairness, i.e., the nodes close to base station take advantage in communication. Figure 12.8 illustrates that our scheme produces better fairness of communication than that of

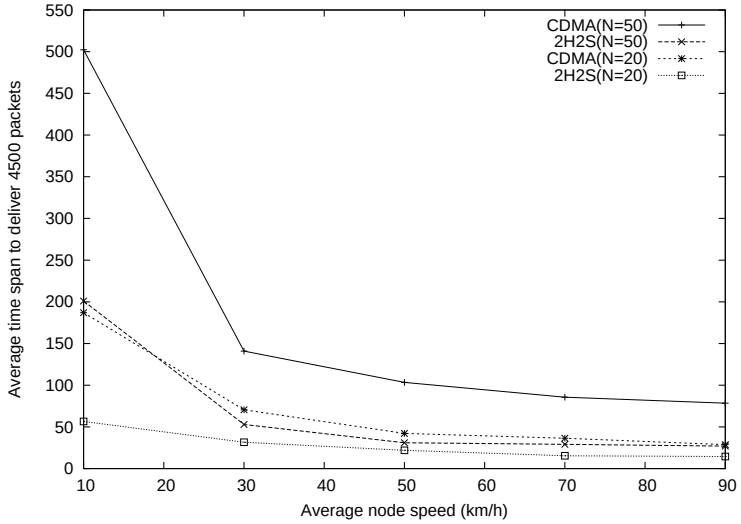

Figure 12.6: Comparison of H2S2 with CDMA at different mobility settings

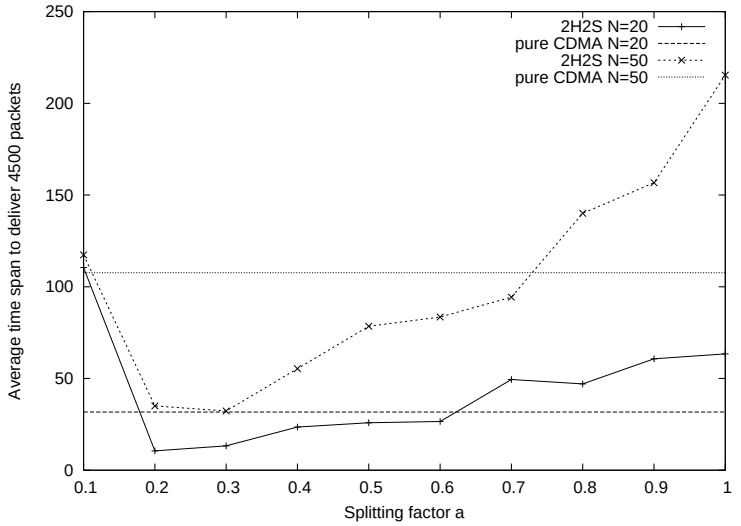

Figure 12.7: Delivery performance using different splitting ratio a (with average node speed 50km/h)

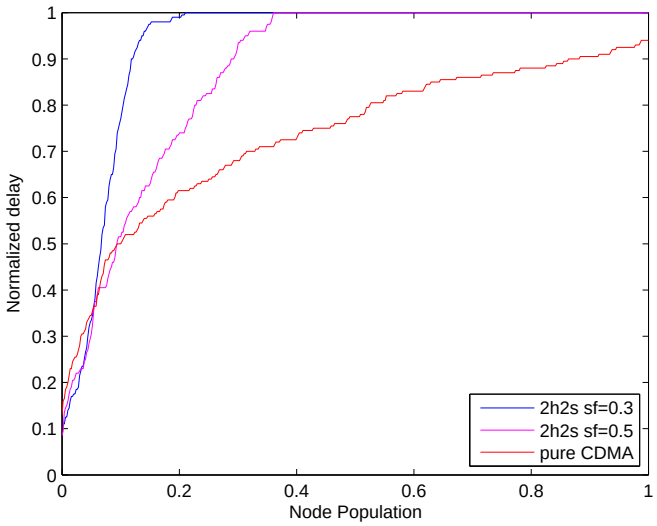

Figure 12.8: CDF of node distribution of average delay

single-hop CDMA. The figure shows the cumulative distribution function (CDF) of average delay of delivering 5000 packets from each node to the base station.

12.5 2H2S—Power Control

In the previous sections we focus on the assumption that all the mobile nodes use a fixed transmit power. However, especially in the inner area $\mathcal{A}_I$, power control is necessarily desirable for the fairness of communications. The fairness problem is described as that the mobile nodes close to the base station will take more radio resources than those are far away from the base station, if all the mobile nodes use a fixed transmit power when communicating with base station.

In this section we consider the power control issue. For practical reasons, we propose that power control is applied only in the inner area A_I, i.e., when the mobile nodes need to transmit to the base station. The outer area power control (i.e., for mobile-to-relay communication) is possible, but leading a way too complex to be implemented: due to the deployment of power control of inner-area nodes, it becomes difficult for the outer area nodes to estimated transmit power, and fast power control (frequent pilot broadcasting from the inner-area nodes) will take too much radio resource. So, we assume that all nodes in $\mathcal{A}_O$ transmit at a constant power P. Power control is deployed only in $\mathcal{A}_I$. As a result, the throughput of $\mathcal{A}_O$-to-$\mathcal{A}_I$ communication is unchanged.

The single-hop CDMA capacity using power control has been explicitly illustrated by (Viterbi & Viterbi 1993) and a large number of related works. Here we apply the similar way to analyse the capacity.

The capacity is measured as the number of accepted mobiles, denoted as K. Considering the inter-cell interference from the first tier, and the accepted user data rate is r_a, we have

$$r_a = \frac{WP_r}{\gamma(I_{ak} + I_{bk} + \nu)} \tag{12.15}$$

where P_r is the signal power at the receiver, I_{ak}, I_{bk} are intra- and inter-cell interference in power control mode, respectively. For a mobile node having a distance to its own base station r_1, its transmit power is given as $P_t(r_1) = P_r r_1^{\alpha}$, and it gives interference to a neighboring base station with distance r_0 as

$$I^*(r_0, r_1) = P_r \left(\frac{r_1}{r_0}\right)^{\alpha} \tag{12.16}$$

I_{ak} is given as $I_{ak} = (K-1)P_r$, in case that all the users are accepted (satisfied), $K = \pi R^2 \rho = \pi\rho$. Note that $R = 1$. I_{bk} is given by

$$I_{bk} = 6 \iint_{\mathcal{B}} \rho P_r \left(\frac{r_1}{r_0}\right)^{\alpha} d\mathcal{B}(x, y)$$

where $\mathcal{B}$ is one of the six neighboring cells, r_1, r_0 are the distances depicted in eq. (12.16), respectively.

The capacity of single-hop CDMA with power control can be obtained as

$$\Gamma_{cdma-pc} = Kr_a = \pi\rho r_a \tag{12.17}$$

In the case of 2H2S, the cells are split into two concentric areas. We apply the same mobile density ρ. For the inner area A_I, the accepted user data rate becomes to be

$$r'_a = \frac{WP_r}{\gamma(I'_{ak} + I'_{bk} + \nu)} \tag{12.18}$$

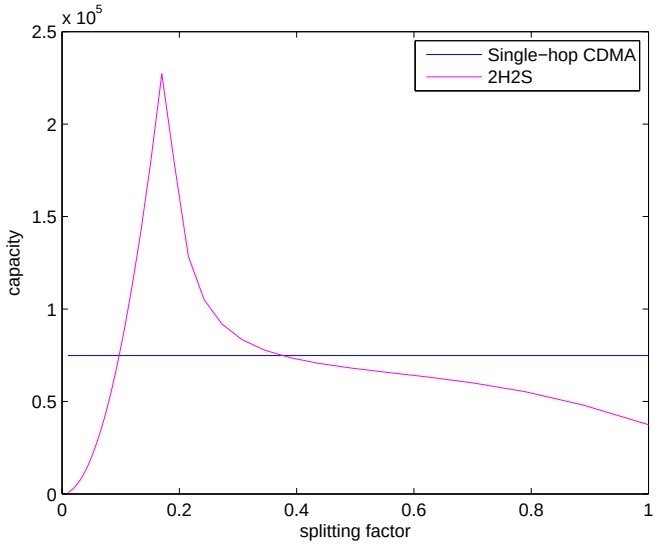

Figure 12.9: Numerical comparison of capacity of single-hop CDMA and 2H2S in power control mode. Parameters are: W=1.25MHz, $\gamma = 10$, $P_r = 0.1$W, $\alpha = 4$, $\nu = 2 \times 10^{-9}$W/Hz, $\rho = 10$

The intra-cell interference becomes to be

$$I'_{ak} = (\pi\rho a^2 - 1)P_r$$

The inter-cell interference is

$$I'_{bk} = 6 \iint_{\mathcal{B}'} \rho P_r \left(\frac{r_1}{r_0}\right)^{\alpha} d\mathcal{B}'(x, y)$$

where $\mathcal{B}'$ is the one inner area of six neighboring cells.

And the capacity of 2H2S becomes to be

$$\Gamma_{2h2s-pc} = K' r'_a/2 = \pi\rho a^2 r'_a/2 \tag{12.19}$$

A numerical result comparing $\Gamma_{cdma-pc}$ and $\Gamma_{2h2s-pc}$ can be seen in Figure 12.9.

12.6 Simulation of Power Control Scheme

The same settings as Sec.10.4 are given in the simulations of power control case. We compare the uplink throughput by initializing 5000 packets to all the nodes

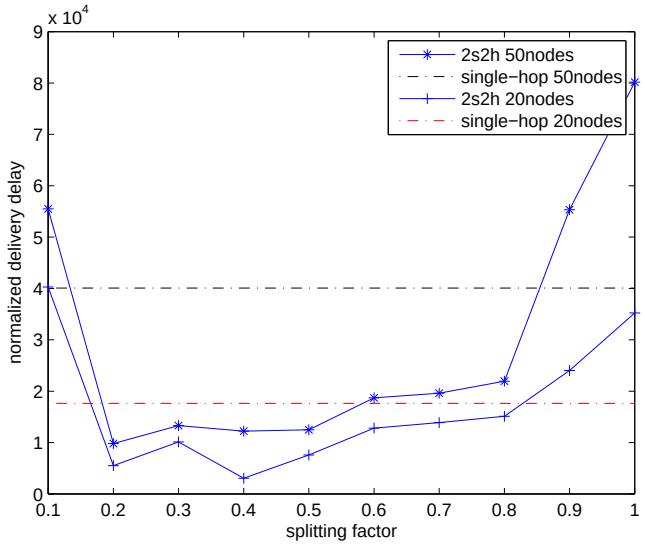

Figure 12.10: Throughput comparison of 2H2S and single-hop CDMA in power control mode

and measure the delivery time. Figure 12.10 shows the simulation results of power control mode with 20 and 50 nodes per cell, respectively. The figure also shows the simulation results of single-hop CDMA using power control in both populations. From the figure one can see that the 2H2S scheme outperforms single-hop CDMA when the splitting factor $a \in (0.2, 0.8)$.

12.7 Outter- and Inner-cell Capacity Estimation

In Section 4.2 we proposed a relay selection scheme. Base on this scheme, the capacity between the outer area $\mathcal{A}_O$ and inner area $\mathcal{A}_I$ can be estimated.

Assume that the node density is high enough so that an outer tier node can always find a relay which has shorter distance than from the tier node to the base station. We consider the situation shown in Figure 12.11. Nodes are uniformly distributed in a half disc of radius a:

$$p_I(d, \phi) = \frac{2}{\pi a^2} d, \quad 0 \le d \le a, \quad -\frac{\pi}{2} \le \phi \le \frac{\pi}{2}$$

Distance between an outer tier and an inner tier node is

$$X^2 = d_I^2 + d_O^2 + 2 d_I d_O \cos(\phi_I - \phi_O),$$

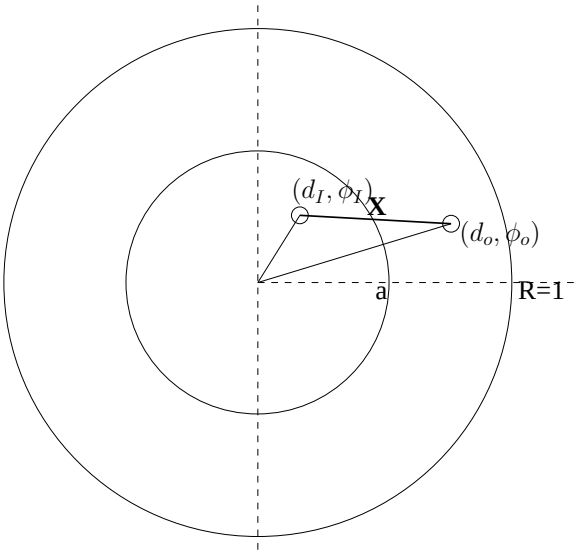

Figure 12.11: Relay selection scheme

then the cummulative density function (CDF) of distance X for $d_i = D_I, \phi_i = \Phi_I$ is given as (12.20). For the uniform distribution of the relay node at (d_o, ϕ_o), the distribution follows (12.21).

$$\Pr(X \leq x) = \Pr(D_I^2 + d_o^2 - 2D_I d_o \cos(\Phi_I - \phi_o) \leq x^2), \quad x \geq 0 \tag{12.20}$$

$$\begin{aligned}\Pr(X \leq x \,|d_o, \phi_o) = \Pr\{\max\{0, (d_o \cos(\phi_I - \phi_o) - \sqrt{d_o^2 \cos^2(\phi_I - \phi_o) - 4z^2})\} \\ \leq d_I \leq \frac{1}{2}(d_o \cos(\Phi_I - \phi_o) + \sqrt{d_o^2 \cos^2(\Phi_I - \phi_o) - 4x^2})\}\end{aligned} \tag{12.21}$$

The distribution of distance x can be found as

$$p(x \,|d_i, \phi_i) = \frac{d}{dx} \Pr(X \leq x \,|d_o, \phi_o) \tag{12.22}$$

Thus the overall capacity of A_O-to-A_I can be derived as

$$\Gamma_{O-I} = \int_{d_o = aR}^{R} \iint_{A_I} p(x \,|d_i, \phi_i) d_i^{-\alpha} d(A_I) d(d_o) \tag{12.23}$$

12.8 Concluding Remarks

In this chapter we proposed a 2-hop 2-slot scheme for the uplink throughput enhancement of packet-switched CDMA cellular networks. By dividing the transmission of mobiles and relays into different time slots, we can greatly reduce the co-channel interference. The scheme is easy to be implemented and the analytical and simulation results indicate that the scheme improves the capacity capacity significantly comparing with a single-hop CDMA network.

13 CONCLUSION

In Chapter 3, we inspected the energy consumption properties of typical radio transceivers in different states, including transmitting, receiving, and sleeping modes. An important energy feature of multihop ad hoc networks is that breaking a long communication path into shorter distance multi-hops will not always be energy-efficient. A protocol that can organize nodes in sleeping mode is more preferable in saving energy.

In Chapter 4, analysis of the probability of finding least-hop route using reactive routing protocols is given. With the assumption that the channel congestion probability is p when a route-finding procedure is progressed, the expected time that the route-finding packet arrives the destination is proportional to $\frac{p}{1-p}$. We also found that when the size and scale of network increase, the probability that the least-hop route will be selected decreases.

In Chapter 5 we inspected the energy efficiency of ad hoc/sensor network when topology control by variant transmit power is available. We define the energy capacity of ad hoc network as the number of bits that can be transmitted by unit power. When the transmit power varies, the network topology is changed as well. An optimal power level is desirable so that end-to-end transportation energy cost is minimized. We found that in a typical local area ad hoc network, the optimal transmit power should keep the expected hop count to be 2 or 3.

Chapter 6 presents an energy-efficient reactive routing protocol based on AODV. The protocol relies on the link state information when the route-finding packet (RREQ) is being flood. This protocol is able to select a more energy-efficient route is a distributed manner. Simulation shows that 20-30% of energy can be saved comparing with original AODV protocol. Later in Chapter 7, this protocol is modified to cope with the communication gray zone problem, because communication gray zone is directly defined by the radio link quality. We obtained significant reduction of packet drop rate and link breaks.

Chapter 8 focuses on clustering issue of large scale ad hoc/sensor networks. A link-state clustering algorithm is proposed. We inspected the routing and clustering overhead of our algorithm and compared it with that of a flat reactive ad hoc network. The simulation results show that the overhead energy consumption of a flat ad hoc network is a dominating factor of overall energy drain. The algorithm can applied to both homogeneous and heterogeneous networks. In order to perform more efficient cluster, and also for deployment of sleep mode, as global synchrnization scheme is proposed in Chapter 9.

Chapters 10 and 11 turn to investigate multi-path routing protocols. Multi-path routing is desirable in the situation that a certain area of network is jammed, but there are still viable routes existing. Multipath routing can greatly improve the delivery performance in terms of packet delivery ratio, jitter, and delay.

In Chapter 12 the interest is to extend CDMA-based wireless cellular networks into multihop hybrid networks. A synchronous 2-hop 2-slot uplink relaying scheme is proposed for uplink time-elastic traffics. By dividing a cell into inner and outter areas the throughput of uplink communication is greatly increased. 2H2S scheme is simple and easy to be implemented.

In this thesis lower protocol layers wireless ad hoc/sensor networks is studied. Different approaches to improve energy efficiency and performance of ad hoc networks, including energy efficient routing, hierarchical clustering, transmit power controlling, and coping with communication gray zone to improve the link quality, are proposed and from these approaches we can see that a cross-layer design is necessary method.

BIBLIOGRAPHY

3GPP (1999), Opportunity driven multiple access, Technical report, Technical Report 3G TR 25.924 v 1.0.0, 3G Partnership Project.

Agarwal, S., Katz, R., Krishnamurthy, S. & Dao, S. (2001), Distributed power control in ad-hoc wireless networks, *in* 'Proceedings of 12th IEEE International Symposium Personal, Indoor and Mobile Radio Communications', Vol. 2.

Aguero, R., Galache, J. & Munoz, L. (2009), Using snr to improve multi-hop routing, *in* 'Vehicular Technology Conference, 2009. VTC Spring 2009. IEEE 69th', pp. 1–5.

Analog Device (2004), 'Datasheet of ad9203 10-bit, 40 msps, 3 v, 74 mw a/d converter'.

Atmel (2006), 'At90s2313 8-bit microcontroller datasheet'.

Bachir, A., Barthel, D., Heusse, M. & Duda, A. (2005), Hidden nodes avoidance in wireless sensor networks, *in* 'Proceedings of Wireless Networks, Communications and Mobile Computing, 2005 International Conference', Vol. 1, pp. 612–617 vol.1.

Baek, S. J. & de Veciana, G. (2007), 'Spatial energy balancing through proactive multipath routing in wireless multihop networks', *Networking, IEEE/ACM Transactions on* **15**(1), 93–104.

Bergamo, P., Maniezzo, D., Giovanardi, A., Mazzini, G. & Zorzi, M. (2002), Dstributed power control for power-ware energy-efficient routing in ad hoc networks, *in* 'Proceedings of EW2002', Florence, Italy, pp. 237–243.

Bettstetter, C. (2002), On the minimum node degree and connectivity of a wireless multihop network, *in* 'Proc. MobiHoc'02', pp. 80–91.

Beyer, D. (1990), Accomplishments of the darpa suran program, *in* 'proc. of MILCOM'90'.

bing Wang, X., zhao Zhan, Y., min Wang, L. & ping Jiang, L. (2008), Ant colony optimization and ad-hoc on-demand multipath distance vector (aomdv) based routing protocol, *in* 'Natural Computation, 2008. ICNC '08. Fourth International Conference on', Vol. 7, pp. 589–593.

Bisnik, N., Abouzied, A. & Busch, C. (2006), Load balanced link reserval routing in mobile wireless ad-hoc networks, *in* 'Proc. of 4th Asian International Mobile Computing Conference'.

Booth, L., Bruck, J., Cook, M. & Franceschetti, M. (2003), Ad hoc wireless networks with noisy links, *in* 'proceedings of IEEE Symposium on Information Theory', pp. 386–386.

Braginshhy, D. & Estrin, D. (2002), Rumor routing algorithm for sensor networks, *in* 'Proc. of the first Workshop on Sensor Networks and Applications (WSNA)'.

Broch, J., Maltz, D., Johnson, D., Hu, Y. & Jetcheva, J. (1998), A performance comparison of multi-hop wireless ad hoc network routing protocols., *in* 'Proceedings of Mobicom'98'.

Buettner, M., Yee, G. V., Anderson, E. & Han, R. (2006), X-mac: a short preamble mac protocol for duty-cycled wireless sensor networks, *in* 'Proceedings of the 4th international conference on Embedded networked sensor systems (SenSys '06)', ACM, New York, NY, USA, pp. 307–320.

Business Week, E. (1999), '21 ideas for the 21st century', *Business Week* **8-30**, 78–167.

Cai, Z., Lu, M. & Wang, X. (2003), 'Channel access-based self-organized clustering in ad hoc networks', *Mobile Computing, IEEE Trans* **2**(2), 102–113.

Cano, J.-C. & Manzoni, P. (2000), A performance comparison of energy consumption for mobile ad hoc network routing protocols, *in* 'Proceedings: 8th International Symposium of Modeling, Analysis, and Simulation of Computer and Telecommunication Systems', pp. 57–64.

Chalhoub, G., Guitton, A., Jacquet, F., Freitas, A. & Misson, M. (2008), Medium access control for a tree-based wireless sensor network: Synchronization management, *in* 'Wireless Days, 2008. WD '08. 1st IFIP', pp. 1–5.

Chavalit, S. & Chien-Chung, S. (2002), Coordinated energy conservation for ad hoc networks, *in* 'ICC 2002: Proceedings of IEEE International Conference on Communications', Vol. 5.

Chen, B., Jamieson, K., Balakrishnan, H. & Morris, R. (2002), 'Span: an energy-efficient coordination algorithm for topology maintenance in ad hoc wireless networks', *Wirel. Netw.* **8**(5), 481–494.

Chen, Y. P., Liestman, A. L. & Liu, J. (2004), *Ad Hoc and Sensor Networks*, Nova Science Publishers, chapter Clustering Algorithms for Ad Hoc Wireless Networks, p. na.

Cho, W. & Kim, S.-L. (2002), A fully distributed routing algorithm for maximizing lifetime of a wireless ad hoc network, *in* 'Proceedings of 4th International Workshop of Mobile and Wireless Communications Network', pp. 670 –674.

Cisco (2004), 'Cisco aironet 350 series client adapters datasheet'.

Clark, M., Leung, K., McNair, B. & Kostic, Z. (2002), Outdoor ieee 802.11 cellular networks: radio link performance, *in* 'IEEE International Conference on Communications, ICC 2002', Vol. 1, pp. 512–516.

CommAccess (2003), 'Commaccess matlab wlan toolbox'.

Cox, D., Jovanov, E. & Milenkovic, A. (2005), Time synchronization for zigbee networks, *in* 'System Theory, 2005. SSST '05. Proceedings of the Thirty-Seventh Southeastern Symposium on', pp. 135–138.

Darrin, M. A. G., Carkhuff, B. G. & Mehoke, T. S. (2004), 'Future trends in miniaturization for wireless applications', *JOHNS HOPKINS APL TECHNICAL DIGEST* **25**, 343–347.

Das, S. R., Perkins, C. E. & Royer, E. M. (2000), Performance comparison of two on-demand routing protocols, *in* 'Proceedings of IEEE INFOCOM 2000', Tel Aviv, Israel.

Dominique, D. & Guerin-Lassous, I. (2003), Experiments with 802.11b in ad hoc configurations, *in* 'Proceedings of 14-th IEEE Personal, Indoor and Mobile Radio Communications (PIMRC 2003)', Vol. 2, pp. 1618–1622.

Doshi, S., Bhandare, S. & Brown, T. X. (2002), 'An on-demand minimum energy routing protocol for a wireless ad hoc network', *Mobile Computing and Communications Review* **6**(2), 50–66.

Doshi, S. & Brown, T. X. (2002), Minimum energy routing schemes for a wireless ad hoc network, *in* 'Proceeding of IEEE INFOCOM'02'.

Dressler, F. (2006), Self-organization in ad hoc networks: Overview and classification, Technical report, University of Erlangen, Dept. of Computer Science.

Dunkels, A., Osterlind, F., Tsiftes, N. & He, Z. (2007), Software-based on-line energy estimation for sensor nodes, *in* 'proc. 4th Workshop on Embedded Networked Sensors (EMNET IV)', Cork, Ireland.

Dyer, T. & Boppana, R. (2001), A comparison of tcp performance over three routing protocols for mobile ad-hoc networks, *in* 'Proc. ACM Mobihoc'01'.

Elshakankiri, M., Moustafa, M. & Dakroury, Y. (2008), Energy efficient routing protocol for wireless sensor networks, *in* 'Intelligent Sensors, Sensor Networks and Information Processing, 2008. ISSNIP 2008. International Conference on', pp. 393–398.

Elson, J. & Estrin, D. (2001), Time synchronization for wireless sensor networks, *in* 'proc. of International Paralle and Distributed Processing Symposium (IPDPS)', San Francisco, USA.

Elson, J., Girod, L. & Estrin, D. (2002), 'Fine-grained network time synchronization using reference broadcasts', *ACM SIGOPS Operating System Review* **36**, 147–163.

Elson, J. & Römer, K. (2002), Wireless sensor networks: A new regime for time synchronization, *in* 'proc. of 1st workshop on hot topics in networks (HotNets-I)', Princeton, New Jersy.

Erdogan, E., Ozev, S. & Collins, L. (2008), Online snr detection for dynamic power management in wireless ad-hoc networks, *in* 'Proceedings of Research in Microelectronics and Electronics', pp. 225–228.

Fall, K. & Varadhan, K. (2003), *The Network Simulator version 2*, Information Sciences Institute (ISI).

Floreen, P., Kaski, P., Kohonen, J. & Orponen, P. (2003), Multicast time maximization in energy constrained wireless networks, *in* 'Proceedings of DIALM-POMC'03', San Diego, California, USA.

Fragouli, C., Le Boudec, J.-Y. & Widmer, J. (2006), 'Network coding: an instant primer', *SIGCOMM Comput. Commun. Rev.* **36**(1), 63–68.

Ganeriwal, S., Kumar, R. & Srivastava, M. (2003), Time-sync protocol for sensor networks, *in* 'Proc. 1st International Conference of Embedded Networked Sensor Systems (SenSys)'.

Ganesan, D., Govindan, R., Shenker, S. & Estrin, D. (2001), Highly-resilient, energy-efficient multipath routing in wireless sensor networks, *in* 'MobiHoc '01: Proceedings of the 2nd ACM international symposium on Mobile ad hoc networking & computing', ACM, New York, NY, USA, pp. 251–254.

Ganjali, Y. & Keshavarzian, A. (2004), Load balancing in ad-hoc networks: Single-path routing vs. multi-path routing, *in* 'Proc. of IEEE INFOCOM'04', Hong Kong.

Gao, C. & Jäntti, R. (2004*a*), Least-hop routing analysis of on-demand routing protocols, *in* 'Proc. IEEE ISWCS 2004', Mauritius.

Gao, C. & Jäntti, R. (2004*b*), A reactive power-aware on-demand routing protocols for wireless ad hoc networks, *in* 'Proc. IEEE VTC 2004 Spring', Milano, Italy.

Gao, C. & Jäntti, R. (2005*a*), Energy capacity in wireless sensor networks, *in* 'Proc. 5th international conference on Intelligent Transportation Systems', Brest, France.

Gao, C. & Jäntti, R. (2005*b*), On clustered ad hoc networks: link-state clustering algorithm and its energy performance study, *in* 'Proc. INTERNATIONAL WORKSHOP ON CONVERGENT TECHNOLOGIES (IWCT)', Oulu, Finland.

Gao, C. & Jäntti, R. (2005*c*), Power-aware routing to cope with communication gray zones in ad hoc networks, *in* 'Proc. 5th international conference on Intelligent Transportation Systems', Brest, France.

Gao, C. & Jäntti, R. (2006*a*), A global synchronization scheme for clustered wireless ad-hoc/sensor networks, *in* 'Proceedings of 6th International Conference on Intelligent Transportation Systems - Telecommunications (ITST'06)', Chengdu, China.

Gao, C. & Jäntti, R. (2006*b*), Link-state clustering based on ieee 802.15.4 mac for wireless ad-hoc/sensor networks, *in* 'Proc. of IEEE Wireless Communication and Networking Conference (WCNC'06)', Las Vegas.

Gao, C. & Jäntti, R. (2006*c*), 'Two-hop two-slot cdma uplink - multi-cell considerations', *Wireless Communications, Networking and Mobile Computing, 2006. WiCOM 2006.International Conference on* **1**, 1–4.

Gao, C., Nethi, S. & Jäntti, R. (2007), Load balanced aodv- an improvement in performance and fairness, *in* 'Proc. 7th international conference on ITS telecommunication (ITST 2007)', Paris, France.

Gao, D., Niu, Y. & Yang, O. (2009), Synchronous sleep andwake in ip-enabled wireless sensor networks, *in* 'Electrical and Computer Engineering, 2009. CCECE '09. Canadian Conference on', pp. 161–164.

G.Bianchi (2000), 'Performance analysis of the ieee 802.11 distributed coordination function', *IEEE JSAC* **18**, pp. 535 – 547.

Geng, L., Lu, F., Liang, Y.-C. & Chin, F. (2008), Secure multi-path construction in wireless sensor networks using network coding, *in* 'Personal, Indoor and Mobile Radio Communications, 2008. PIMRC 2008. IEEE 19th International Symposium on', pp. 1–5.

Goel, A. & Khanna, S. (2008), On the network coding advantage for wireless multicast in euclidean space, *in* 'Information Processing in Sensor Networks, 2008. IPSN '08. International Conference on', pp. 64–69.

Gomez, J. & Campbell, A. (2004), A case for variable-range transmission power control in wireless multihop networks, *in* 'INFOCOM 2004. Twenty-third AnnualJoint Conference of the IEEE Computer and Communications Societies', Vol. 2, pp. 1425–1436 vol.2.

Gomez, J., Campbell, A. T., Naghshineh, M. & Bisdikian, C. (2003), 'Paro: Supporting dynamic power controlled routing in wireless ad hoc networks'.

Grossglauser, M. & Tse, D. N. C. (2002), 'Mobility increases the capacity of ad hoc wireless networks', *IEEE/ACM TRANSACTIONS ON NETWORKING* **10**(4), 477–486.

Guimaraes, R. P. & Cerda, L. (2007), Improving reactive routing on wireless multi-rate ad-hoc networks, *in* 'proceedings of 13th European Wireless 2007'.

Gupta, N. & Das, S. (2001), A capacity and utilization study of mobile ad hoc networks, *in* 'Proceedings of 26th IEEE conference on Local Computer Networks (LCN2001)', pp. 576–583.

Gupta, P. & Kumar, P. (2000), 'The capacity of wireless networks', *IEEE Trans. Information Theory* **46**(2), 388–404.

Gupta, P. & Kumar, P. R. (1998), 'Critical power for asymptotic connectivity in wireless networks', *A Volume in Honor of W.H. Fleming in Stochastic Analysis, Control Optimization, and Applications* **in Honor of W.H. Fleming**, 547–566.

Handy, M., Haase, M. & Timmer-mann, D. (2002), Low energy adaptive clustering hierarchy with deterministic cluster-head selection, *in* 'Mobile and Wireless Communications Network, 2002. 4th International Workshop on', pp. 368–372.

Hassanein, H. & Zhou, A. (2001), Routing with load balancing in wireless ad-hoc networks, *in* 'ACM Workshop on Modeling, Analysis and Simulation of Wireless and Mobile Systems'.

Healy, M., Newe, T. & Lewis, E. (2008), 'Wireless sensor node hardware: A review', *Sensors, 2008 IEEE* **1**, 621–624.

Heinzelman, W., Kulik, J. & Balakrishnan, H. (1999), Adaptive protocols for information dissemination in wireless sensor networks, *in* 'proc. Mobicom'99'.

Hohlt, B., Doherty, L. & Brewer, E. (2004), Flexible power scheduling for sensor networks, *in* 'IPSN '04: Proceedings of the 3rd international symposium on Information processing in sensor networks', ACM, New York, NY, USA, pp. 205–214.

Hou, T.-C. & Tsai, T.-J. (2001), 'An access-based clustering protocol for multihop wireless ad hoc networks', *IEEE Journal of Selected Area Communications* **19**(1), 1201–1210.

Howard, S. L., Schlegel, C. & Iniewski, K. (2006), 'Error control coding in low-power wireless sensor networks: when is ecc energy-efficient?', *EURASIP J. Wirel. Commun. Netw.* **2006**(2), 29–29.

IEEE (2003), Wireless medium access control (mac) and physical layer (phy) specifications for low-rate wireless personal area networks (lr-wpans), Technical report, IEEE802.15.4 WorkGroup.

IEEE (2006), Ieee standard 802.15.4, Technical report, IEEE 802.15 work group.

IEEE, W. G. (1999), Ieee std 802.11b-1999: Wireless lan medium access control (mac) and physical layer (phy) specifications: Higher- speed physical layer extension in the 2.4 ghz band., Technical report, IEEE.

Imran, A., Sorav, B., Gupta, R., Misra, A., Razdan, A. & Shorey, R. (2002), Energy efficiency and throughput for tcp traffic in multi-hop wireless networks, *in* 'Proceedings of IEEE INFOCOM'2002 conference', New York, USA.

Intanagonwiwat, C., Govindan, R., Estrin, D., Heidemann, J. & Silva, F. (2003), 'Directed diffusion for wireless sensor networking', *IEEE/ACM Trans. Netw.* **11**(1), 2–16.

Jäntti, R. & Ki, S.-L. (2005), 'Joint data rate and power allocation for lifetime maximization in interference limited ad hoc networks', *to appear in IEEE Transactions on Wireless Communications* **1**, 1.

Jardosh, S., Zunnun, N., Ranjan, P. & Srivastava, S. (2008), Effect of network coding on buffer management in wireless sensor network, *in* 'Intelligent Sensors, Sensor Networks and Information Processing, 2008. ISSNIP 2008. International Conference on', pp. 157–162.

Jennic Co. Ltd. (2006), 'Jennic JN5139 IEEE802.15.4 and ZigBee Wireless Microcontrollers datasheet'.

Johson, D., Maltz, D., Hu, Y.-C. & Jetcheva, J. (2001), The dynamic source routing (dsr) protocol for mobile ad hoc networks, Internet draft, IETF.

Jung, E.-S. & Vaidya, N. H. (2005), 'A power control mac protocol for ad hoc networks', *Wirel. Netw.* **11**(1-2), 55–66.

Karn, P. (1990), Maca - a new channel access method for packet radio, *in* 'proc. of the 9th ARRL Computer Networking Conference'.

Kawadia, V. & Kumar, P. (2003), Power control and clustering in ad hoc networks, *in* 'Proc. Infocom 2003'.

Khurana, S., Gupta, N. & Aneja, N. (2006), 'Reliable ad-hoc on-demand distance vector routing protocol', *Mobile Communications and Learning Technologies, Conference on Networking, Conference on Systems, International Conference on* **0**, 98.

Kim, W., Lee, J., Kwon, T., Lee, S.-J. & Choi, Y. (2007), Quantifying the interference gray zone in wireless networks: A measurement study, *in* 'Communications, 2007. ICC '07. IEEE International Conference on', pp. 3758–3763.

Kleinrock, L. & Tobagi, F. A. (1975), 'Packet switching in radio channels: Part i - carrier sense multiple-access modes and their throughput-delay characteristics', *IEEE Trans. Commun.* **vol. COM-23**, pp. 1400–1416.

Koskinen, H. (2004), On the coverage of a random sensor network in a bounded domain, *in* 'Proceedings of 16th ITC Specialist Seminar', pp. 11–18.

Krishnamachari, B., Estrin, D. & Wicher, S. (2002), Modelling data-centric routing in wireless sensor networks, *in* 'Proc. of IEEE Infocom 2002'.

Kulik, J., Henzelman, W. R. & Balakrishnan, H. (2002), 'Negotiation-based protocols for disseminating information in wireless sensor networks', *Wireless Networks* **8**, pp. 169–185.

Kwon, T. J. & Gerla, M. (2002), 'Efficient flooding with passive clustering (pc) in ad hoc networks', *SIGCOMM Comput. Commun. Rev.* **32**(1), 44–56.

Lee, S. & Gerla, M. (2001), Dynamic load-aware routing in ad hoc networks, *in* 'Proc. IEEE ICC'01', Helsinki, Finland, pp. 3201–3205.

Li, Q., Aslam, J. & Rus, D. (2001), Online power-aware routing in wireless ad-hoc networks, *in* 'MobiCom '01: Proceedings of the 7th annual international conference on Mobile computing and networking', ACM Press, New York, NY, USA, pp. 97–107.

Li, Q. & Rus, D. (2004), Global clock synchronization in sensor networks, *in* 'proc. of IEEE INFOCOM'04'.

Li, X. & Cuthbert, L. (2004), 'Stable node-disjoint multipath routing with low overhead in mobile ad hoc networks', *Modeling, Analysis, and Simulation of Computer Systems, International Symposium on* **0**, 184–191.

Li, X.-Y., Wan, P.-J., Wang, Y. & Frieder, O. (2001), Constrained shortest paths in wireless networks, *in* 'Proceedings of Military Communications Conference, 2001. MILCOM 2001', Vol. 2, pp. 884 –893.

Lim, C. H. & Lee, P. J. (1994), More flexible exponentiation with precomputation, *in* 'Precomputation, Advances in Cryptology - CRYPTO 94', pp. 95–107.

Lin, C.-H. & Tsai, M.-J. (2006), 'A comment on "heed: A hybrid, energy-efficient, distributed clustering approach for ad hoc sensor networks", *Mobile Computing, IEEE Transactions on* **5**(10), 1471–1472.

Lin, Y.-D. J. & Hsu, Y.-C. (2000), Multihop cellular: A new architecture for wireless communications, *in* 'Proceedings of INFOCOM'00', pp. 1273–1282. URL: `citeseer.ist.psu.edu/lin00multihop.html`

Liu, J.-S. & Lin, C.-H. (2003), ower-efficiency clustering method with power-limit constraint for sensor networks, *in* 'Proceedings of the 2003 IEEE International Performance, Computing, and Communications Conference', pp. 129 –136.

Lundgren, H., Nordström, E. & Tschudin, C. (2002), Coping with communication gray zones in ieee 802.11b based ad hoc networks, *in* 'Proceedings of The Fifth International Workshop on Wireless Mobile Multimedia, WOWMOM 2002', Atlanta, Georgia.

Maheshwari, R., Jain, S. & Das, S. R. (2008), A measurement study of interference modeling and scheduling in low-power wireless networks, *in* 'SenSys '08: Proceedings of the 6th ACM conference on Embedded network sensor systems', ACM, New York, NY, USA, pp. 141–154.

Maróti, M., Kusy, B., Simon, G. & Lédeczi, A. (2004), The flooding time synchronization protocol, *in* 'SenSys '04: Proceedings of the 2nd international conference on Embedded networked sensor systems', ACM, New York, NY, USA, pp. 39–49.

MAXIM Semiconductor (2001), Block diagram for 2.4ghz ieee802.11b dsss wlan transceiver application, Application note, Maxim-Dallas Semiconductor Co. Ltd.

MAXIM Semiconductor (2003), 'Max2242 2.4ghz to 2.5ghz linear power amplifier datasheet'.
URL: `http://pdfserv.maxim-ic.com/en/ds/MAX2242.pdf`

Mills, D. L. (1994), Internet time synchronization: The network time protocol, *in* Z. Yang & T. Marsland, eds, 'Global States and Time in Distributed Systems', IEEE Computer Society Press.

Minoli, D. (1979), 'Packet radio monitoring via repeater-on-packets', *IEEE Transactions on Aerospace and Electronic Systems* **AES-15**, 466–473.

Monks, J., Ebert, J.-P., Wolisz, A. & Hwu, W. (2001), A study of the energy saving and capacity improvement potential of power control in multi-hop wireless networks, *in* 'Local Computer Networks, 2001. Proceedings of LCN 2001. 26th Annual IEEE Conference on', pp. 550 – 559.

Nethi, S., Gao, C. & Jäntti, R. (2007), Localized multiple next-hop routing protocol, *in* 'Proc. 7th international conference on ITS telecommunication (ITST 2007)', Paris, France.

Olafsson, S. (2004), *Mobile and Wireless Communications: Key Technologies and Future Applications*, IEE, chapter 7, pp. 117–135.

Oliveira, P. & Barros, J. (2008), 'A network coding approach to secret key distribution', *Information Forensics and Security, IEEE Transactions on* **3**(3), 414–423.

Park, S.-J. & Sivakumar, R. (2002), Load sensitive transmission power control in wireless ad-hoc networks, *in* 'Proceedings of IEEE Global Communications Conference (GLOBECOM)', Taipei, Taiwan.

Park, V. & Corson, S. (2001), Temporally-ordered routing algorithm (tora) version 1, Internet draft, IETF.

Penrose, M. D. (1997), 'The longest edge of the random minimal spanning tree', *The Annals of Appl. Prob.* **7**(2), 340–361.

Perkins, C. E. & Bhagwat, P. (1994), Highly dynamic destination-sequenced distance vector (dsdv) for mobile computers, *in* 'Proc. of the SIGCOMM 1994 Conference on Communications Architectures, Protocols and Applications', pp. 234–244.

Perkins, C. E. & Royer, E. M. (1999), Ad-hoc on-demand distance vector routing, *in* 'Proceedings of IEEE WMCSA 1999', New Orleans, LA.

Perkins, C. E. & Royer, E. M. (2001), Ad hoc on demand distance vector (aodv) routing, Technical report, IETF Internet Draft.

Poon, E. & Li, B. (2003), Smartnode: achieving 802.11 mac interoperability in power-efficient ad hoc networks with dynamic range adjustments, *in* 'Proceedings of 23rd International Conference on Distributed Computing Systems', pp. 650–657.

Popa, L., Raiciu, C., Stoica, I. & Rosenblum, D. (2006*a*), Reducing congestion effects in wireless networks by multipath routing, *in* 'Network Protocols, 2006. ICNP '06. Proceedings of the 2006 14th IEEE International Conference on', pp. 96–105.

Popa, L., Raiciu, C., Stoica, I. & Rosenblum, D. (2006*b*), Reducing congestion effects in wireless networks by multipath routing, *in* 'ICNP '06: Proceedings of the Proceedings of the 2006 IEEE International Conference on Network Protocols', IEEE Computer Society, Washington, DC, USA, pp. 96–105.

Radwan, A. & Hassanein, H. S. (2006), Multi-hop cdma cellular networks with power control, *in* 'IWCMC '06: Proceedings of the 2006 international conference on Wireless communications and mobile computing', ACM Press, New York, NY, USA, pp. 325–330.

Raghunathan, V., Schurgers, C., Park, S. & Srivastava, M. (2002), 'Energy-aware wireless microsensor networks', *IEEE Signal Processing Magazine* **vol.19**, pp.40–50.

Raju, G., Hernandez, G. & Zou, Q. (2000), Quality of service routing in ad hoc networks, *in* 'Proceedings of IEEE WCNC: Wireless Communications and Networking Conference', Vol. 1, pp. 263 –265.

Ramanathan, R. & Redi, J. (2002), 'A brief overview of ad hoc networks: Challenges and directions', *IEEE Communications Magazine* **40**(5), 20–22.

Ramathandran, L., Kapoor, M., Sarkar, A. & Aggarwal, A. (2002), Clustering algorithms for wireless ad hoc networks, *in* 'Proceedings of the 4th international workshop on Discrete algorithms and methods for mobile computing and communications', Boston, Massachusetts, United States, pp. 54–63.

Rhee, I., Warrier, A., Aia, M., Min, J. & Sichitiu, M. L. (2008), 'Z-mac: a hybrid mac for wireless sensor networks', *IEEE/ACM Trans. Netw.* **16**(3), 511–524.

Rhee, I., Warrier, A., Min, J. & Xu, L. (2006), Drand: distributed randomized tdma scheduling for wireless ad-hoc networks, *in* 'MobiHoc '06: Proceedings of the 7th ACM international symposium on Mobile ad hoc networking and computing', ACM, New York, NY, USA, pp. 190–201.

Rodoplu, V. & Meng, T. (2002), Bit-per-joule capacity of energy-limited ad hoc networks, *in* 'Proceedings of IEEE Global Telecommunication Conference 2002', Vol. 1, pp. 16–20.

Römer, K. (2001), Time synchronization in ad hoc networks, *in* 'MobiHoc '01: Proceedings of the 2nd ACM international symposium on Mobile ad hoc networking & computing', ACM Press, New York, NY, USA, pp. 173–182.

Ross, S. (2006), *Introduction to Probability Models*, Elsevier Science & Technology Books.

Santi, P. & Blough, D. M. (2002), An evaluation of connectivity in mobile wireless ad hoc networks, *in* 'Proceedings of the International Conference on Dependable Systems and Networks', pp. 89–98.

Schurgers, C. & Sribastava, M. (2001), Energy efficient routing in wireless sensor networks, *in* 'proc. MILCOM 2001'.

Schwartz, M. (2005), *Mobile Wireless Communications*, Cambridge University Press.

Shah-Mansouri, V. & Wong, V. (2008), Maximum-lifetime coding subgraph for multicast traffic in wireless sensor networks, *in* 'Global Telecommunications Conference, 2008. IEEE GLOBECOM 2008. IEEE', pp. 1–6.

Sheu, S.-T. & Chen, J. (2001), A novel delay-oriented shortest path routing protocol for mobile ad hoc networks, *in* 'IEEE International Conference on Communications (ICC2001)', Vol. 6, pp. 1930 –1934.

Sheu, S.-T., Shih, Y.-Y. & Lee, W.-T. (2009), 'Csma/cf protocol for ieee 802.15.4 wpans', *Vehicular Technology, IEEE Transactions on* **58**(3), 1501–1516.

Shin, K.-Y., Song, J., Kim, J., Yu, M. & Mah, P. S. (2007), Rear: Reliable energy aware routing protocol for wireless sensor networks, *in* 'Advanced Communication Technology, The 9th International Conference on', Vol. 1, pp. 525–530.

Sikora, A. (2004), 'Design challenges for short-range wireless networks', *Communications, IEE Proceedings* **151**, 473–479.

Singh, C., Vyas, O. & Tiwari, M. (2008), An overview of routing protocols of sensor networks, *in* 'Computational Intelligence for Modelling Control & Automation, 2008 International Conference on', pp. 873–878.

Singh, S. & Raghavendra, C. (1998), 'Pamas: power aware multi-access protocol with signalling for ad hoc networks', *ACM Computer Communication Review* **28**(3), 5–26.

Singh, S., Woo, M. & Raghavendra, C. S. (1998), Power-aware routing in mobile ad hoc networks, *in* 'MobiCom '98: Proceedings of the 4th annual ACM/IEEE international conference on Mobile computing and networking', ACM Press, New York, NY, USA, pp. 181–190.

Slama, I., Jouaber, B. & Zeghlache, D. (2008), A free collision and distributed slot assignment algorithm for wireless sensor networks, *in* 'Global Telecommunications Conference, 2008. IEEE GLOBECOM 2008. IEEE', pp. 1–6.

Sommer, P. & Wattenhofer, R. (2008), Symmetric clock synchronization in sensor networks, *in* 'REALWSN '08: Proceedings of the workshop on Real-world wireless sensor networks', ACM, New York, NY, USA, pp. 11–15.

Song, J.-H., Wong, V. & Leung, V. (2004), 'Efficient on-demand routing for mobile ad-hoc wireless access networks', *IEEE Journal on Selected Areas in Communications* **22**(7), 1374–1383.

Song, N. O., Kwak, B. J., Song, J. & Miller, L. (2003), Enhancement of ieee 802.11 distributed coordination function with exponential increase exponential decrease backoff algorithm, *in* 'Proc. VTC 2003 (Spring)'.

Srinivasan, K. & Levis, P. (2006), RSSI is Under-Appreciated, *in* 'EmNetS, 2006'.

Swetha, N., Kawadia, V., Screenivas, R. & Kumar, P. (2002), Power control in ad-hoc networks: Theory, architecture, algorithm and implementation of compow protocol, *in* 'Proceedings of the European Wireless Conference - Next Generation Wireless Networks: Technologies, Protocols, Services and Applications', Florence, Italy, pp. 156–162.

Tan, C.-W. & Bose, S. (2005), Investigating power aware aodv for efficient power routing in manets, *in* 'Information, Communications and Signal Processing, 2005 Fifth International Conference on', pp. 584–588.

Tan, C. & Zou, J. (2007), A multicast algorithm based on network coding for wireless sensor network, *in* 'Wireless, Mobile and Sensor Networks, 2007. (CCWMSN07). IET Conference on', pp. 1043–1046.

Tang, Z., Glover, I., Evans, A. & He, J. (2007), Energy efficient transmission protocol for distributed source coding in sensor networks, *in* 'Communications, 2007. ICC '07. IEEE International Conference on', pp. 3870–3875.

Texas inst. (2007*a*), 'Cc2420 2.4ghz ieee 802.15.4/zigbee-ready rf transceiver'.

Texas Inst. (2007*b*), 'Digital temperature sensor with i2c interface datasheet'.

The Mathworks, Inc. (n.d.), 'Matlab - the language of technical computing'.

Tobagi, F. A. & Kleinrock, L. (1975), 'Packet switching in radio channels: Part ii - the hidden terminal problem in carrier sense multiple-access modes and the busy-tone solution', *IEEE Trans. Commun.* **vol. COM-23**, pp. 1417–1433.

Toledo, A. & Wang, X. (2006), Efficient multipath in sensor networks using diffusion and network coding, *in* 'Information Sciences and Systems, 2006 40th Annual Conference on', pp. 87–92.

Toumpis, S. & Goldsmith, A. (2000), Ad hco network capacity, *in* 'Proceedings of the 24-th Asilomar Conference of Signals, Systems and Computers', Vol. 2, pp. 1265–1269.

Trung, T. & Kim, S. (2002), Implementation of an energy-efficient routing protocol: Time delay on-demand routing algorithm (tdor), *in* 'proc. IEEE Conference on Mobile and Wireless Communications Networks', Stockholm, Sweden.

Tseng, Y.-C., Ni, S.-Y., Chen, Y.-S. & Sheu, J.-P. (2002), 'The broadcast storm problem in a mobile ad hoc network', *Wireless Networks* **8**, 153–167.

Tubaishat, M. & Madria, S. (2003), 'Sensor networks: an overview', *IEEE Potentials* **22**, 20–23.

van Dam, T. & Langendoen, K. (2003), An adaptive energy-efficient mac protocol for wireless sensor networks, *in* 'SenSys '03: Proceedings of the 1st international conference on Embedded networked sensor systems', ACM, New York, NY, USA, pp. 171–180.

Veijalainen, J., Ojanen, E., Haq, M. A., Vahteala, V.-P. & Matsumoto, M. (2002), 'Energy consumption tradeoffs for compressed wireless data at a mobile terminal', *IEICE Transaction of Fundamentals/Communications/Electron/Inf. & Syst.* **E85-A/B/C/D**, 1123–1130.

Viterbi, A. & Viterbi, A. (1993), 'Erlang capacity of a power controlled cdma system', *IEEE Journal on Selected Areas in Communications* **11**, 892–900.

Wameke, B. & Pister, K. S. J. (2002), Mems for distributed wireless sensor networks, *in* 'Proc. of 9-th Int'l Conf. on Electronics, Circuits and Systems'.

Wang, N. & Lin, J. (2008), Network coding for distributed data storage and continuous collection in wireless sensor networks, *in* 'Wireless Communications, Networking and Mobile Computing, 2008. WiCOM '08. 4th International Conference on', pp. 1–4.

Weisstein, E. W. (2005), 'Hybercube line picking', From MathWorld–A Wolfram Web Resource.
URL: `http://mathworld.wolfram.com/HypercubeLinePicking.html`

Wu, H., Qiao, C., De, S. & Tonguz, O. (2001), 'Integrated cellular and ad hoc relaying systems: icar', *IEEE JOURNAL ON SELECTED AREAS IN COMMUNICATIONS* **19**(10), 2105–2115.

Xu, K. & Gerla, M. (2002), A heterogeneous routing protocol based on a new stable clustering scheme, *in* 'MILCOM 2002, Proceedings', Vol. 2, pp. 838–843.

Xu, Y., Heidemann, J. & Estrin, D. (2001), Geography-informed energy conservation for ad hoc routing, *in* 'MobiCom '01: Proceedings of the 7th annual

international conference on Mobile computing and networking', ACM Press, New York, NY, USA, pp. 70–84.

Ya, X., Heidemann, J. & Estrin, D. (2000), Adaptive energy-conserving routing for multihop ad hoc networks, Technical report, USC/ISI.

Yamamoto, K. & Yoshida, S. (2004), 'Analysis of reverse link capacity enhancement for cdma cellular systems using two-hop relaying', *IEICE TRANS. FUNDAMENTALS* **E87**(7), 1712–1719.

YDI-Wireless, C. L. (n.d.), *Diamond WLAN Card Quick Start Guide*, YDI-Wireless, Co. Ltd.

Ye, F., Chen, A., Liu, S. & Zhang, L. (2001), A scalable solution to minimum cost forwarding in large sensor networks, *in* 'proc. 10th International Conference on Computer Communications and Networks (ICCCN)'.

Ye, W., Heidemann, J. & Estrin, D. (2002), An energy-efficient mac protocol for wireless sensor networks, *in* 'Proceedings of the 21st International Annual Joint Conference of the IEEE Computer and Communications Societies (INFOCOM 2002)', New York, NY, USA.

Younis, O. & Fahmy, S. (2004), Distributed clustering in ad-hoc sensor networks: A hybrid, *in* 'Proceedings of the IEEE Conference on Computer Communications (INFOCOM), Hong Kong (2004)'.

Yu, D. & Li, H. (2003), On the definition of ad hoc network connectivity, *in* 'Proceedings ICCT 2003: International Conference on Communication Technology', Vol. 2, pp. 990–994.

Zabin, F., Misra, S., Woungang, I., Rashvand, H., Ma, N.-W. & Ahsan Ali, M. (2008), 'Reep: data-centric, energy-efficient and reliable routing protocol for wireless sensor networks', *Communications, IET* **2**(8), 995–1008.

Zadeh, A. & Jabbari, B. (2001*a*), On the capacity modeling of multi-hop cellular packet cdma networks, *in* 'Proc. IEEE MILCOM'01', Vol. 1, pp. 600 – 604.

Zadeh, A. N. & Jabbari, B. (2001*b*), Performance analysis of multihop packet cdma cellular networks, *in* 'Proc. IEEE GLOBCOM'01', San Antonio.

APPENDICES

Appendix for Least-hop Analysis

Probability of k collisions on a H-hop path

From (Ross 2006) we have such a proposition:

Proposition 1 *There are* $\binom{n+r-1}{r-1}$ *distinct nonnegative integer-value vectors denoted as* $(x_1, \ldots, x_r)$ *such that* $x_1 + \ldots + x_r = n$

In reactive routing such as AODV and DSR, a Route REQuest (RREQ) packet is flood through the whole network. Suppose that a path from source node to destination node has H ($H \geq 1$) hops, and the probability that the radio channel is congested on a single hop is p. If there are k ($k \geq 0$) congestions occur over the path, for a single case of k congestions, the probability is $p^k(1-p)^H$. We have

$$\Pr(H,k) = \binom{H-1+k}{H-1} p^k (1-p)^H = \binom{H-1+k}{k} p^k (1-p)^H \qquad (1)$$

Expected Delay of the Least Hop Route

We have

$$\begin{aligned} E(T_H) &= \sum_{i=0}^{\infty} T_{H,i} \Pr(H,i) = \sum_{i=0}^{\infty} (i\tau_c + H\tau_p) \binom{H-1+i}{i} p^i (1-p)^H \\ &= (1-p)^H \tau_c \sum_{i=0}^{\infty} \binom{H-1+i}{i} i p^i + (1-p)^H H \tau_p \sum_{i=0}^{\infty} \binom{H-1+i}{i} p^i \end{aligned}$$

The summation $\sum_{i=0}^{\infty} C_{H-1+i}^{H-1} p^i$ in the second part can be seen by different H:

$$H = 1, \quad \sum_{i=0}^{\infty} C_i^0 p^i = 1 + p + p^2 + ... + p^i + ... = \frac{1}{1-p}$$
$$H = 2, \quad \sum_{i=0}^{\infty} C_{i+1}^1 p^i = 1 + 2p + 3p^2 + ... + (k+1)p^i + ... = \frac{1}{(1-p)^2}$$

By these two observations, we assume that when $H = k$

$$\sum_{i=0}^{\infty} C_{k-1+i}^{k-1} p^i = 1 + kp + \frac{(k+1)k}{2!} p^2 + ... + \frac{(k-1+i)!}{i!(k-1)!} p^k + ... = \frac{1}{(1-p)^k}$$

then when $H = k+1$, let

$$\sum_{i=0}^{\infty} C_{i+k}^{k} p^{k+1} = 1 + (k+1)p + \frac{(k+2)(k+1)}{2!} p^2 + ... + \frac{(k+i)!}{k!i!} p^k + ... = S$$

Let (2) subtract (2), we get

$$\begin{aligned} S - \sum_{i=0}^{\infty} C_{k-1+i}^{k-1} p^i &= 0 + p + \frac{2(k+1)}{2!} p^2 + ... + \frac{(i+k-1)...(k+1)k}{k!} p^k + ... \\ &= p(1 + (k+1)p + \frac{(k+2)(k+1)}{2!} p^2 + ... + \frac{(k+i)!}{k!i!} p^k + ...) \\ &= pS \end{aligned}$$

Thus we have

$$\sum_{i=0}^{\infty} C_{i+k}^{k} p^{k+1} = \frac{1}{(1-p)^{k+1}} \qquad \text{for all } k \tag{2}$$

The summation $\sum_{i=0}^{\infty} C_{H-1+i}^{H-1} i p^i$ can be deduced by

$$\begin{aligned} \sum_{i=0}^{\infty} C_{H-1+i}^{H-1} i p^i &= \sum_{i=1}^{\infty} C_{H-1+i}^{H-1} i p^i \\ &= p \sum_{i=0}^{\infty} C_{H-1+i}^{H-1} i p^{i-1} = p \sum_{i=0}^{\infty} C_{H-1+i}^{H-1} \frac{\partial}{\partial p} p^i = p \frac{\partial}{\partial p} \sum_{i=0}^{\infty} C_{H-1+i}^{H-1} p^i \\ &= p \frac{\partial}{\partial p} \frac{1}{(1-p)^H} \\ &= \frac{Hp}{(1-p)^{H+1}} \end{aligned}$$

Therefore the expected delay is

$$E(T_H) = H\tau_c \frac{p}{1-p} + H\tau_p \tag{3}$$

Appendix for Energy-aware Capacity

The expected hop count in a grid topology network

We have

$$\begin{aligned} E\{|x|\} &= \frac{1}{n}\sum_{i=0}^{n-1}\frac{1}{n-1}\sum_{j=0,j\neq i}^{n-1}|i-j| \qquad (4)\\ &= \frac{1}{n(n-1)}\Bigg[\underbrace{(1+2+\ldots+n-1)}_{\text{S is the 1st node}} + \underbrace{(1+1+2+\ldots+n-2)}_{\text{S is the 2nd node}} + \ldots \\ &\quad + \underbrace{(1+2+\ldots+n-1)}_{\text{S is the last node}}\Bigg] \\ &= \frac{1}{n(n-1)}\left[\left(\frac{n(n-1)}{2}+0\right) + \left(\frac{(n-1)(n-2)}{2}+1\right) + \right. \\ &\quad \left. \ldots + \left(0+\frac{n(n-1)}{2}\right)\right] \\ &= \frac{1}{n(n-1)} 2\sum_{i=0}^{n}\frac{(n-i)(n-1-i)}{2} \\ &= \frac{1}{n(n-1)}\sum_{i=0}^{n}(n-i)(n-1-i) \\ &= \frac{n+1}{3} \qquad (5) \end{aligned}$$

Here the summation $\sum_{i=0}^{n}(n-i)(n-1-i)$ can be derived by

$$\begin{aligned}\sum_{i=0}^{n}(n-i)(n-1-i) &= \sum_{i=0}^{n}\left(n^2-(2i+1)n+i^2+i\right)\\ &= n^2(n+1)-n\sum_{i=0}^{n}(2i+1)+\sum_{i=0}^{n}(i^2+i)\\ &= n^2(n+1)-n(n+1)^2+\frac{n(n+1)(2n+1)}{6}+\frac{n(n+1)}{2}\\ &= \frac{n(n-1)(n+1)}{3} \qquad (6)\end{aligned}$$